THE MATHEMATICAL MODELLING OF MIXING IN NATURAL STREAMS

THE MATHEMATICAL MODELLING OF MIXING IN NATURAL STREAMS

By

ROBERT CHARLES HUDSPITH, B. Eng.

A Thesis
Submitted to the Faculty of Graduate Studies
in Partial Fulfillment of the Requirements
for the Degree
Master of Engineering

McMaster University
May, 1970

MASTER OF ENGINEERING
(Chemical Engineering)

McMASTER UNIVERSITY
Hamilton, Ontario.

TITLE: The Mathematical Modelling of Mixing in Natural Streams

AUTHOR: Robert Charles Hudspith, B. Eng. (McMaster University)

SUPERVISOR: Dr. J. D. Norman

NUMBER OF PAGES: 163, xi

SCOPE AND CONTENTS:

A method of modelling the mixing phenomenon in natural streams is presented. A wide range of mixing situations can be characterized using a lumped parameter model consisting of a network of ideally mixed components. The components represent two ideal states of mixing: complete mixing of the total component volume, and the other extreme where no mixing occurs in the direction of flow through the component volume. The use of frequency response techniques to match the mathematical model to the real situation is also discussed.

Experimental work was carried out on a small natural stream to illustrate how the method is to be applied. The frequency response was obtained using sinusoidal, pulse, and impulse inputs and fluorometric dye tracing techniques. The non-linear model parameters were evaluated using the principles of least squares. The mathematical model chosen for this particular stream illustrates how the phenomenon of stagnant or

slow moving regions can be included. The necessary data was collected on several days under different flow conditions to show how the model can be made a function of stream flow.

ACKNOWLEDGEMENTS

The author wishes to express his sincere gratitude to: his wife, Barbara, for her patience and understanding throughout the year and for the typing of this manuscript, to Dr. J. D. Norman, for his suggestions and advice throughout the project, and to his fellow students, for their assistance in the understanding of the theoretical background and for their practical help during the experimental part of this work.

Financial assistance provided by the National Research Council and the Department of Chemical Engineering, McMaster University, is appreciated.

TABLE OF CONTENTS

PAGE NUMBER

LIST OF TABLES

LIST OF FIGURES

CHAPTER 1

1. INTRODUCTION

1.1 Statement of the Problem

A river can be regarded as a complex and dynamic system involving the interaction of physical, chemical and biological forces.

For effective water quality management it is desirable to be able to predict the extent of a change in water quality for a specific input. In order to do this, a good description of the system must be available. The way in which the overall system is formulated will depend on the water quality parameter of interest. For example, to predict the change in dissolved oxygen for an input of an organic waste, factors such as photosynthesis, bottom deposits, temperature, the extent of mixing and the biochemical reaction rate, will need to be included in the formulation. But in the case of a radioactive waste, if one is only interested in the concentration of that specific component at a given point downstream, the only factors that will need to be considered are, the extent of mixing, the radioactive decay rate, and any loss to the stream bed by adsorbtion or deposition. The major factor common to both of the above examples is the mixing phenomenon. Even for a conserved substance, where no reaction is occurring,

it is necessary to have an adequate characterization of the mixing in order to predict the distribution in the water body.

A system is usually described with the use of mathematical models. When several factors are involved, the system can usually be subdivided. Each subsystem can then be modelled separately. The mixing phenomenon is one of the basic subsystems to all water quality systems.

An adequate characterization of this phenomenon should fulfill the following criteria:

(a) the method should be flexible in that complex, as well as simple flow regimes that are encountered in natural streams can be handled;

(b) the model should be formulated in such a way that it can be easily coupled with other subsystems such as reaction rates and stream flow;

(c) the model proposed should be as mechanistic as possible so that conversion predictions for non-linear reactions will be accurate; and

(d) the field data required should be easily obtainable.

1.2 Objective

The objective of this work will be to describe a method of modelling mixing that has been used on various reactors in industry as well as the waste treatment field and to demonstrate its application to natural streams.

It will be shown how the proposed method satisfies all the criteria mentioned in section 1.1.

1.3 General Approach

It is possible to model the mixing phenomena using either a lumped parameter model or a distributed parameter model. Within these two broad categories, many different models could be proposed.

Any model that defines the extent of mixing continuously at every location within the fluid is described as a distributed parameter model in this work. An example of this approach is the dispersion model which has been extensively applied to natural streams. Other examples and further details of this method will be given in Chapter 2 in conjunction with the review of previous work.

In the field of reactor design there are two ideal flow reactors which describe two extreme states of mixing. For a plug flow, slug flow, or piston flow reactor there may be lateral mixing of the fluid but there must be no mixing of the fluid longitudinally along the flow path. A necessary and sufficient condition for plug flow is to state that the residence time in the reactor is the same for all elements of the fluid. The reactor will be denoted as PFTR. The other extreme is the backmix or completely stirred tank reactor. The contents of this tank reactor are well stirred and uniform in composition throughout. Thus the exit stream from this reactor has the same composition as the fluid

within the reactor. This reactor will be denoted as a CSTR. A network of these ideal reactors, with various interconnecting flows can be used to simulate the nonideal flow occurring in a natural stream. The arrangement of the elements can be made to approach the actual state of mixing. This modular approach is what is meant by a lumped parameter model in this work.

One of the most important criteria to be satisfied by any model is that reaction conversion prediction be simple and accurate. In the case of a reaction with rate linear in concentration, i.e. first order kinetics, the model only has to correctly predict the exit age distribution in order for the predicted performance to be good. But in the case of a nonlinear rate equation the prediction will only be accurate if the model has a correspondence with fact. The ability to model a wide variety of complex and simple mixing situations and at the same time reflect reality is a strong feature of the modular approach. No one distributed parameter model has this flexibility. The conversion of each reactor in the network can be calculated individually and this information applied to a succeeding reactor as one moves through the network, making conversion prediction simple and straightforward.

The lumped parameter approach is chosen as a general approach to model natural streams. Parameter evaluation

techniques and details of the field data required will be discussed in Chapters 3 and 4 after the previous work in this field has been reviewed.

CHAPTER 2

2. LITERATURE REVIEW

2.1 Introduction

The mathematical modelling of the mixing phenomenon is not new, especially in the chemical reactor field. Development of a model involves three different activities. First, a model or at least a modelling approach must be selected. The system response must be then obtained, i.e. data must be collected, so that the model can be compared to the real situation. Lastly, the parameters of the model must be evaluated. Modelling attempted in the past will be reviewed in this chapter under the three activities described above. Work in the general area of chemical reactor engineering and in the area of streams and natural water bodies will be considered separately. The chapter will conclude with an evaluation of the previous work and a brief description of the methods chosen for this study.

2.2 Modelling of Mixing in the Chemical Reactor Field

2.2.1 Types of Models

Numerous models have been proposed for a variety of situations. Commercial continuously stirred tank reactors have been the subject of much study and the models proposed for them approach the case of perfect mixing. On the other hand, many reactors are designed to be as close as possible

to plug flow; several models have been developed to account for deviations from this extreme mixing condition. However, some models and modelling approaches are general enough to describe almost any type of mixing. Types of models proposed for these specific or general situations, as well as some other special cases, will be briefly discussed in this section.

Van De Vusse (116) proposed a three parameter model for a CSTR in terms of circulation loops around the mixer. He also showed how his model could be used for batch mixing. Gibilaro et al (44) showed how the above model could be formulated using probability or statistical methods. A two tank model, involving the evaluation of only one parameter, has been suggested by Esterson (86) and a two tank model coupled by a region of plug flow was proposed by Dysinger (34). Corrigan's (22) model for the CSTR involved the interaction of a stagnant region within the tank.

Both distributed and lumped parameter models have been proposed to model mixing conditions that approach plug flow.

The most popular distributed parameter model is the dispersion or diffusion model. In this model the process that causes the deviation from ideal plug flow is considered to be analogous to molecular diffusion. Taylor (106, 107, 108), Hays et al (95) and Aris (6) used this model in their study of mixing in a pipe. Bischoff and Levenspiel (11)

discuss how the model can be used to describe both axial and radial diffusion. They also generalize the model to a wide variety of boundary conditions. Further discussion on how to use this model is given by Clements (20), and Levenspiel and Smith (72).

There are also many examples of the modular approach, i.e. the use of a lumped parameter model, to describe deviations from plug flow. Deans and Lapidus (24) modelled a fixed bed reactor using a series of CSTRs. This one dimensional model was expanded to two dimensions to include the effect of radial mixing. They also compare this series model to the dispersion model. Whereas the usual tank in series model only allows mixing in one direction, a backflow cell model has also been studied (94, 102, 61). As Adler et al (2) points out, this backflow model is equivalent to the dispersion model expressed in finite difference terms. Rippin (93) has proposed another model consisting of a PFTR with recycle, and shows how one form of it is analogous to a series of CSTRs and to the dispersion model.

The modular approach, using CSTRs and PFTR has been shown to be flexible enough to handle almost any mixing situation. Levenspiel (71) and Chollette and Cloutier (17, 18) have presented models and methods to account for short-circuiting and stagnant regions as well as partial mixing. A four parameter finite stage model is described by Adler et al (2); it has been shown to be flexible enough to

handle a wide variety of mixing situations and at the same time approximate the real system. Clements (19) used this model in his studies of an extraction column and found it far better than the dispersion model. A parallel flow situation has been studied by Melnyk (75) using the mixed model or modular approach.

Wolf and Resnick (91) present a general function, rather than a specific model, to characterize the various kinds of mixing described above. The recycle model of Rippin (93) can also be used for any flow situation between the two extremes of ideal mixing.

There are two different ways of treating 'dead space', 'dead volume', or 'stagnant zones'. Most workers treat this region by considering it to have a large residence time compared to the major bulk of the fluid. The model discussed by Adler (1) accomplished this with a parallel CSTR having a slow exchange rate with an in-series CSTR. Levenspiel (71), on the other hand, considers this region to be completely dead or inactive, i.e. no interaction with the active volume. He feels that this approximation will cause an error of a few per-cent for most conversion predictions. White (118) points out the importance of distinguishing which method is being used. A very general time delay model, to account for stagnancy, has been proposed by Buffham and Gibilaro (14). This model is very flexible and has many other delay models as subcases. Naor and Shinnar (101) derive a function that

can be used to determine if stagnancy or parallel flow is significant in the system being studied.

Some of the methods and models described above have been used to characterize a variety of the unit processes in the sanitary engineering field. Sawyer (97, 98) used the modular approach to model a chlorine contact tank. He found that the mixing could be characterized by a CSTR, a PFTR and a completely dead region. The hydraulic efficiency of a sedimentation basin has been studied and modelled by Kebhun and Argamen (90). The mathematical relationships used by them to model the mixing are equivalent to the components used by Sawyer (97). One further example is the application of the dispersed plug flow model to a spiral flow aerator by Murphy and Boyko (76).

2.2.2 System Response Determination

The system response can be measured using any one of many inputs or forcing functions. Most mixing systems are usually studied in either the time domain, the frequency domain, or the Laplace domain. (In most scientific fields, the Laplace domain, s-plane and frequency domain are considered to be synonomous. Mathematically, the s-plane is a complex plane with $s = \sigma + jw$ (where σ is the real part, w, the frequency, is the imaginary part, and $j = \sqrt{-1}$). However, in this work, to be consistent with the literature reviewed, use of the positive imaginary part of the s-plane will be referred to as the frequency domain and use of the positive

real part of this plane as the Laplace domain. When the term s-plane is used, it will refer to both domains.) The type of domain to be used will restrict the allowable kinds of inputs. Rooze (95) discusses the use of these three domains and others.

Representation of the system response in the time domain has been the most popular method in the past. When an impulse (Dirac-delta function) of a tracer is used as an input, the concentration-time curve at the output defines the distribution of ages of fluid molecules in the exit stream. This curve is called a residence time distribution (RTD). If a step is used as an input, the resulting response is a cumulative RTD and is sometimes referred to as the transient response. These two response curves are also called C and F curves respectively. Dankwerts (23) has derived the F and C curves for a CSTR and a PFTR and other workers (91, 90) express their models in terms of these curves.

The complexity of most models in the time domain has resulted in a more recent emphasis on the frequency and Laplace domains.

The frequency response of a system can be defined as the steady state response to a periodic stimulus. This definition is somewhat misleading since almost any kind of input can be used. Although sinusoidal inputs have been used (98, 75, 63), they have been found to be an inefficient and impractical method of data collection.

The use of pulse inputs to obtain the frequency response has been studied extensively (98, 36, 53, 31, 32, 34). These thorough treatments of the subject study the effect of pulse shape and width as well as other possible sources of error. There are many examples of the pulse testing procedure being used to model the mixing phenomena (98, 53, 34). Frequency response techniques, especially pulse testing, is described in greater detail in a later chapter.

Both random and step inputs can be used to obtain the frequency response of a system. The use of steps is discussed by Schechter and Wissler (100) and Nyguist et al (80). Random inputs with the corresponding outputs can be transformed to the frequency domain through the use of statistical correlation techniques (8, 4).

Use of the Laplace domain is somewhat similar to frequency response techniques in the frequency domain in that the form of the input is not restricted. Rooze (95), Adler (1), Clements (19), and Williams et al (119) have shown how experimental data can be transformed into this domain. However, as Clements (19) points out, no investigation has been made concerning the propagation of errors in the transformations.

No matter what domain is used, the model must be expressed in that domain for the purpose of parameter evaluation. Most models are in the form of a differential equation in the time domain. Analytical solutions for these equations are usually not possible except for some simple mathematical definable inputs. This makes comparison of the experimental

response to model response for an arbitrary input very difficult. However, when the model differential equation is transformed into the s-plane, the equation becomes algebraic. This function is called the transfer function and is independent of the type of input. The model can also be expressed in the frequency domain by merely substituting jw (where w = frequency, and $j = \sqrt{-1}$) for the Laplace variable s. Use of frequency domain or Laplace domain involves the evaluation of the experimental transfer function which is to be compared to the model transfer function. Wen and Chang (117) present a dictionary of transfer functions for many models proposed in the past. They also give the time domain responses of these models for some well defined periodic and non-periodic inputs.

2.2.3 Parameter Evaluation

Some of the main methods that have been used to evaluate the model parameters will be briefly discussed in this section.

Models that have been expressed in terms of an F curve are usually exponential relationships (90, 71, 91). If the experimentally measured transient response is plotted on semi-log paper as ln (1-F) against t/θ (where t is time and θ is the average residence time) the points should lie on a straight line. The parameters can be evaluated from the slope and intercept of this line. Any deviation from a straight line relationship will indicate model deficiency.

Use of moments in general and the variance of the time-concentration curve specifically has been a popular

method. Otto and Stout (85) have shown how moments calculated from the model transfer function can be compared to the ratio of moments of the input and output pulses. The variance of the RTD, if an inpulse is used for the input, or the variance of both the input and output curves has been used to evaluate the coefficient of dispersion (11, 72).

The experimental transfer function in terms of the frequency response can be represented graphically using a dual plot known as a Bode diagram. Sawyer and King (98) describe the use of a template on a normalized Bode diagram to evaluate the parameters of their model.

The use of non-linear least squares estimation is becoming more popular. This procedure not only gives the statistically best parameter values but also indicates how well the model fits the data. In the time domain, the RTD of the model is fitted to measured concentration-time curve (20, 1, 95, 52). Hays (51) has shown how the least squares principle is applied in the frequency domain. Similarly, Williams et al (119) has shown how parameters can be estimated in the Laplace domain using this procedure. They also found that by choosing certain real positive values of s, the method will weight the more accurate portion of the curve.

Other workers have attempted to evaluate model parameters by relating them to hydraulic properties (107), and to mixer speeds (116). Proposed models could also be matched to experimental data by simulation on an analogue computer (74).

2.3 Modelling of Mixing in Natural Streams and Estuaries

2.3.1 Types of Models

In chapter one it was stated that a river could be considered as a water quality system. The major part of the interest in this system has resulted from a desire to know the effect of a waste load on the oxygen resources.

Early workers attempted to describe the whole system by one equation. The well-known model proposed by Streeter and Phelps (105) only considered the effects of decaying organic material and atmospheric reaeration. Since then, their basic equation has been altered and terms added to include the effects of such things as sedimentation, sludge deposits, photosynthesis, waste loads along the stream and fluctuating conditions at the effluent outfall.

While most of these equations do not consider the mixing phenomena explicitly, a type of mixing is implied. It can be shown that the stretch of river, for which the model is being applied, is assumed to be a PFTR. O'Conner (83, 82) shows how the effect of longitudinal dispersion can be included in the usual equations, however, he feels that this phenomena is only important in an estuary. Dobbins (26) also feels that dispersion is not an important phenomena in streams, accounting for only a three per-cent error in conversion predictions.

Thomann (114) discusses the systems analysis approach to the problem. He shows how a complex system

can be divided into subsystems which can be analysed separately and later combined to give an overall picture of the system. Most of the study of the mixing phenomena separately (i.e. as a subsystem) has been with the dispersed plug flow model described in section 2.2.1.

This one dimensional dispersion model has been applied to natural streams (35, 40, 39, 46, 64) and to estuaries (83, 59, 47, 45). Many of the researchers (35, 40, 41, 39) have attempted to relate the dispersion coefficient to hydraulic parameters so that the effect can be predicted without being measured using tracers. Usually the coefficient is considered to be an average over a tidal cycle, but other workers point out that intertidal effects need more consideration. The effect of a varying cross-sectional area or width (88, 48), varying velocity, as well as a varying dispersion coefficient (45) on the model as it applies to an estuary has also been studied. Leeds and Bybee (68) studied the effect of the various parameters using an electrical circuit analogue of the model. Hydraulic scale models, usually in conjunction with the prototype, have also been used to study dispersion (66,9).

When an impulse of tracer is applied to a stream, the resulting response has been observed to deviate from that predicted by the dispersion model. The most striking deviation that has been observed (35, 40, 46, 39, 110) is long tails indicating some kind of time delay mechanism.

A model, developed by Hays (52), accounts for this effect using a 'dead zone' concept where there is a slow rate interchange between these regions and the main flow. Thackston and Krenkel (111) studied this 'dead zone' concept in a laboratory flume using bricks along the bottom. They found that this had a significant effect on the measured dispersion coefficient. Patterson (86) proposes a model similar to Hays' except the dead volume is considered to be a stationary volume of ion exchange media.

While the dispersion model, a distributed parameter model, has been used so extensively, the lumped parameter or modular approach has only been used recently. Hoover and Arnoldi (54) divided the river under study into many sections and considered each section to be completely mixed (i.e. a CSTR). They also included an effective dispersion coefficient to allow mixing between sections. However, they did not experimentally verify the validity of this approach to the mixing phenomena. Another attempt to use the modular approach to mixing was carried out by Quirk and Eder (89) ; relatively slow moving areas were modelled with a PFTR whereas rapids and flow over dams were considered to be similar to a CSTR. They too did not verify these assumptions.

There are a few examples of other kinds of models in the literature. Thayer and Krutchkoff (113) used a probability approach to formulate a stochastic model for

the biochemical oxygen demand (BOD) and the dissolved oxygen (DO) in a stream. However, they did not explicitly consider the mixing phenomena. A slightly different use of the dispersion approach was proposed by Orlob et al (84); an estuary is divided into a network of ideal channels, as suggested by Shubinski et al (103), and the diffusion equation is applied to these channels.

2.3.2 System Response Determination

As mentioned in section 2.2.2, there are three usual ways of studying the mixing system: in the time domain, in the frequency domain using frequency response techniques, and in the Laplace domain. However, most workers concerned with applying models to the mixing phenomena in natural streams or estuaries have usually employed some form of a time response. Frequency response techniques have been used in applying the dispersed plug flow model to flow in a pipe (53) and in an extraction column (19), but have not been used to study natural systems. Use of the Laplace domain has also been limited to chemical reactor type systems.

The time domain response has been obtained using various kinds of inputs. Godfrey and Frederick (46) used a simulated plane source in their studies. A point source was used by Patterson and Gloyna (87) to measure both radial and longitudinal dispersion. There are also many examples (39, 40) of the use of an arbitrary closed pulse of dye as

an input for the purpose of measuring dispersion coefficients. These inputs have been applied to hydraulic scale models (9, 104, 81) as well as the prototype.

Cederwall and Hansen (16) have employed a unique method in studying their system. Their input consisted of two tracers with different decay rates. The tracers were continuously pumped into the receiving water at the effluent. After allowing steady state condition to be reached, samples were taken at various points in the bay. From the relative concentrations of the two dyes, they were able to calculate the average residence time and the amount of dilution. However, this does not determine the amount or kind of mixing that occurred between the effluent and the sample point.

If the dispersion model is being used, Glenne and Selleck (45) have demonstrated that the system may not need to be tested in the usual way. They suggest that concentration distributions of certain water quality parameters can be used to measure dispersion coefficients.

As pointed out in the preceeding section (2.3.1), many workers have attempted to predict dispersion coefficients rather than measure them. If this approach is used, the system response is not obtained, but extensive hydraulic data, such as velocity profiles, shear velocity and cross-sectioned area, are still required (35, 40, 39).

2.3.3 Parameter Evaluation

Since the most widely used model to describe the mixing phenomena in streams and estuaries has been the dispersed plug flow model, methods of evaluating the major parameter of this model (i.e. the dispersion coefficient) have been studied extensively.

Many attempts have been made to predict this parameter using either a theoretical formulation or some empirical relationship. Which ever method is used, the coefficient is related to some measurable hydraulic properties of the system. Fisher (40) and Hays and Krenkel (52) provide excellent reviews to this approach.

The time domain response has also been widely used for parameter evaluation. The use of the variance, or second moment, with respect to time (64, 87, 65) and with respect to distance (39) has been employed. Fisher (39) attempts to verify the parameter value chosen by a routing procedure; by application of the dispersion model (i.e. use of the predicted or measured dispersion coefficient and the average velocity) to an upstream time-concentration curve, the observed curve at a downstream point should result. Godfrey and Frederick (46) have shown how a Pearson Type III distribution can be fitted to the observed time-concentration curve; the dispersion coefficient is related to the properties of this type of curve. A statistical method based on the principle of maximum likelihood, involving only the

use of the first moment, to estimate the parameters of the dispersion equation has been suggested by Harris (49). It should be noted that the last two mentioned methods require that the input be an impulse. Thackston et al (110) suggests that the use of a non-linear least squares technique is the only reliable and accurate way of determining dispersion coefficients from time-concentration curves.

Other methods of evaluating the parameter of the dispersion model include the use of salinity profiles (47) and other water quality data (82).

Hays and Krenkel (52) suggest the use of the least squares procedure mentioned above to evaluate the parameter of the 'dead zone' model. However, in a recent paper, Thackston and Schnelle (112) describe how they have attempted to correlate the parameters of this model with the hydraulic properties of the natural stream instead of measuring them.

2.4 Evaluation of Previous Work

A natural stream can be viewed as a biochemical reactor. The state of mixing within such a reactor strongly affects most rate processes such as mass transfer and chemical reaction. In order to predict the extent of any chemical reaction, the mixing phenomenon must be adequately characterized. This has been long recognized in the chemical reactor engineering field as evidenced by the number of models that have been proposed and studied in an attempt to accurately define this phenomenon.

In the past there has been a tendency to use one analytical equation in the time domain to describe or model a natural stream or estuary. These models are usually derived to give the dissolved oxygen and biochemical oxygen demand profiles. In order to treat the complex system in such a manner, many simplifying assumptions are required. In some cases it is necessary to use unrealistic parameter values (i.e. quite different from measured or predicted values) in order to fit the observed dissolved oxygen profile. This would indicate: 1) that the model is incomplete (i.e. all the important factors have not been included), 2) that some of the assumptions used in deriving the model are too gross, or 3) that other parameter values are incorrect. The first two of the above three possible reasons for model failures are due to oversimplification. Most of the models in use today assume that the river acts as a plug flow vessel or PFTR. This may be a reasonable approximation in some cases but could lead to gross errors in other situations. It is desirable to study each factor or phenomenon separately and then to couple these together to give an overall model. The ability to study complex systems in detail, through the concept of sub-division, has come about because of sophisticated numerical techniques and the availability of the high speed computer.

The only model that has been used, to any extent, to study mixing in natural streams is the dispersion model or the modified dispersion model employing the 'dead zone' concept.

These distributed parameter models may be applicable to many streams but are not flexible enough to handle all the states of mixing that can occur in nature.

A far more flexible approach would be to use a lumped parameter model involving a network of CSTRs and PFTRs (described in section 1.3) to model the natural system. These lumped parameter models have been used extensively to model chemical reactors. They can be used to characterize a wide range of mixing states including complete mixing, plug flow, short circuiting and situations where relatively stagnant regions are significant. Reaction conversion prediction for any given network is simple and direct. This latter feature is not shared by the distributed parameter models for any reaction that is other than first order.

Use of a distributed parameter model implies that one can predict concentrations at any point within the system; a lumped parameter model can only be used to predict a concentration at one point in the system (i.e. the output). However, when a particular section of a stream is being studied the data for either type of model is collected in the same manner (i.e. at the upstream and downstream ends of the section) and represents the overall effect of the various mixing processes occurring between the two points. To then use the distributed parameter model to predict anything within the section, between these two points, would be questionable. Furthermore, it is often only required to

know concentrations at specific points such as the nearest town downstream from a particular effluent; a lumped parameter model provides this kind of information.

The use of frequency response techniques appears to be the best procedure to use in testing the system. The major advantage of this technique is that almost any type of input (eg. impulses, steps, pulses, random signals) can be employed. Many time domain techniques require the use of ideal inputs which are difficult to simulate in a natural stream. The Laplace domain technique also has this same advantage, but, as pointed out in the literature review, the errors associated with this technique have not been thoroughly investigated.

It also seems clear, that the non-linear least squares procedure, or an equivalent optimization procedure would be best for parameter evaluation. Not only do these methods provide the statistically best values of the parameters but also give an indication of how well the model fits the data.

To summarize, a review of the previous work indicates that mixing is significant, and that the use of the modular approach, frequency response techniques and least squares parameter estimation appears to be the best way to model this phenomenon.

CHAPTER 3

3. THEORETICAL BACKGROUND AND METHOD OF ANALYSIS

3.1 Introduction

Mixing, although a subsystem to many other more complex systems, can be studied as a dynamic system in itself. Experimental procedures for the development of mathematical models to characterize the dynamics are based on the concept that a system can be described by a differential equation:

$$a_n \frac{d^n y(t)}{dt^n} + \ldots + a_1 \frac{dy(t)}{dt} + a_o y(t) =$$

$$b_m \frac{d^m x(t)}{dt^m} + \ldots + b_1 \frac{dx(t)}{dt} + b_o x(t) \qquad 3.1\text{-}1$$

where y(t) is the response or output as a function of time, x(t) is the forcing function or input as a function of time, $\frac{d}{dt}$ is the differential operator and the a's and b's are system parameters. Equation 3.1-1 can be written in a simpler form by defining p to be the differential operator. Thus

$$y(t) = G(p)\, x(t) \qquad 3.1\text{-}2$$

where $$G(p) = \frac{a_n p^n + \ldots + a_1 p + a_o}{b_m p^m + \ldots + b_1 p + b_o}$$

The system can be experimentally analysed or tested using either periodic, non-periodic or random inputs. The theoretical model is then compared to the experimental response and the system parameters are then evaluated.

There are many advantages to be gained by modelling in the Laplace or frequency domain as opposed to the time domain. Often the differential equations describing the system cannot be solved analytically in the time domain. However, recalling that the Laplace transform F(s) of a function f (t) is defined as

$$F(s) = \int_0^{\infty} f(t)e^{-st}dt \qquad 3.1\text{-}3$$

and assuming all initial conditions of the system to be zero, equation 3.1-2 can be transformed by substituting the Laplace variable s for p, Y(s) for y(t) and X(s) for x(t). Therefore, equation 3.1-2 becomes

$$Y(s) = G(s)\ X(s)$$

$$\text{or} \qquad G(s) = \frac{Y(s)}{X(s)} \qquad 3.1\text{-}4$$

Equation 3.1-4 can be used to obtain the frequency response by simply substituting jw for s, i.e.

$$G(jw) = \frac{Y(jw)}{X(jw)} \qquad 3.1\text{-}5$$

where w is the frequency and $j = \sqrt{-1}$. G(s) or G(jw) is called the transfer function of the system. Now the describing differential equation has been replaced by an algebraic equation; this is one of the major advantages. It should also be noted that since the transfer function is equal to the Laplace transform of the output over the Laplace transform of the input (under zero initial conditions), almost any input, along with its corresponding output, can be used to describe the system. These advantages make this approach very attractive.

If the frequency domain is to be used to fit the model to the real system, the experimental frequency response of the system must be obtained. When the input x(t) is varied sinusoidally at a frequency w, the output will also vary sinusoidally at the same frequency if the system is linear. However, the output may have a different amplitude and there may exist a phase difference between the two waveforms. This amplitude or magnitude ratio (M.R.) and phase shift are measured as a function of frequency. In order to describe the experimental frequency response adequately, a number of sinusoidal tests must be performed. Not only must a pure sine wave be generated but each test must be run until the transient response of the system has died out and the output is at steady state. This is a severe disadvantage in most cases.

Fortunately, the same frequency response can be obtained from one test. Theoretically an arbitrary closed pulse contains an infinite frequency spectrum, i.e. the pulse can be represented analytically by a Fourier transform. The frequency spectrum of a pulse varies with the shape and width of the pulse, but if an input pulse is chosen properly the system will be excited well enough at the important frequencies to give a good representation of the frequency response. Using similar principles to those employed in pulse testing, steps and random inputs can also be used.

The rest of this chapter will discuss in detail modelling using the modular approach in the frequency domain, obtaining the experimental frequency response using pulse testing, and how the model is fitted to the experimental response.

3.2 The Modular Approach to Modelling in the Frequency Domain

For the modular approach, the real reactor (here a natural stream) is simulated by a network of ideal flow regions. The two extremes in mixing, the PFTR and the CSTR (as described in the introduction (Chapter 1) and in further detail in Levenspiel (71)) are the ideal flow elements or mixing modes used. Many models have been proposed to approximate physical situations such as parallel flow (75), shortcircuiting (17, 71), reflux or backmixing (94, 102, 61), recycle (93), dead or stagnant regions with interchange with the main stream (14, 1) and cross flow (71). Some of these are illustrated in Figure 3-1.

Figure 3-1 Model Examples

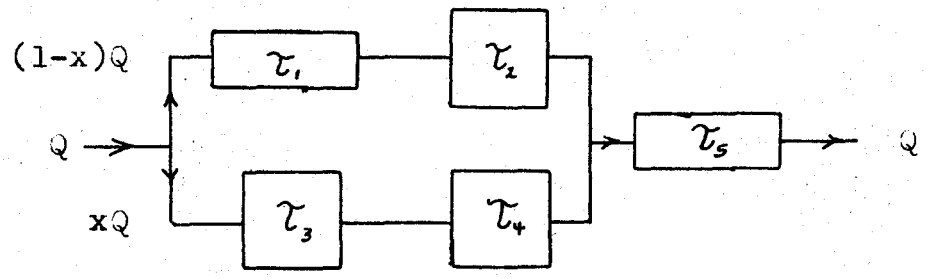

a. Parallel Flow

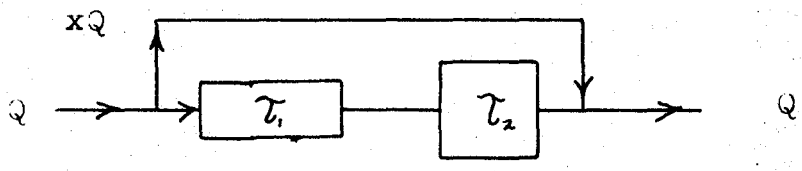

b. Short Circuiting

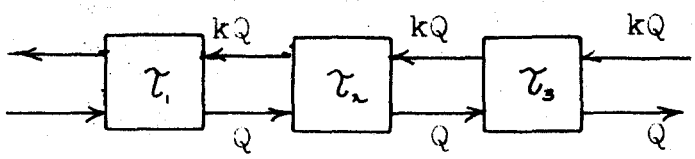

c. Reflux or Backmixing

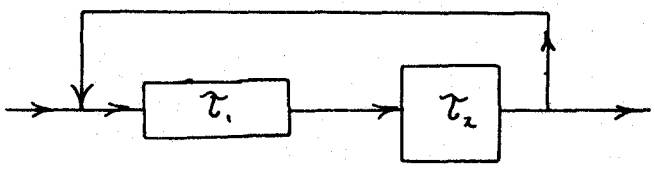

d. Recycle

Figure 3-1 (Cont.)

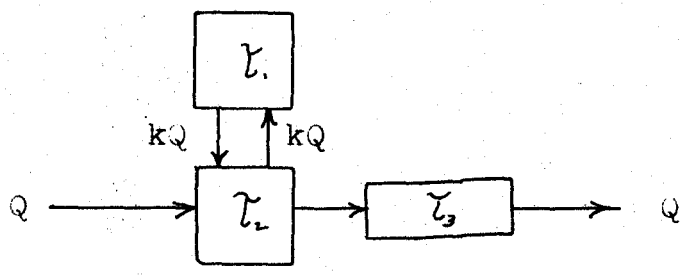

e. Stagnant Zones

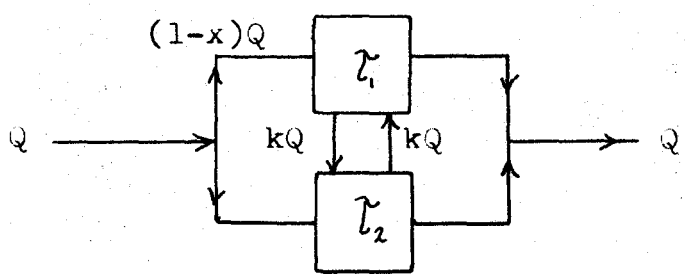

f. Cross Flow

Key:

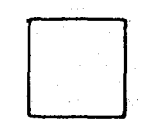

CSTR

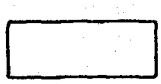

PFTR

τ Residence Time

Q Flowrate

Each element or, in some cases, group of elements in the network has a transfer function. If the transfer function is expressed in the Laplace or frequency domain, the overall transfer function of the network can be found by a simple combination of the individual functions within the network as outlined in most texts on control theory (28). For series networks the system transfer function is simply the product of the individual functions. Melnyk (75) describes how parallel flow paths are handled.

The transfer function for each element or group of elements is derived from the describing differential equation. The differential equation, on the other hand, is derived by taking a mass balance around the element. The transfer functions for a CSTR, PFTR and the model proposed by Adler and Horvoka (1) (hereafter called Stagnant Zone Model) are derived in Appendix C.

3.3 Analysis of the Experimental Data in the Frequency Domain

Unless sinusoidal testing is done, the response of the system to an arbitrary input must be transformed into the frequency domain, using a Fourier transform, for comparison with the model transfer function.

The forcing function for dynamic testing can be a step, an arbitrary pulse or a random signal. Methods of obtaining the Fourier transform of the data for the above inputs and their corresponding outputs have been outlined by many in the past few decades (4, 29, 70, 80, 51, 100, 2, 31, 55, 95). An excellent review of all the major methods is

given by Murrell, Pike and Smith (78). Most of the methods are numerical, i.e. developed for use on a digital computer, but Teasdale (109) shows how the frequency response can be obtained graphically if one of three ideal inputs are used, and Reynolds (109) has developed a machine to perform the Fourier transform.

A numerical method of obtaining the frequency response from pulse testing will be outlined in detail here since the major part of the experimental work employed this type of input. Two major studies of pulse testing were performed by Clements (19) and Dreifke (30). Recalling section 3.1, the transfer function of a system is, for any set of input-output functions,

$$G(s) = \frac{Y(s)}{X(s)} = \frac{\int_0^\infty y(t)e^{-st}dt}{\int_0^\infty x(t)e^{-st}dt} \qquad 3.3\text{-}1$$

(with zero initial conditions) or in terms of frequency when jw is substituted for s,

$$G(jw) = \frac{\int_0^\infty y(t)e^{-jwt}dt}{\int_0^\infty x(t)e^{-jwt}dt} \qquad 3.3\text{-}2$$

If the input and output are measured experimentally as illustrated in Figure 3-2, the integrals in equation 3.3-2 must be evaluated numerically. Applying the identity $e^{-jwt} = \cos(wt) - j\sin(wt)$ to the integrals we can write

$$G(jw) = \frac{\int_0^{T_y} y(t)\cos(wt)dt - j\int_0^{T_y} y(t)\sin(wt)dt}{\int_0^{T_x} x(t)\cos(wt)dt - j\int_0^{T_x} x(t)\sin(wt)dt} \qquad 3.3\text{-}3$$

where the infinite limits have been replaced by the duration of the closed pulses, i.e. Tx = duration of input pulse, and Ty = duration of output pulse . If

$$A = \int_0^{T_y} y(t)\cos(wt)dt \ , \qquad 3.3\text{-}4$$

$$B = \int_0^{T_y} y(t)\sin(wt)dt \ , \qquad 3.3\text{-}5$$

$$C = \int_0^{T_x} x(t)\cos(wt)dt \ , \qquad 3.3\text{-}6$$

and $$D = \int_0^{T_x} x(t)\sin(wt)dt \ , \qquad 3.3\text{-}7$$

we can write equation 3.3-3 as

$$G(jw) = \frac{A - jB}{C - jD} = \frac{AC + BD}{C^2 + D^2} + j\,\frac{AD - BC}{C^2 + D^2} \qquad 3.3\text{-}8$$

Figure 3-2 Typical Time-Concentration Curves For Pulse Runs

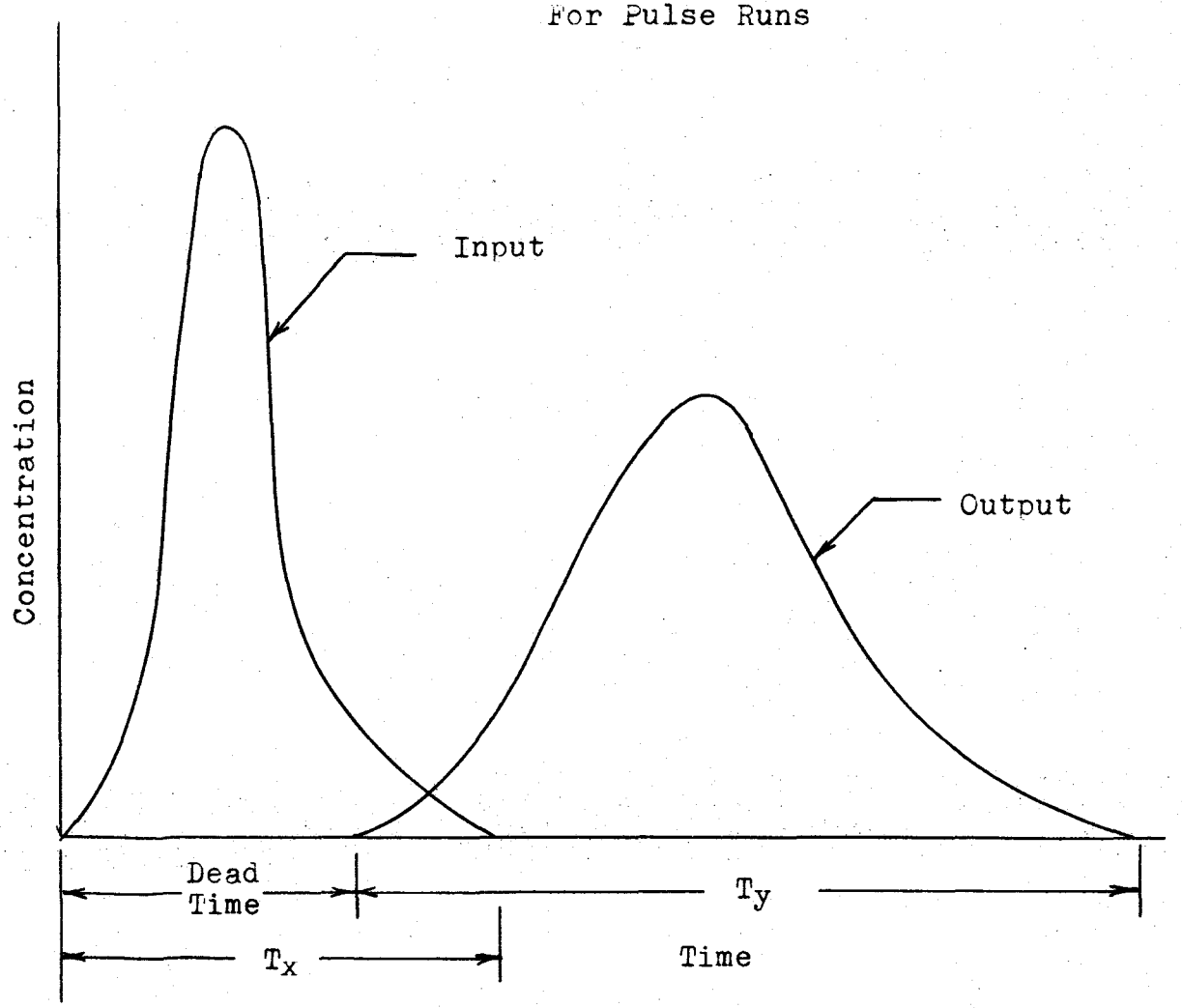

Therefore,

$$Re(w) = \frac{AC + BD}{C^2 + D^2} \qquad 3.3\text{-}9$$

and

$$Im(w) = \frac{AD - BC}{C^2 + D^2} \qquad 3.3\text{-}10$$

where Re(w) is the real part and Im(w) is the imaginary part of the complex number G(jw). It can also be written in another complex form as

$$G(jw) = MR(w)e^{-jPA(w)} \qquad 3.3\text{-}11$$

where MR(w) is called the magnitude ratio and PA(w) is called the phase angle. Comparing equation 3.3-11 to equation 3.3-3 and using the rules of complex algebra

$$MR(w) = \sqrt{Re^2(w) + Im^2(w)} \qquad 3.3\text{-}12$$

and

$$PA(w) = \tan^{-1} \frac{Im(w)}{Re(w)} \qquad 3.3\text{-}13$$

Evaluation of integrals A, B, C, D using ordinary quadrature formulae such as the trapezoidal rule or Simpson's rule, breaks down at high frequencies making the calculations completely useless. This difficulty has been removed by

some special approximation methods. A small portion of the input or output curve is approximated by some function and this expression is then multiplied by sin(wt) or cos(wt). The resulting equation is then integrated analytically and this represents the area under one segment of the product curve. The total integral is the sum of all such segments between the limits of integration. Large values of w do not introduce error into the quadrature since the trigonometric integration is done analytically. Several approximations to the pulse curve are discussed by Clements (34). The most popular method is the one outlined by Filon (42).

Filon's quadrature formula for the integrals $\int_a^b f(t)\sin(wt)$ and $\int_a^b f(t)\cos(wt)$ is based on a parabolic approximation to segments of the time curve. To apply his formula the curve is divided into an odd number, $2n+1$, of points at intervals Δt. These points are denoted by $I_0, I_1, I_2, \ldots I_{2n}$ where $I_0 = f(a)\sin(wa)$ and $I_{2n} = f(b)\sin(wb)$. Let

$$S_{2n} = \tfrac{1}{2}I_0 + I_2 + \ldots + I_{2n-2} + \tfrac{1}{2}I_{2n}, \qquad 3.3\text{-}14$$

$$S_{2n-1} = I_1 + I_3 + \ldots + I_{2n-1}, \qquad 3.3\text{-}15$$

$$\theta = w\Delta t, \qquad 3.3\text{-}16$$

$$\alpha = \frac{1}{\theta} + \frac{\sin 2\theta}{2\theta^2} - 2\,\frac{\sin^2\theta}{\theta^3}, \qquad 3.3\text{-}17$$

$$\beta = 2\left[\frac{\cos^2\theta + 1}{\theta^2} - \frac{\sin 2\theta}{\theta^3}\right], \qquad 3.3\text{-}18$$

$$\gamma = 4\left[\frac{\sin\theta}{\theta^3} - \frac{\cos\theta}{\theta^2}\right], \qquad 3.3\text{-}19$$

and then

$$\int_a^b f(t)\sin(wt)dt \approx \Delta t\Big\{\alpha\big[f(a)\cos(wa) - f(b)\cos(wb)\big] + \beta S_{2n} + \gamma S_{2n-1}\Big\}. \qquad 3.3\text{-}20$$

Now denoting I_0 by f(a)cos(wa) and I_{2n} by f(b)cos(wb),

$$\int_a^b f(t)\cos(wt)dt \approx \Delta t\Big\{\alpha\big[f(a)\cos(wa+\pi/2) - f(b)\cos(wb+\pi/2)\big] + \beta S_{2n} + \gamma S_{2n-1}\Big\}, \qquad 3.3\text{-}21$$

When θ is small ($<$ .35 rad.) Taylor series expansion of equation 3.3-17-3.3-14 must be used to prevent a loss of significant figures (see Appendix D).

It should be noted that the same technique can be used when an ideal impulse input is assumed and when a step (not necessarily ideal) is employed.

A computer program was written to perform the above calculations. The program will accept two different time increments for each pulse; the input can be an assumed impulse, a step or an arbitrary pulse; the integrals will be calculated using both the trapezoidal rule and Filon's method; the program converts the raw data to concentration vs. time data before the transformation is calculated; and the program output consists of the magnitude ratio, phase shift (with and without dead time), real and imaginary parts of the transfer function, and the frequency content of both the input and output pulse (defined below), at selected frequencies. A detailed description and listing of the program is given in Appendix D.

Care must be taken, in going from one domain to another, to minimize those factors which could cause errors in the transformation. The extent to which a system responds to a certain frequency depends on the frequency content of the input pulse. The normalized frequency content of a pulse is defined as

$$S_n(w) = \frac{\int_0^T f(t)e^{-jwt}dt}{\int_0^T f(t)e^{-j(0)}dt} \qquad 3.3\text{-}22$$

and can be computed numerically by

$$S_{xn}(w) = \frac{(\sqrt{C^2 + D^2})_w}{(C)_{w=0}} \qquad 3.3\text{-}23$$

for the input pulse and

$$S_{yn}(w) = \frac{(\sqrt{A^2 + B^2})_w}{(A)_{w=0}} \qquad 3.3\text{-}24$$

for the output pulse. The input frequency content depends on the shape and width of the pulse (19, 30). A pulse should be chosen so that it has the greatest frequency content without distorting the system. On the other hand, the output pulse frequency content indicates the degree to which the system responded to the input. Hays (51) suggests that when this value approaches the experimental error, the reliability of the calculation degenerates. The effect of truncating the output pulse before it has reached zero has been studied by Hougen and Walsh (55), Dreifke (33) and Clements (19) and they have found that the error is negligible unless there is severe truncation. Clements (19) also found that the data from the recorded pulse curves need only be read to two or three significant figures without affecting the accuracy of the computations. Details of how these sources of errors were dealt with in this work will be discussed later.

3.4 Graphical Representation of Model and Experimental Data

The system transfer function can be written in complex number form

$$G(jw) = Re(w) + jIm(w) \quad , \qquad 3.4\text{-}1$$

the complex polar form

$$G(jw) = MR(w)e^{-jPA(w)} \quad , \qquad 3.4\text{-}2$$

or as a polynomial

$$G(jw) = \frac{a_n(jw)^n + a_{n-1}(jw)^{n-1} + \ldots + a_o}{b_m(jw)^m + b_{m-1}(jw)^{m-1} + \ldots + b_o} \qquad 3.3\text{-}3$$

The transfer function can also be presented graphically in three ways:

(a) as a curve on a polar plot on which each point is represented by a vector whose magnitude is equal to MR(w) and whose direction is equal to the phase angle PA(w). This can also be considered as a plot of Re(w) vs. Im(w),

(b) the magnitude ratio in decibels ($20 \times \log_{10} MR(w)$) is plotted against the phase angle (PA(w))in degrees, or,

(c) a Bode plot, where the magnitude ratio (in decibels) and the phase angle are plotted against frequency.

The Bode plot has been most popular since it can sometimes be used to evaluate parameters or at least give an indication of the mathematical form of the system.

One principle advantage of the Bode diagram can be realized when the overall transfer function of a system is the simple product of component transfer functions. The phase angle vs. frequency plot for the system is just the sum of the individual phase angle plots since in the multiplication of two complex numbers, their associated angles are simply added together. Since the logarithims of the magnitude ratios are plotted instead of the ratios themselves, the magnitude ratios (in decibels) are also additive. These features can be applied to a series network of PFTRs and CSTRs as described in section 3.2.

The amplitude ratio curve of a system can be represented by straight line segments which have a slope of an integer number times 20 decibels/decade. The numerator and denominator of the polynomial form of the transfer function (equation 3.4-3) can be factored. These factors are called the zeros and poles respectively. A zero would be drawn as straight line of slope + 20 decibels/decade and a pole as a line with a slope of -20 decibels/decade. The zeros and poles start at a point on the Bode plot equal to the root value of the appropriate factor.

The parameters of complex flow networks cannot always be evaluated graphically from Bode diagrams.

However, the magnitude of the slope of the amplitude ratio vs. frequency plot at high frequencies is always indicative of the relative order of the numerator and denominator polynomials in equation 3.4-3 (i.e. if there are n poles and m zeros, the slope at high frequencies will be (m - n) X 20 decibels/decade).

Only features relevant to this work have been discussed here. A fuller treatment of parameter evaluation from Bode diagrams is given by Murrill, Pike and Smith (78).

To illustrate some of the points discussed above, the Bode plots for the two ideal elements, the PFTR and the CSTR, are shown in Figure 3-3. The transfer function of a CSTR is $^{1}/(1 + jw\tau)$ where τ is the residence time. Noting that there is one pole and no zeros, the amplitude ratio curve can be represented by two straight line segments, one of zero slope and the other of slope - 20 decibels/decade. The frequency at which the two lines intersect is called the break point or break frequency and is equal to the reciprocal of the residence time. The phase angle curve for the CSTR has an "S" shape, approaching -90° at high frequencies. The transfer function of a PFTR is $e^{-jw\tau_p}$ where τ_p is its residence time. It can be seen that the magnitude ratio is equal to one for all frequencies and that the phase angle increases (negatively) with frequency.

Figure 3-3 Bode Diagram of an Ideal CSTR

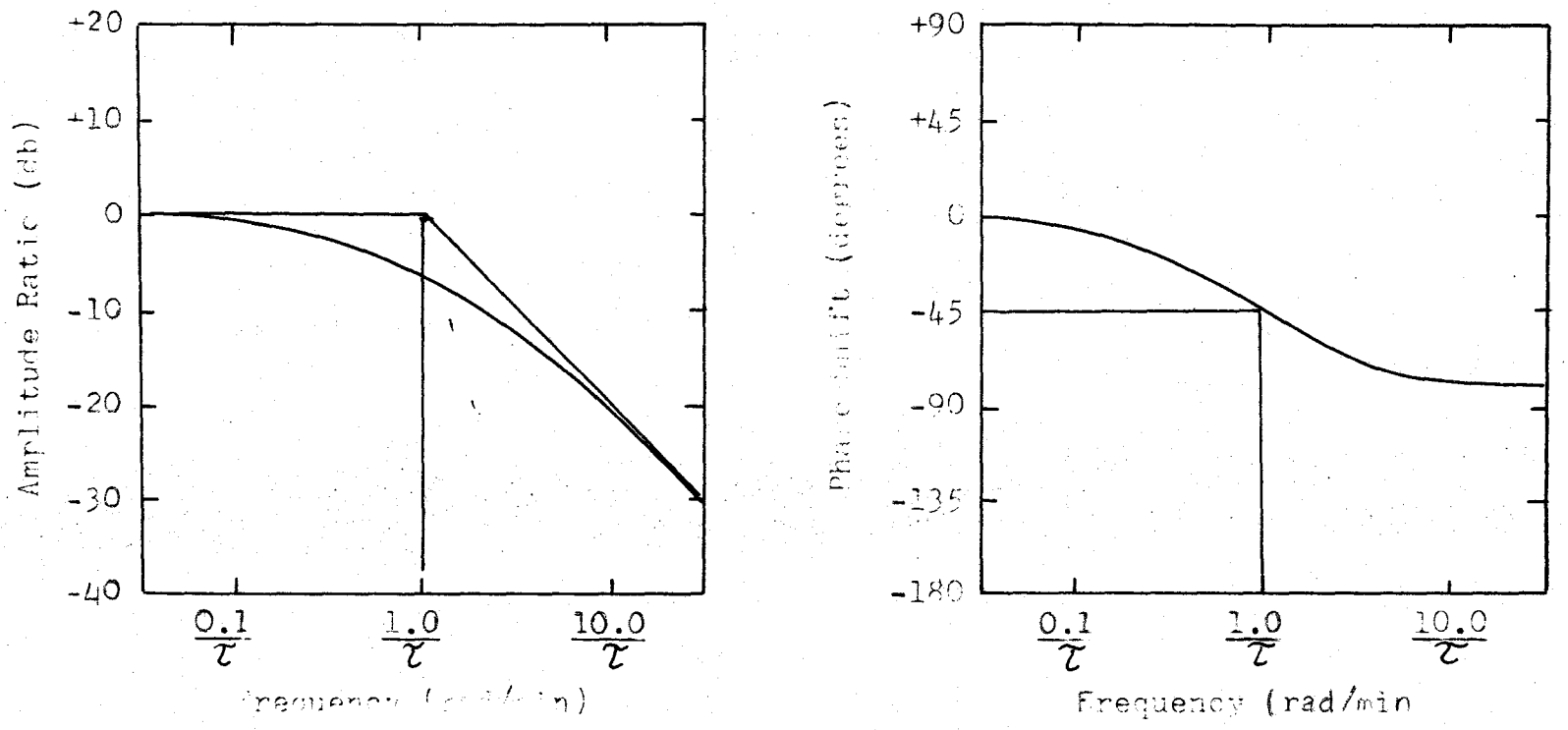

Figure 3-3 (Cont.) Bode Diagram of Ideal PFMR

3.5 Model Selection and Parameter Evaluation

Modelling involves two steps: formulation of a mathematical description of the system, and the evaluation of the statistically best values of the parameters of the mathematical relationship.

The equations describing the system can also be derived in two ways. The black box approach involves fitting the output to the input by some expression, usually a polynomial, without any reference to what is going on within the system. On the other hand, where the system can be examined, the dominant mechanisms causing the phenomena under study should be identified. Some of the mechanisms that could occur in a natural stream are: 'dead zones' or relatively stagnant regions with a slow interchange with the main flow, short circuiting, and parallel flow. Using the modular approach, several possible models are then synthesized using the basic elements of a CSTR and a PFTR, combined in such a way as to approximate the real mixing mechanisms; this has been further described and illustrated in section 3.2.

To evaluate the parameters of the proposed models the theoretical transfer functions are fitted to the experimental data using the principle of least squares. The sum of the squares of the deviations between the predicted and observed curves is used as a measure of deviation and is therefore minimized. In the time domain

this function is written as

$$\phi = \int_{t_a}^{t_b} (y_o(t) - y_p(t))^2 dt \qquad 3.5\text{-}1$$

where t_a to t_b is the region of interest of the independent variable t over which the deviation between $y_o(t)$, the observed results, and $y_p(t)$, the predicted results, is to be compared. It has been shown by Hays (51) how to derive the expression for ϕ in the frequency domain. Defining the deviation to be

$$d(t) = y_o(t) - y_p(t) \qquad 3.5\text{-}2$$

and assuming $d(t) = 0$ for $t < t_a$ and $t > t_b$ we can write

$$\phi = \int_0^{\infty} (d(t))^2 dt = \int_{t_a}^{t_b} (d(t))^2 dt \qquad 3.5\text{-}3$$

Parseval's Theorem states that

$$\int_0^{\infty} (d(t))^2 dt = \frac{1}{\pi} \int_0^{\infty} |D(jw)|^2 dw \qquad 3.5\text{-}4$$

where D(jw) is the Fourier transform of d(t). We can also write D(jw) as

$$D(jw) = Y_o(jw) - Y_p(jw) \qquad 3.5\text{-}5$$

or

$$D(jw) = ((Re_o(w) + j\ Im_o(w)) - (Re_p(w) + j\ Im_p(w))) \qquad 3.5\text{-}6$$

where Re(w) and Im(w) are the real and imaginary parts as before. Substituting equation 3.5-6 into 3.5-4 we have

$$\phi = \frac{1}{\pi}\int_0^{\infty}\left\{(Re_o(w) - Re_p(w))^2 + (Im_o(w) - Im_p(w))^2\right\}dw \qquad 3.5\text{-}7$$

It can be noted that where the deviation is based on the square of a scaler in the time domain, it is based on the square of the vectorial distance between predicted and observed results in the frequency domain.

Instead of using the integral form of ϕ as in 3.5-7, the function to be minimized could be weighted to a specific region by defining ϕ to be the summation of vectorial deviation of discrete points and selecting more points in that region. This was done in this work as will be described later.

Any non-linear least squares procedure could be used to minimize ϕ. The general optimization procedure outlined by Rosenbrock (96) was used here.

After all the proposed models have been fitted to one set of experimental data the best model must be chosen from these. When two proposed models have the same number of parameters the minimized sum of squares can be compared directly. The lower the sum of squares the better the model fits the data. However, this can only be used as an indication of a better model and final choice depends on other fundamental considerations. For example, if one model is derived on the basis of an approximation of the physical situation and the other is merely a polynomial curve fit, then the former should be the one chosen even though it may give a slightly higher sum of squares. If two proposed models have a different number of parameters, an F test can be used. Although this may not be strictly correct, since the models are non-linear, it will serve as an indication.

CHAPTER 4

4. EXPERIMENTATION

4.1 Introduction

This chapter describes the experimentation undertaken to illustrate the practical application of this modelling approach. Included are a description of the stream where the work was undertaken, a section dealing with the tracer selection, a description of the experimental apparatus and details of the actual tests performed.

4.2 Ancaster Creek

The experimental aspects of this study were carried out on a small creek flowing through the West Campus of McMaster University. This spring fed creek is known by several names: Cold Water Creek, Clear Water Creek and the most common being Ancaster Creek. The creek is a tributary of Spencer Creek which flows through Coote's Paradise into Burlington Bay at the west end of Lake Ontario. Figure 4-1 shows the creek with its drainage basin of approximately nine square miles.

The section where all the dye runs were conducted is approximately 2,000 feet in length and is shown in detail in Figure 4-2. The gradient in this reach is about 1 foot in every 1,200 feet. Through the campus a flood plain has been constructed to handle 7,200 c.f.s., but the usual flow ranges from 1 c.f.s. in August to about 50 c.f.s. during spring runoff. The flow in the stream responds rapidly to

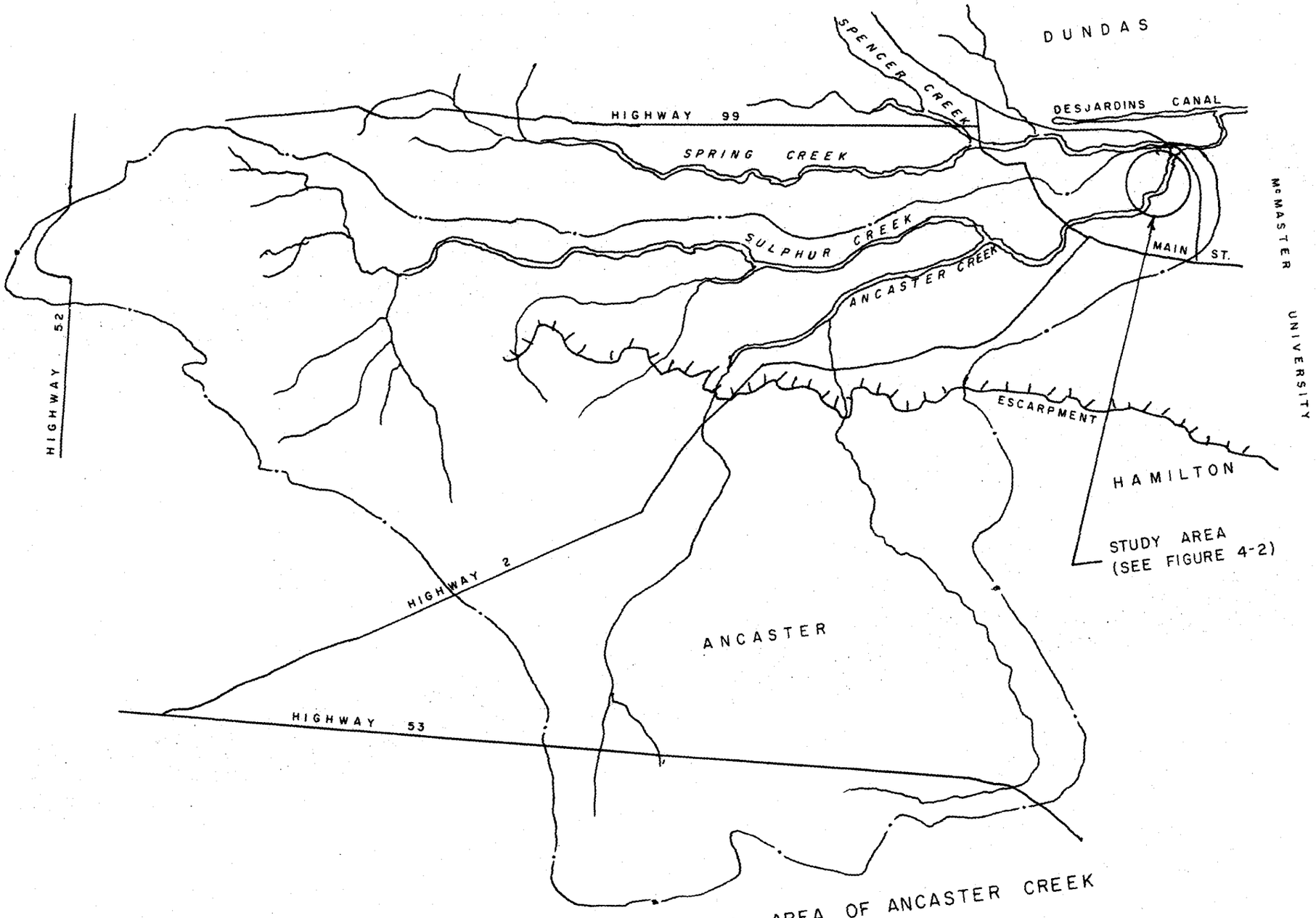

FIGURE 4-1 DRAINAGE AREA OF ANCASTER CREEK

0 0.5 1.0

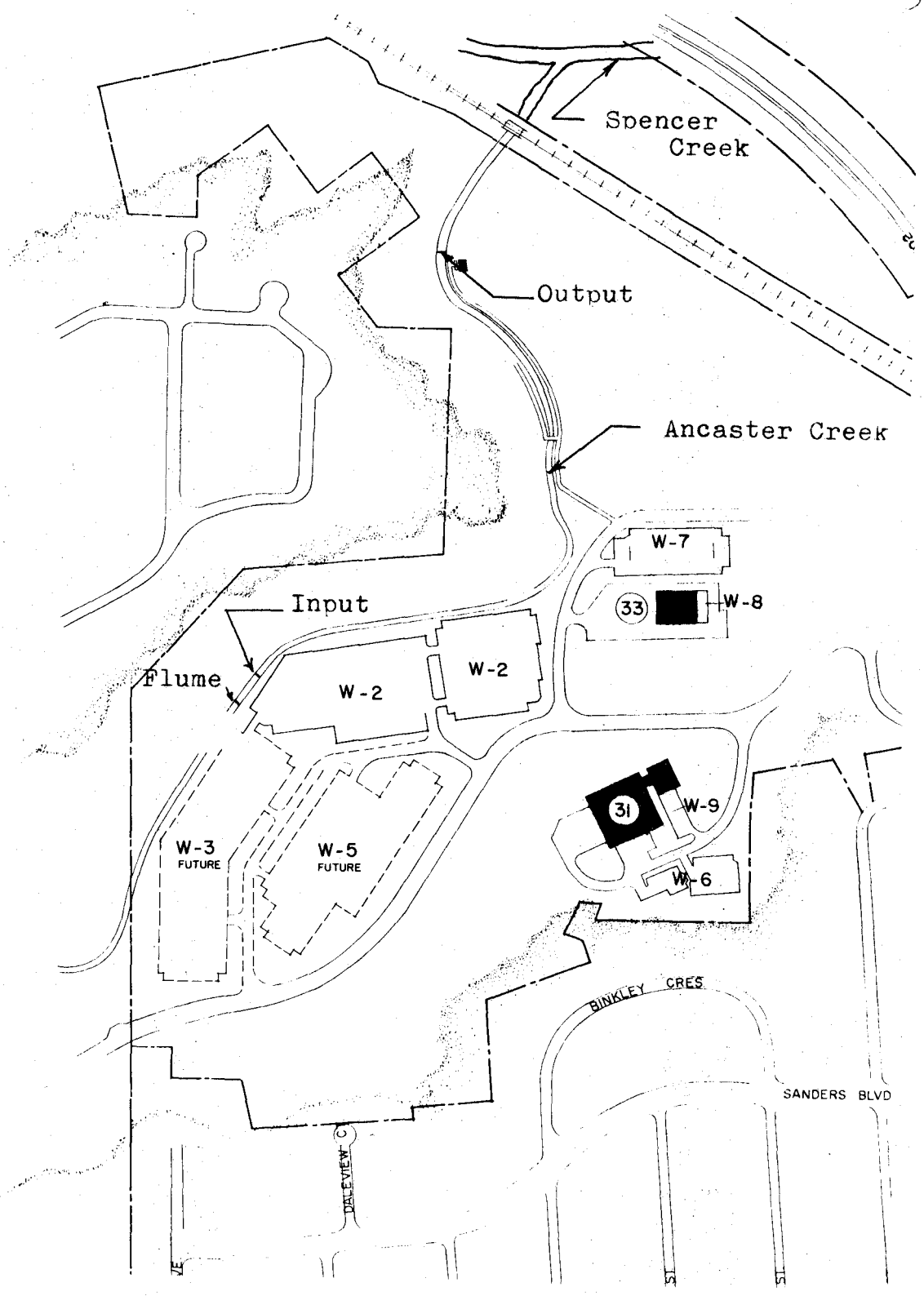

Figure 4-2 Section of Creek Modelled

a rainfall, the flow sometimes increasing fourfold. The water quality is greatly impaired because of the large number of storm sewers and septic tanks entering the creek upstream.

4.3 Selection of Tracer

An ideal tracer to be used in this type of investigation would possess the following characteristics:

(a) the tracer should be stable in a natural environment, i.e. not affected by light, bacteria, pH, temperature, algae, adsorption, or by chemicals such as chlorine that might be present in the system;

(b) the tracer should be non-toxic at levels employed;

(c) the tracer should be easily measured in situ, detectable at low concentrations, and measured accurately over the whole range used without requiring large quantities;

(d) the tracer should not have a large or variable background; and

(e) the tracer should be inexpensive, easily handled and water soluble.

A search of the literature was undertaken to find a tracer that would satisfy all or most of the above criteria.

There has been an extensive use of tracers in the field of Sanitary Engineering. They have been employed in hydrological studies such as time-of-travel measurements (13, 121), dispersion studies (25, 40, 46, 56, 81, 99, 104) and discharge measurements (10, 57, 58, 60). The hydraulic characteristics of a primary clarifier (3), aeration

tanks (115, 77, 99), settling basins (79), and chlorine contact tanks (97) have also been studied using tracers. Many good reviews of tracers, listing advantages and disadvantages as well as comparison with other tracers, are available in the literature (27, 37, 42, 120, 5).

Of the three generally used, i.e. various salts, fluorescent dyes, and radioactive tracers, the least desirable method seems to be the use of a salt where the ionic concentration is measured by conductivity. The disadvantage of this tracer in a natural system results from, the need for large quantities of salt solution to obtain detectable concentration, large and possibly variable background and possible density effects.

Archibald (5) discusses the use of radioactive tracers for various flow tests. He concludes that the technique is far superior to any dye or salt techniques. The superior characteristic of the use of radiotracers is the ability to detect minute quantities at a very high accuracy. However, there is an associated high cost and possible health hazard. It has been pointed out by Frederick and Godfrey (43) that unless there are no finite boundaries within 3 to 4 feet of any side of the crystal used in radiation detection, the sensing apparatus must be calibrated in situ; this limits their use to large bodies of water unless relative readings are satisfactory.

The dye techniques, compared by Archibald (5) to radiotracers, have been greatly improved since 1949.

Feuerstein and Sellach (37) have studied three widely used fluorescent dyes: Rhodamine B, Pontacyl Brilliant Pink B and fluorescein. The effect of temperature, salinity, pH value, background level, and turbidity or suspended solid concentration, on the analytical determination of concentration was ascertained. Wilson has written a manual on Fluorometric Procedures for Dye Tracing (120) and includes in his comparison of dyes, Rhodamine WT, as well as those mentioned above. A manual on fluorometry published by C. K. Turner Associates (42) mentions that Rhodamine WT is favoured over other fluorescent dyes by those engaged in water tracing studies in recent years.

Fluorometric techniques have developed to such an extent in the past ten years that they are now more generally favourable than radioactive techniques. This may not be the case where there is a need for very accurate measurements and where calibration can be done in situ, or where large bodies of water are being studied. Of all the fluorescent dyes available, Rhodanine WT and Pontacyl Brilliant Pink appear to be the best. The only important difference between these two is the cost and therefore, Rhodanine WT, being the less expensive, was chosen for this study.

Although the properties of Rhodamine WT have not been formally reported, the information is available in many published reviews of various dye applications (12, 60, 99, 42, 120). The properties of this dye are listed below in the same order as those for an ideal tracer given at the

beginning of the section.

(a) The dye is slightly less adsorbed, on most materials, than Pontacyl Brilliant Pink and far less than Rhodamine B. It can be considered negligible in short reaches of a few miles. The concentration is affected by sunlight but the decay rate is believed (42) to be small enough to be ignored for the period the dye was exposed in this study. The concentration has been found to be independent of pH between the values of 5-10 but is very sensitive to temperature. The dependence on temperature has been measured (37, 15) and one can easily correct for this factor.

(b) The tolerance level for human consumption of the dye has been set at .75 mg/day which is equivalent to 2½ qts. at 370 ppb and at that concentration the dye is a brilliant red.

(c) The concentration of the dye can be easily and continuously measured using a flow-through fluorometer. It can be detected at concentrations as low as 2 ppb and the fluorescent intensity is linear with concentration in the range employed.

(d) The background from natural sources was found to be small and easily corrected for. The indirect form of background or interference due to turbidity is appreciable at high concentrations of suspended solids but can be ignored at the levels found in the stream studied.

(e) The dye is available as a 20% solution and is relatively inexpensive; the cost of the dye for this total project was less than $5.

It can be seen that Rhodamine WT fulfills many of the criteria of an ideal tracer for this work.

4.4 Flow Measurement

A Parshall flume was constructed and placed upstream of the test section as shown on Figure 4-2. The purpose of the flume was to give an indication of the magnitude of the flow during a test run as well as to indicate the variation occurring during the longer sine runs. For runs performed on the same day, the flume readings provided a check on the flow calculations made by another method to be described later. The hydraulic jump at the exit to the flume provided an excellent location for tracer injection so that the dye would be uniformly mixed across the cross-section of the creek.

The flume was a standard Parshall flume with a 1.5 ft. throat and was constructed with 3/4 inch plywood. The stream was dammed off by two walls of sand bags, forcing the flow through the flume. Due to the fact that the walls were not perfectly water-tight, and that the one end of the flume tended to settle over time, the readings could not be used for absolute flow calculations but only for comparison purposes.

4.5 Sampling Apparatus

The creek was sampled at two locations downstream of the flume so that the dye concentration could be continuously monitored as it passed each site. The location nearest the flume is considered as the input to the system and the other as the output. The sample was pumped through the flow-through door of the fluorometer using a self-priming pump. In order to obtain a representative sample for the whole cross-section, the creek was sampled at four evenly spaced points. These 1/4 inch I.D. polyethylene lines were held in place by a framework of aluminum rods set into the creek bed.

It is usually suggested, in manuals of fluorometric procedures, that the sample be drawn through the fluorometer as opposed to being pumped through. This is to prevent possible interference which can be formed as the sample passes through the pump and by bubbles, which can give erroneous readings. The pumps used did not have enough suction head to do this. However, it was found that if the flow was limited to about 500 ml./min., by means of a valve, no bubbles were formed. Each of the four sample lines were also valved to ensure that each sampled the same amount.

The sampling apparatus is shown on Figure 4-3. A detailed list of the tubing, valves, pumps etc. used is given in Appendix A.

Figure 4-3 Sampling Apparatus

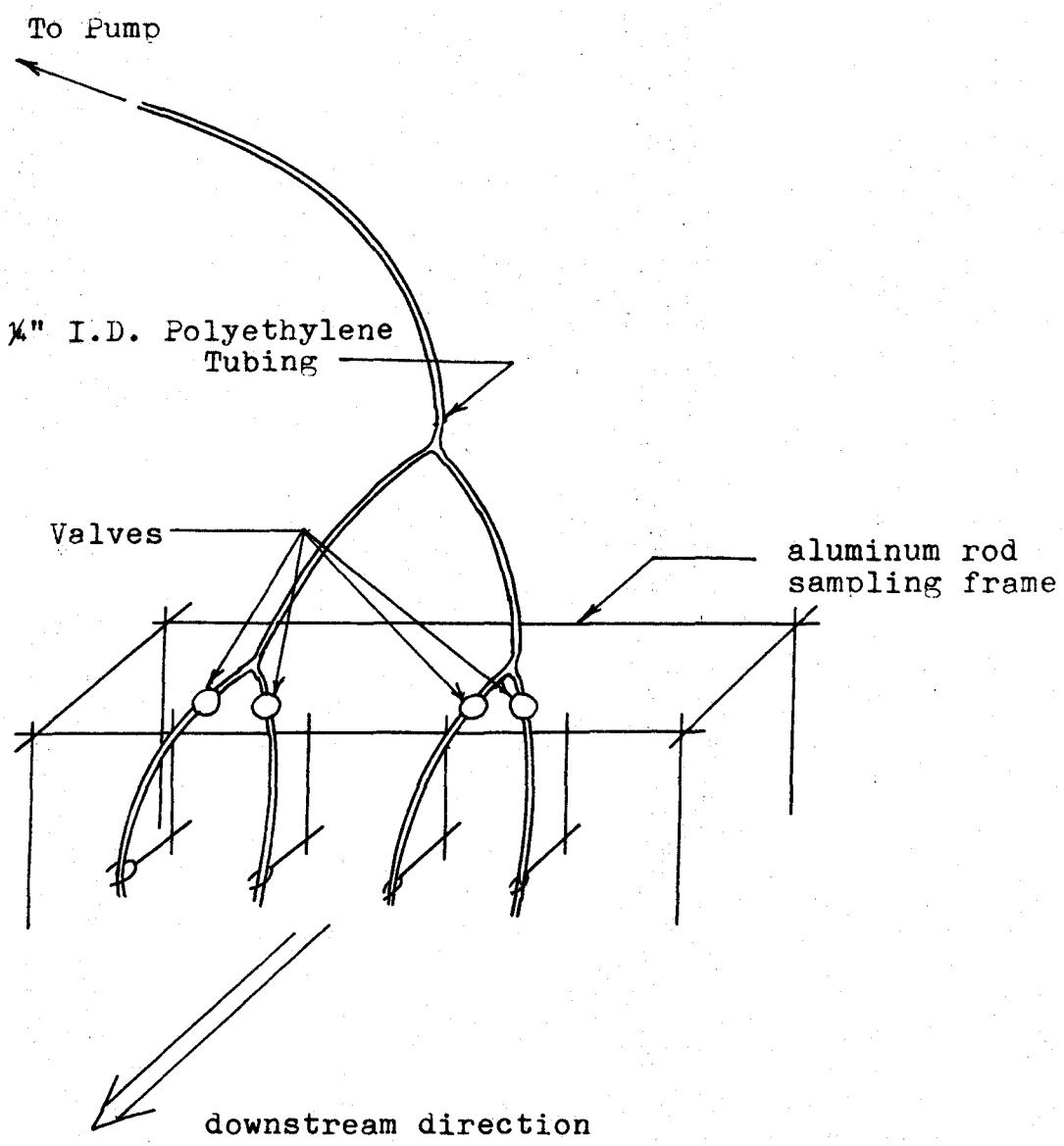

4.6 Monitoring Apparatus

The unit used to measure the dye concentration was a Turner III fluorometer equipped with a 5 c.c. flow-through door. The polyethelene tubing was covered with black tape for five feet on both sides of the door to ensure no light entered the fluorometer. The far UV lamp, No. 546 primary filter and No. 590 secondary filter were used as recommended for Rhodamine WT.

A Honeywell 10 inch Electronik 19 recorder was used to continuously monitor the output of the fluorometer. This recorder features variable chart speed control with 10 speeds ranging from 1 inch/sec. to 1 inch/5 min. The recorder used for the input had a 2-position zero while the output recorder had an 11-position zero so that small ranges of the output could be amplified for better accuracy during the high frequency sine runs.

A 3,000 watt gasoline generator was used to supply the necessary power to the recorder, fluorometer and pump. Ahead of the fluorometer, a 120 volt-amp constant voltage transformer was used to reduce the output voltage fluctuation of the generator. It was found that this transformer was too small and one twice the size is recommended for future work.

At first the temperature was just measured periodically using a standard 0-100°C thermometer but during the later runs, it was continuously measured with a YSI thermometer.

The two sets of monitoring apparatus were placed on 3 foot x 4 foot plywood platforms that were constructed at both the

input and output sites. The platform had a framework above it so that it could be covered with a black polyethylene tarpaulin in case of rain and to shade the fluorometer from the sun.

Figure 4-4 illustrates what has been described above. Appendix A gives a detailed list of the equipment used.

4.7 Injection Apparatus

Three different kind of tracer inputs were applied to the system: impulse, arbitrary pulse, and sinusoidal.

An impulse was attempted at the input site by spreading, as evenly as possible, some concentrated dye solution across the stream. Since the creek is only about eight inches deep at this point this input approximated a plane source.

An arbitrary pulse was formed in two ways. One of the methods involved pumping the dye solution for one minute, using a positive displacement peristaltic pump, into the flow at the throat of the flume. The other method involved an instantaneous injection of 100 ml. of concentrated dye solution at the flume throat. Because of the large amount of backmixing just downstream of the flume, the dye was well mixed with the whole stream. The pulse at the input site from either of these injection methods was sharp peaked with a duration of about eight minutes as will be illustrated later.

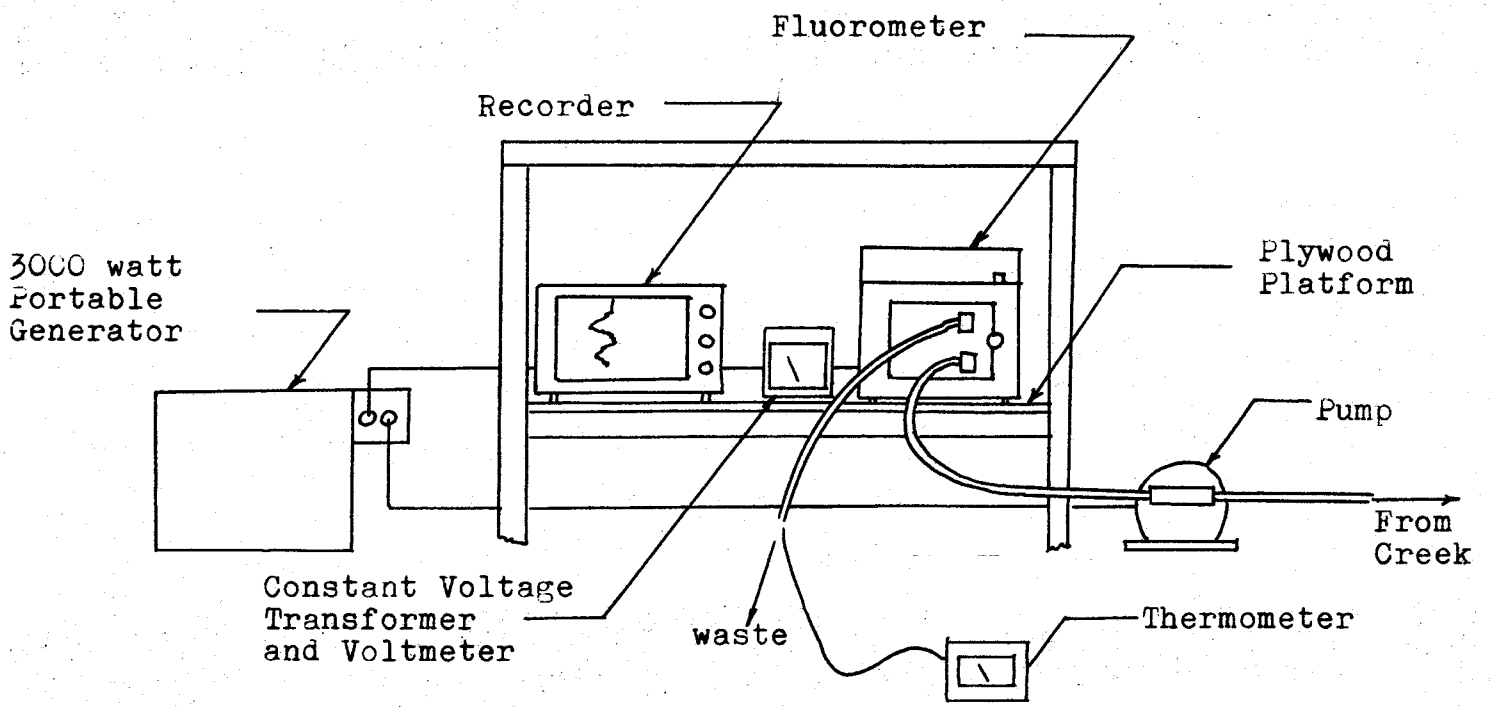

Figure 4-4 Monitoring Apparatus

The sinusoidal input was induced by varying the speed of the feed pump in the appropriate manner. The volume output of the peristaltic pump is directly proportional to the speed of the DC drive motor. The voltage to the motor was varied sinusoidally using a mechanical sine generator described elsewhere (75). Here a gear ratio of 100:1 was used to accurately vary the frequency in the range of interest.

The power source for the sine generator and pump was a 1,500 watt gasoline generator.

The equipment was placed on a platform at the flume. A tarpaulin was used, as for the monitoring apparatus, for weather protection.

The apparatus is illustrated in Figure 4-5. A detailed list of the equipment is given in Appendix A.

4.8 Experimental Procedure for a Pulse Run

(i) All the necessary equipment is taken to the input site at the creek and set up. After the generator has been started the pump is started first and each of the four sampling points are checked to ensure that they are all functioning properly. The recorder, and then the fluorometer are turned on. The fluorometer is started last so that it will not be damaged by the large voltage fluctuations that may occur when the other electrical equipment is put into operation.

(ii) The same procedure is followed at the output site. Allow two hours for the fluorometers to warm up.

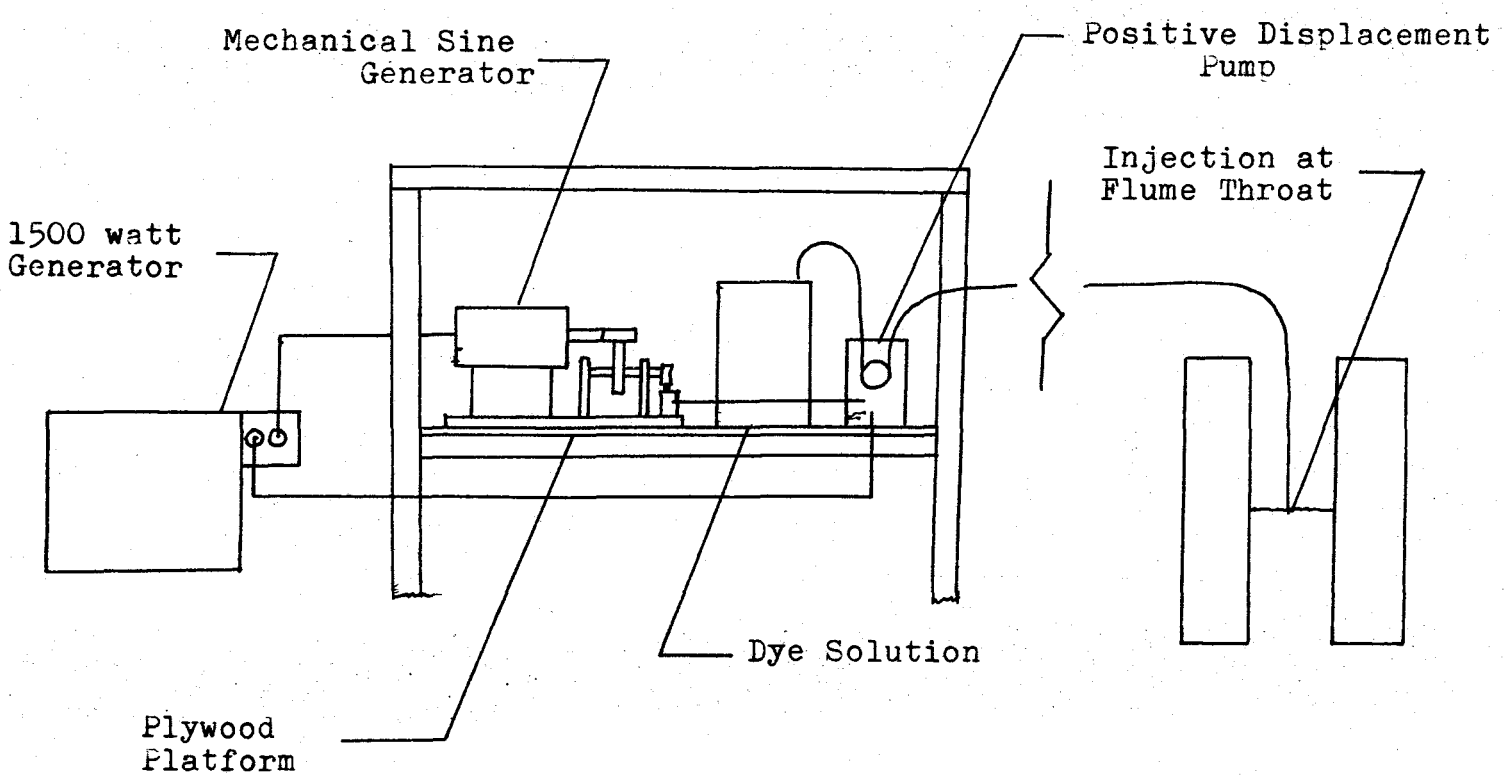

Figure 4-5 Injection Apparatus

(iii) Pieces of cardboard are placed in front of both the primary and secondary filters and the zero adjustment knob of the fluorometer is adjusted until the recorder reads zero. This is true zero.

(iv) The sampling rate is adjusted to a flow that eliminates bubbles on the discharge side of the pump.

(v) With the cardboard removed, background readings are taken on each scale. The fluorometer is left on the 3x aperature opening.

(vi) The dye solution is injected at the flume.

(vii) The chart speed of the recorder is set to 2 min./in.

(viii) A timer is started and the time is marked on the chart.

(ix) The dye concentration is monitored as it passes the input site. The fluorometer is adjusted to a less sensitive scale as soon as the reading reaches 95% full scale on the recorder and is still increasing. The scale is changed in the opposite direction as soon as the reading falls low enough to be within 90 and 100% full scale of a larger aperature opening.

(x) Record periodically the temperature of the stream and the sample after it has passed through the fluorometer.

(xi) The time should also be marked on the chart periodically in order to correct the chart speed and to relate the input to the output.

(xii) Once the reading drops to approximately the background concentration, the recorder is put on standby.

(xiii) Steps (iii) - (xi) are repeated at the output site except that step (viii) is omitted and the fluorometer is set on the most sensitive scale to start.

(xiv) Once the concentration at the output drops low enough that it will reach the background level before another pulse arrives, another run can be started.

(xv) Record the average voltage output of each of the generators for calibration purposes.

(xvi) Record the flume reading at the beginning and end of a run.

4.9 Experimental Procedure of a Sine Run

Much of the procedure for doing sine runs is the same as for pulse runs. The differences are explained in the following list.

(i) The dye is injected into the throat of the flume, with the concentration varying sinusoidally, using the apparatus described previously. This is done first, before the fluorometers are started.

(ii) The fluorometers are started as in section 4.8.

(iii) After the two hour warm-up, an appropriate scale is selected for the input fluorometer such that fluorometer output signal is displayed over most of the recorder chart. Because of the amplitude attenuation at the output site, the 11-position zero feature of the recorder may be needed

to expand the scale about the average concentration in order to give an accurate representation of the output sine curve.

(iv) Readings are taken until steady-state is reached. (This usually took about 6 hours).

(v) The background readings on the scale used can only be taken after the dye injection has been stopped and the system has been flushed.

(vi) Time, temperature, voltages, and flume readings should be taken and noted as described in section 4.8.

4.10 List of Experimental Runs

Table 4-1 gives a complete list of the experimental runs performed.

4.11 Calibrations

Some of the factors that could change the calibration of the fluorometer have been reported (120) to be: jarring during transportation, voltage surges, and changing the lamp or filters. The first two factors could be important here. The fluorometers were taken to and from the field each day of testing. Care was taken by transporting them in the backseat of a car, but some jarring was inevitable. Due to the unreliable nature of the generators, voltage surges could also have occurred. Because of these factors, the two fluorometers were calibrated three times on different occasions during the month of testing.

TABLE 4-1

List of Experimental Runs

No.	Date	Type of Input
1	June 30/70	Impulse
2	July 1/70	Pulse- pump for 1 min. at flume
3	July 1/70	Pulse - 100 ml. at flume
4	July 1/70	Pulse - 100 ml. at flume
5	July 3/70	Pulse - (generator failure)
6	July 3/70	Pulse - 100 ml. at flume
7	July 6/70	Sine - w = .162 rad/min
8	July 7/70	Pulse - 100 ml. at flume
9	July 7/70	Sine - w = .28 rad/min
10	July 8/70	Sine - w = .225 rad/min
11	July 8/70	Pulse - 100 ml. at flume
12	July 12/70	Pulse - 100 ml. at flume
13	July 13/70	Sine - w = .12 rad/min
14	July 16/70	Pulse - 100 ml. at flume
15	July 16/70	Pulse - 100 ml. at flume
16	July 16/70	Pulse - 100 ml. at flume
17	July 16/70	Pulse - 100 ml. at flume

The effect of temperature on dye fluorescence has been discussed in section 4.2. Since the temperature coefficients reported in the literature are not consistent, it was decided to carry out another experimental determination of this effect. The calibrations and the temperature coefficient determination are described in greater detail, along with the results, in Appendix B.

CHAPTER 5

5. EXPERIMENTAL RESULTS, INTERPRETATION AND DISCUSSION

5.1 Calibrations and Experimental Technique

Although the calibrations are given in detail in Appendix B, some pertinent points and recommendations should be included in this chapter. Possible improvements in the experimental technique are also to be discussed here.

The factors that could cause the calibration of the fluorometers to change has been discussed in section 4.10. Three different calibrations were carried out over the period of testing, and each time the resulting relationship between dye concentration and fluorometer reading was different. For those runs that were performed on days in-between calibrations, a decision must be made as to which set of calibration curves should be used. Depending on when the change occurred, and on how many small changes occurred between calibration days, the concentration calibrations would be in error for some runs. This error is especially evident when going from readings at one scale of fluorometer light intensity to another. Figure 5-1 illustrates this problem for Run 15. It can be seen from the output pulse that there is an unexpected rise in concentration at about fifty-eight minutes. This occurred at a point of scale change. The Bode plot is also affected by this error (see Figure 5-3).

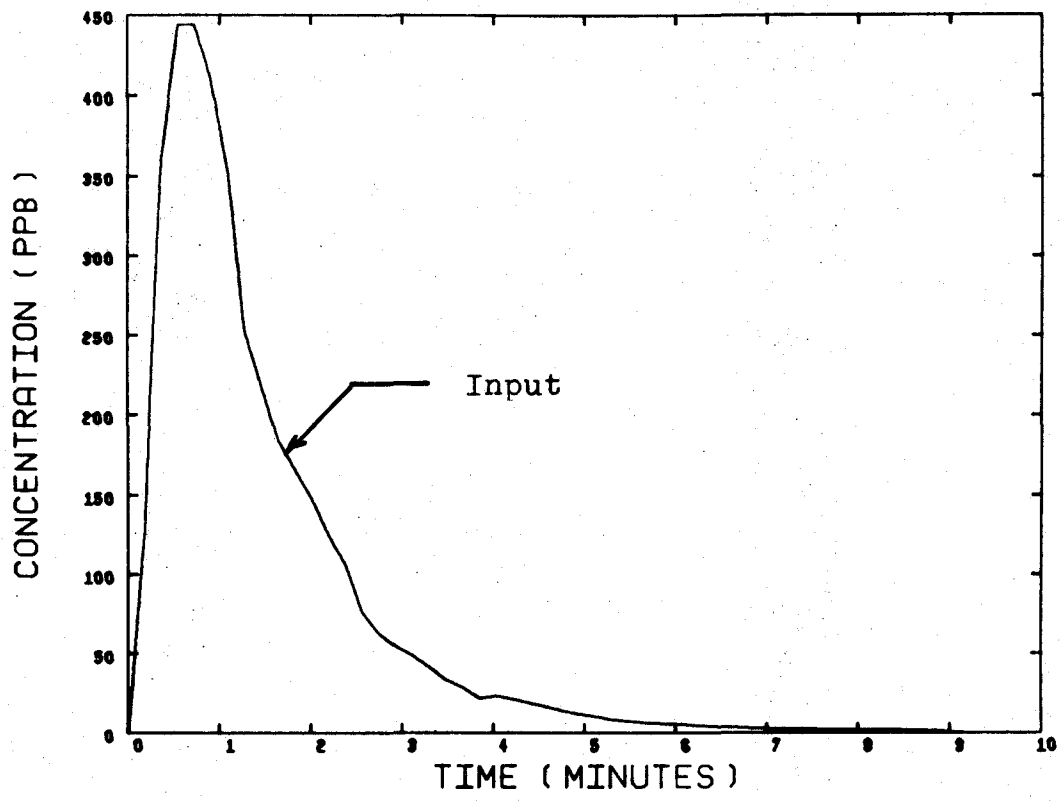

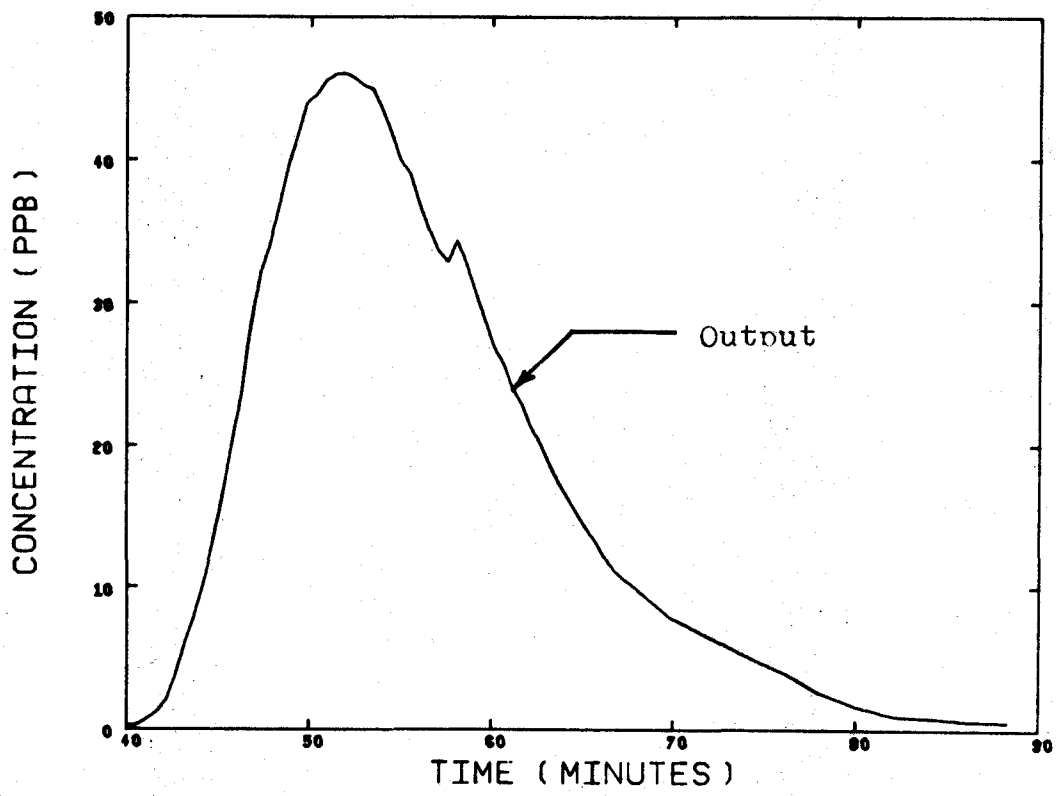

Figure 5-1 Input-Output Curves for Run 15 to Illustrate the Effect of Calibration Errors

The importance and the magnitude of the temperature fluctuation was not fully appreciated at first (see Appendix B for the effect of temperature on concentration). Since the flow through the clear polyethylene sample lines was fairly slow (about a one minute delay between stream and fluorometer), the water was heated as much as 3C° when the sun was out. However, when clouds temporarily blocked the direct sunlight, the temperature rise was as little as 1C°. While for the first half of the runs the temperature was only measured periodically, it was later monitored continuously using a YSI continuous reading thermometer. The use of a larger flow-through door would not only provide greater sensitivity but a shorter sample delay time resulting in a more constant temperature.

To summarize, several recommendations concerning experimental technique can be made. The experiments should be designed so that only one scale of the fluorometer would be required to monitor the complete range of concentrations. This would alleviate the need to calibrate every scale and eliminate the type of error that occurs at scale changes. It is important to calibrate the fluorometer often, at the end of each day of field use if possible. For short runs it is necessary to continuously monitor the concentration in the field. For these situations, it would be advisable to use the largest flow-through door, and to continuously monitor the temperature of the sample

at the output of the fluorometer. However, for longer runs, it should be possible to define the pulses well enough using discrete samples. In this case, samples could be taken in the field at a selected time interval and then the concentration measured later in the lab using a constant temperature door on the fluorometer.

5.2 Flow Rate Calculations

The flume, the pulse data, the sinusoidal data, and the dead time measurements can all be used to either calculate the stream flow or at least give an indication of the relative magnitude from one run to the next. The assigning of a numerical value for the stream flow at each run proved to be a real exercise in engineering judgment.

The flume used in this study was the type requiring only one measurement to calculate the flowrate through it. However, several factors made the measurements only useful for comparison purposes. Some of the problems that occurred were: settling of the upstream end of the flume over the month of testing, leaks through and around the sandbag walls used to divert the flow through the flume, and sedimentation after a storm. Some of the rain storms experienced during the month were large enough to increase the flow in the creek to four times the average magnitude. It was found that the readings before a particular storm could not be compared, even on a relative basis, with readings after the storm.

It is possible to calculate the flowrate from pulse data using the following formula:

$$Q = \frac{V_1 C_1}{\int C dt} \qquad 5.2\text{-}1$$

where Q = the flowrate,

V_1 = the volume of dye used,

C_1 = the concentration of the dye, and

$\int C dt$ = the area under the input or output curves.

As will be discussed in section 5.3, the accuracy of the area calculations is limited by the calibrations. The concentration of the dye solution used must also have been carefully determined.

Data from the sine runs can also be used to calculate flowrate. The formula used is

$$Q_{ST} = \frac{C_{IN}\, Q_{IN}}{C_{ST}} \qquad 5.2\text{-}2$$

where Q_{ST} = the flowrate in the stream,

Q_{IN} = the flowrate at which the dye solution is pumped into the stream,

C_{IN} = the concentration of the dye solution used, and

C_{ST} = the steady state concentration in the stream.

The positive displacement kinetic clamp pump, used to feed the dye solution into the stream, was calibrated only once. It was discovered, after all the tests had been run, that the calibration changes each time the rubber tubing is attached to the pump. Depending on the tubing and the tightness of the clamp, the flowrate could vary as much as thirty percent. This severely limited the trustworthiness of the stream flow calculations using this method.

One further measurement that can be used as an indication of relative flowrates is the dead time. This is a measurement of the amount of time that elapses between the detection of the dye at the input to the detection at the output.

The procedure used for the pulse run was to first calculate the flow based on the average of the areas under the input and output curve. This value was then compared to the flume and dead time measurements for consistency. For the sine runs, most of the weight was placed on the comparison with the pulse runs and flume readings (usually on the same day) rather than the use of equation 5.2-2.

All the data used for these calculations along with the chosen flowrates, is summarized in Table 5-1.

TABLE 5-1

Date	Run No.	Flume Reading (ft.)	Pulse Calc. Eqn. 5.2-1 (cfs)	S.S. Calc. Eqn. 5.2-2 (cfs)	Dead Time (min.)	Chosen Flowrate (cfs)
June 30/70	1	1.04			48.0	
July 1/70	2	1.02	3.38 ± .03		54.2	4.0
	3	1.02	3.94 ± .15		55.4	4.0
	4	1.02	4.10 ± .17		55.2	4.0
3/70	5	*				
	6	1.50	7.84 ± .14		36.2	7.8
6/70	7	.97		3.42		3.5
7/70	8	.95	3.18 ± .06		60.0	3.2
	9	.93		2.84		2.9
8/70	10	.99		3.32		3.4
	11	1.02	3.55 ± .10			3.5
12/70	12	1.03	4.30 ± .06		47.8	4.3
13/70	13	.93		3.71		4.0
16/70	14	1.21	6.77 ± .12		40.2	6.8
	15	1.18	6.71 ± .32		40.1	6.4
	16	1.17	5.99 ± .30		40.2	6.2
	17	1.14	5.54 ± .01		42.6	5.5

* Generator Failure, Run aborted

The chosen flow rates are considered to be accurate to approximately five percent. Considering the total range of flows, this accuracy is sufficient.

The accuracy of the flow calculations using pulse or sine data could possibly be improved to be within two percent in any future work. Calibrations of pumps used in sine runs are simple and should be made every time. Also, recommendations made in section 5.1 concerning calibrations and experimental technique should be followed to improve the accuracy of the calculations based on the pulse data.

5.3 Pulse Runs

From each of the eleven pulse runs obtained at different stream flows, a continuous recording of fluorometer readings versus time was obtained for both the input and the output. Using the results of the calibration study (Appendix B) these curves were transformed into time-concentration plots. Between fifty and eighty points were used to describe each curve. Some of these time histories have been plotted up using a Benson-Lehner plotter. This plotter joins given points by straight lines. It can be seen from Figures 5-1, 5-4 and 5-7 that enough points have been chosen to give a sufficiently detailed description of the curves.

Table 5-2 lists the area under both the input and output curves, as well as the percent recovery for each run. The areas were used to calculate the stream flow as described in section 5.2.

TABLE 5-2

Run	Area Input (ppb - min)	Area Output (ppb - min)	Percent Recovery (%)
2	657	653	99.3
3	1,247.2	1,290.7	103.5
4	1,268.1	1,171.0	92.3
6	649.2	626.7	96.5
8	1,592.9	1,547.7	97.2
11	1,371.3	1,447.2	105.5
12	1,147.3	1,179.8	102.8
14	725.4	751.2	103.5
15	707.6	780.9	110.4
16	877.6	791.4	90.2
17	901.7	903.3	100.2

It can be seen from the above table that the percent recovery ranges from 90.2 to 110.4, but with the majority within 5% of the theoretically expected 100% recovery. If the dye had adsorbed into the stream bed, or if the tail of the output curve was not monitored long enough, there would be less than one hundred percent recovery. However, in this work, this is not believed to be significant since the dye is a non-adsorbing type, especially in such a short reach, and the tail would have to be extremely long to account for an error of only a few percent. Since there are just as many

calculated recoveries above one hundred as there are below, the deviation is most likely due to experimental error. The greatest source of experimental error is in the calibrations as was described in section 5.1. This problem was especially evident in the two extreme cases, Runs 15 and 16. Since the shape of the curve rather than the absolute numerical value is important in the frequency response calculations, an error of five percent in the percent recovery is considered quite acceptable.

The computer program listed in Appendix D and described in section 3.3 was then used for the frequency response calculations. The Filon and the trapezoidal quadrature formulae gave essentially the same answers. A typical program output is also listed in Appendix D. The Filon result was used to construct the Bode plots using the Benson-Lehner plotter. Examples of these plots are shown in Figure 5-2, 5-3, 5-5 and 5-6.

It has been suggested in the literature (51) that the calculated response should not be considered reliable beyond the frequency where the frequency content of the output pulse approaches the experimental error. In this study the curves are truncated at a frequency content of five percent.

As a further check on the required accuracy of the time-concentration curves, a few program runs were repeated with the data from the original recorder graphs accurate to

only two significant figures. It was found that this had an insignificant effect on the corresponding Bode plot (not shown).

5.4 Sinusoidal Runs

A series of runs involving a sinusoidal input of dye at different frequencies was carried out in order to compare the results with the pulse method of obtaining the frequency response of the system. This data was also used as a check on the numerical method used in the pulse testing procedure.

Table 5-3 lists these results along with a rough approximation to the experimental error involved. Appendix E outlines, as an example, the calculations involved in reducing the observed results to amplitude ratio and phase shift data.

TABLE 5-3

Run	Amplitude Ratio (Decibels)	Phase Shift (Degrees)	Stream Flow (cfs)
7	$-12.8\ ^{-1.3}_{+1.1}$	732 ± 25	3.5
9	$-27.5\ ^{-6.1}_{+3.5}$	1,270 ± 55	2.9
10	$-19.3\ ^{-2.4}_{+1.9}$	985 ± 25	3.4
13	$-\ 6.94\ ^{+.7}_{-.6}$	524 ± 20	4.0

These results are also shown on Figure 5-2 along with the results of four pulse runs in the same flow range.

The error calculations for the amplitude ratio data were based on an assumed error of two percent in graph reading and calibration. It can be seen that the effect on the reliability of the amplitude ratio at high frequencies is

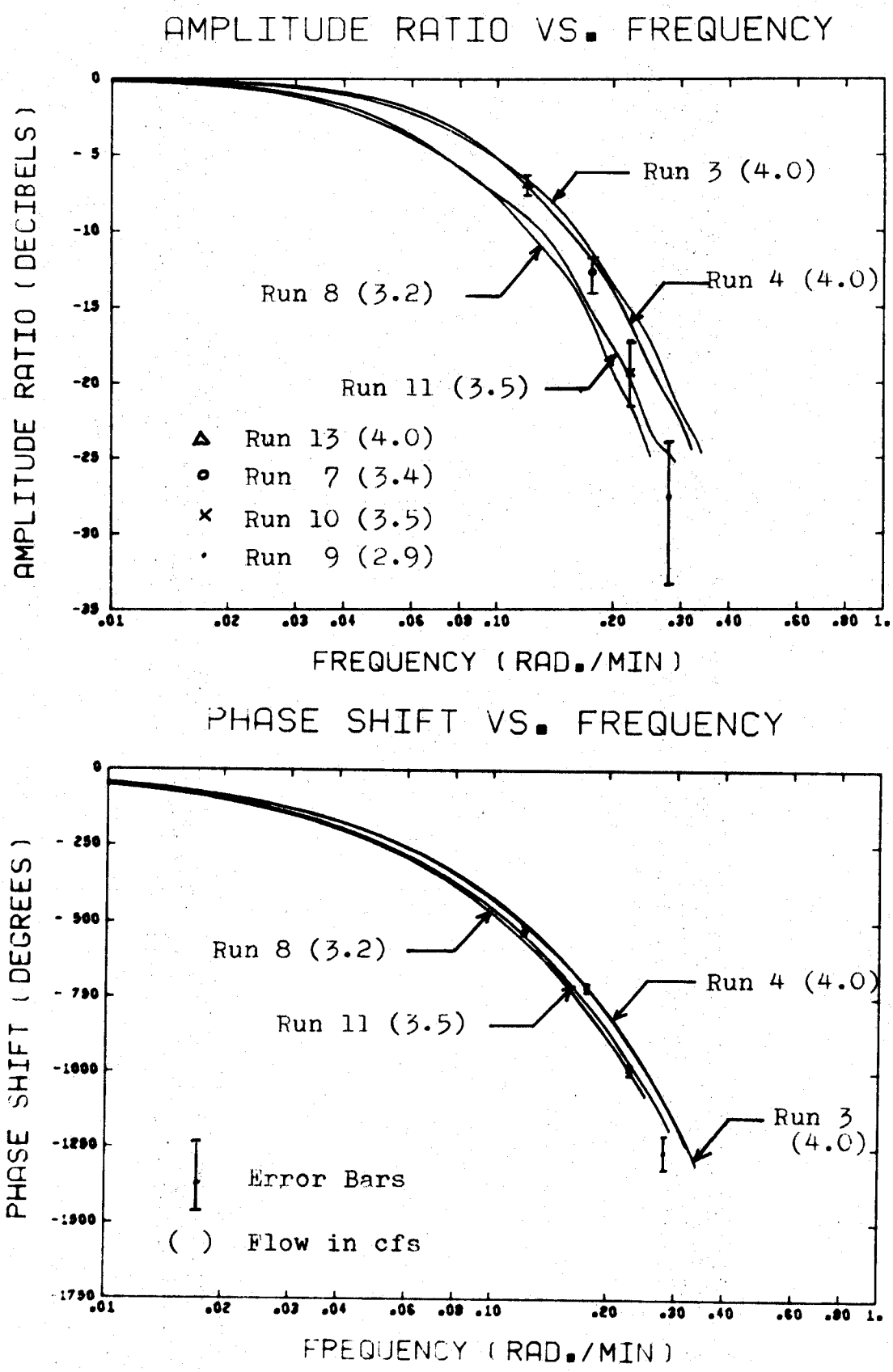

Figure 5-2 Comparison of Sine Data to Pulse Data

quite significant. This is simply due to the fact that the output amplitude is severely attenuated, and therefore, difficult to measure at high frequencies. The accuracy of the time of the peak concentration for both the input and output sine curves, used in the calculation of the phase shift, was estimated for each individual run. This error was found to be less than four percent.

In spite of the large experimental errors involved, it can be seen from Figure 5-1, that the results are in good agreement with the frequency response calculated from the pulse runs.

One of the purposes of using sinusoidal inputs was to compare this method of obtaining the frequency response to the pulse procedure. The possible accuracy, using the fluorescent dye techniques outlined in this study, limits the usefulness of the sine approach, especially at high frequencies. Not only does each test have to be run for a considerable length of time until steady state conditions are reached, but one run provides only one point on each of the Bode plots. In order to sufficiently define the frequency response curves several sinusoidal runs would be necessary at each stream flow. It is clear that the pulse testing method is a more efficient and practical method of obtaining the frequency response.

5.5 Reproducibility

Since no two runs were performed at exactly the same flowrate, reproducibility of the Bode plots is difficult to show. However, two pairs of runs are felt to be at close enough flowrates to be used as an indication. Runs 3 and 4 at a flow of 4.0 cfs and Runs 14 and 15 at an average flow of 6.6 cfs are shown in Figure 5-3. Unfortunately, Run 15 has more error associated with it due to the problem described in section 5.1.

These curves give an indication of the overall experimental variability involved in determining the frequency response from pulse data. It can be seen that the results are fairly reproducible, especially for the phase shift curves.

5.6 Effect of Different Inputs

Three different types of inputs were used for three consecutive runs to show that the resulting frequency response does not depend on the input. An impulse (Run 1) was simulated by dumping the dye as a line source across the creek at the input site. For Run 2 the dye solution was pumped into the creek at the flume for a period of one minute. The third type of input (Run 3) was created by dumping 100 ml. of concentrated dye solution, in one shot, into the throat of the flume.

The concentration-time curves for two of the inputs and all three of the outputs are shown in Figure 5-4. The impulse input is not shown since it is essentially a delta

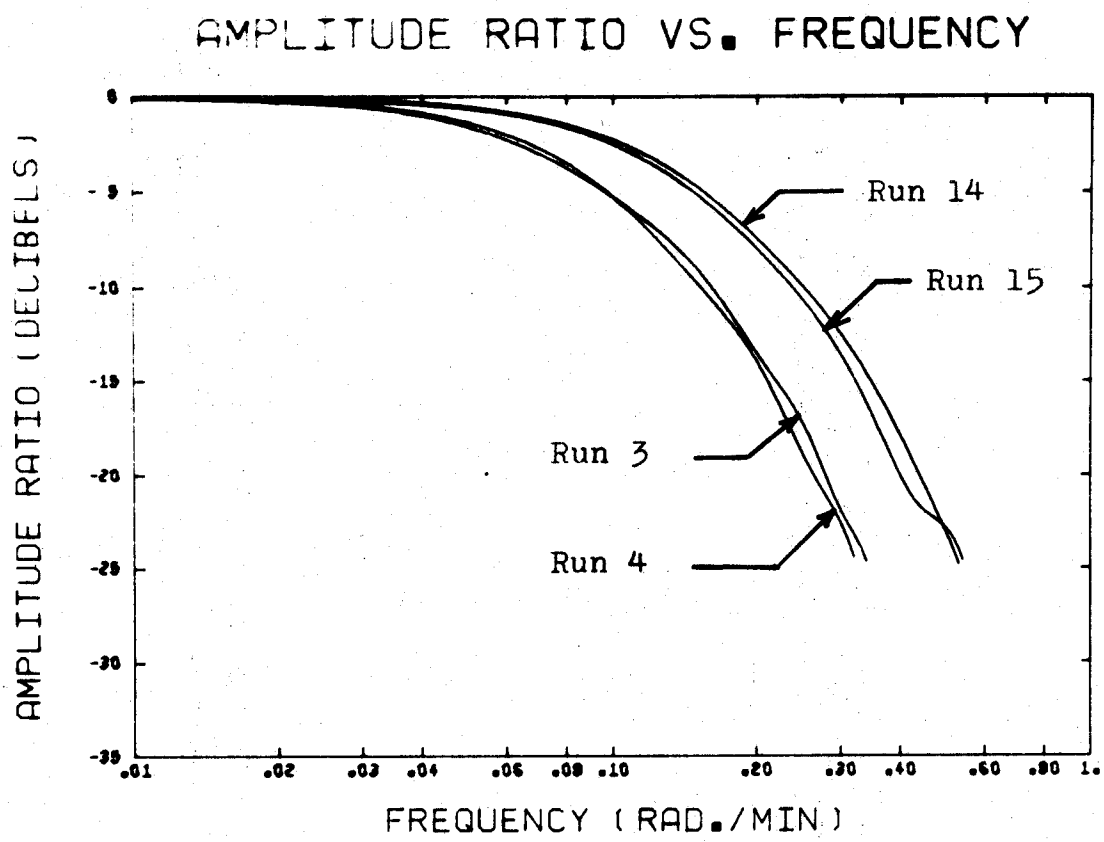

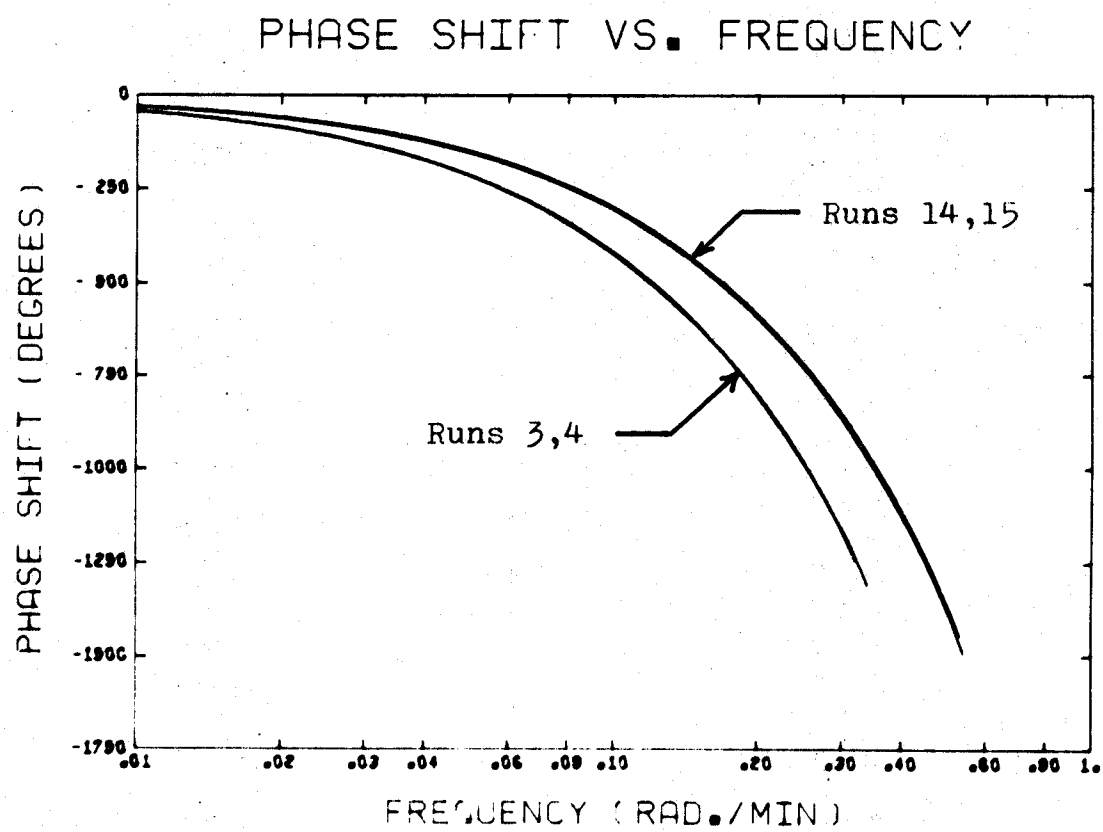

Figure 5-3 Bode Plots of Runs 3,4,14,15 to Illustrate Reproducibility

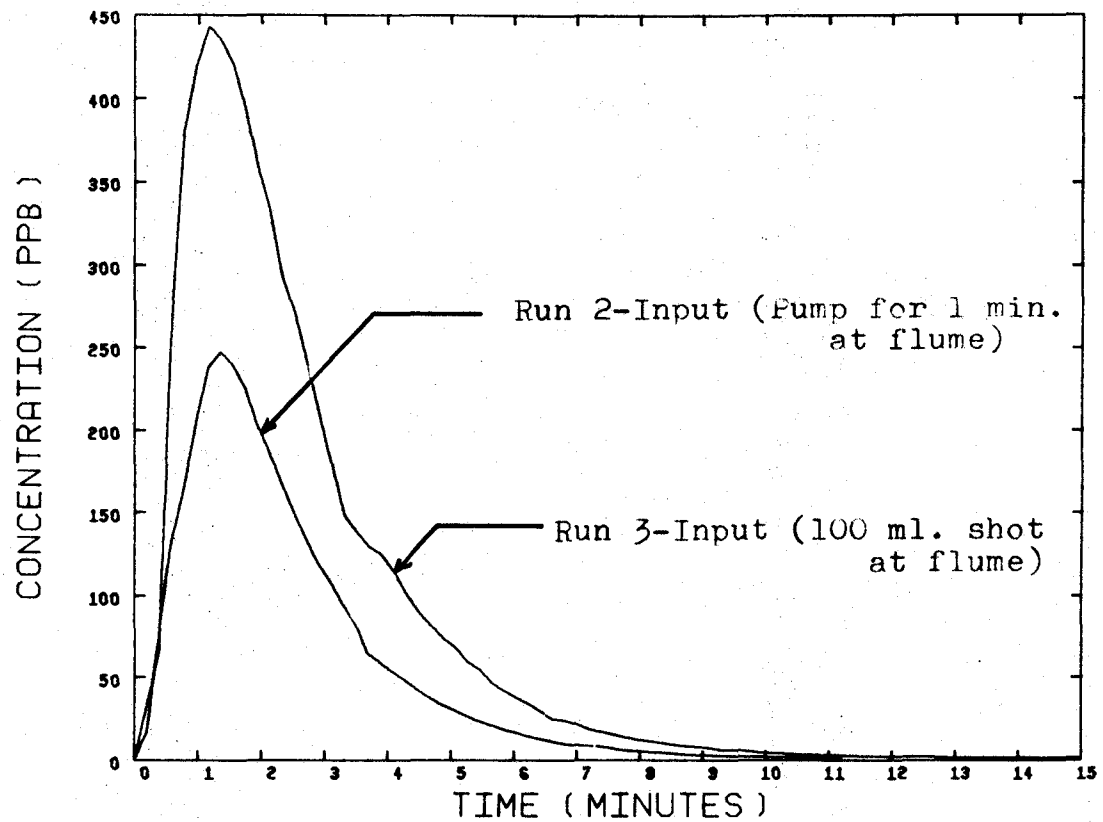

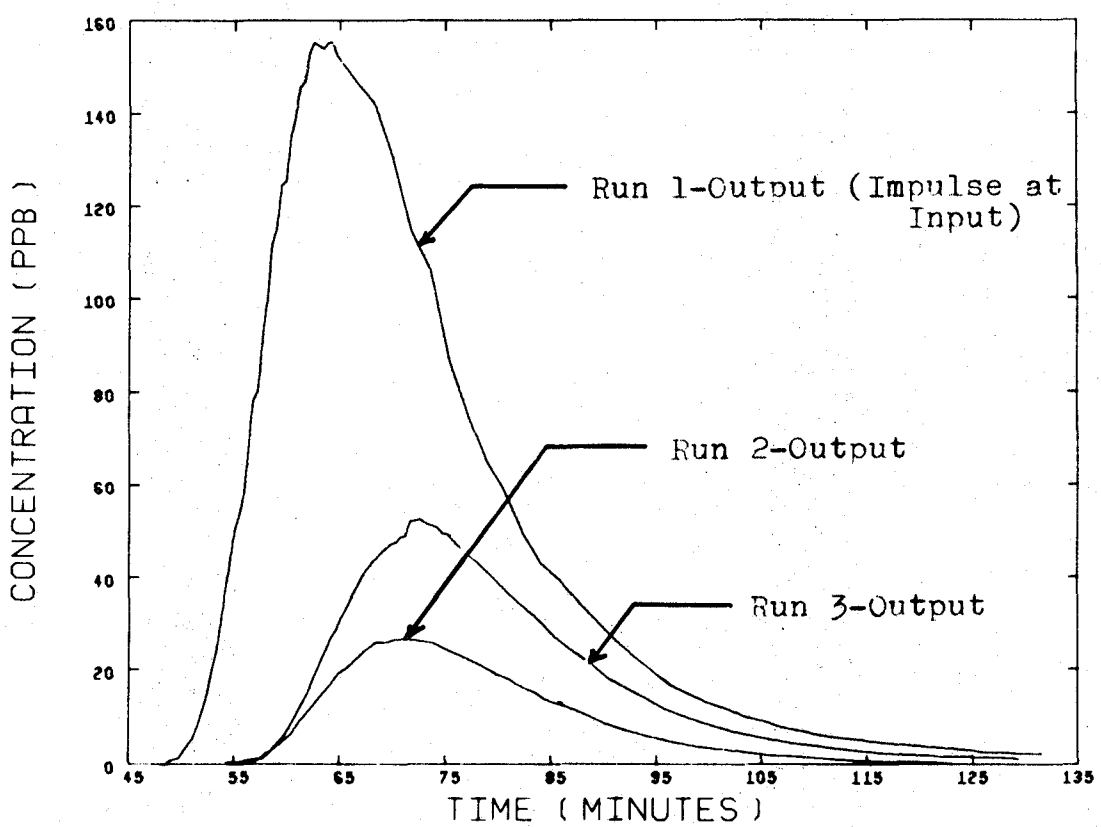

Figure 5-4 Input-Output Curves to Illustrate the Effect of Different Types of Input

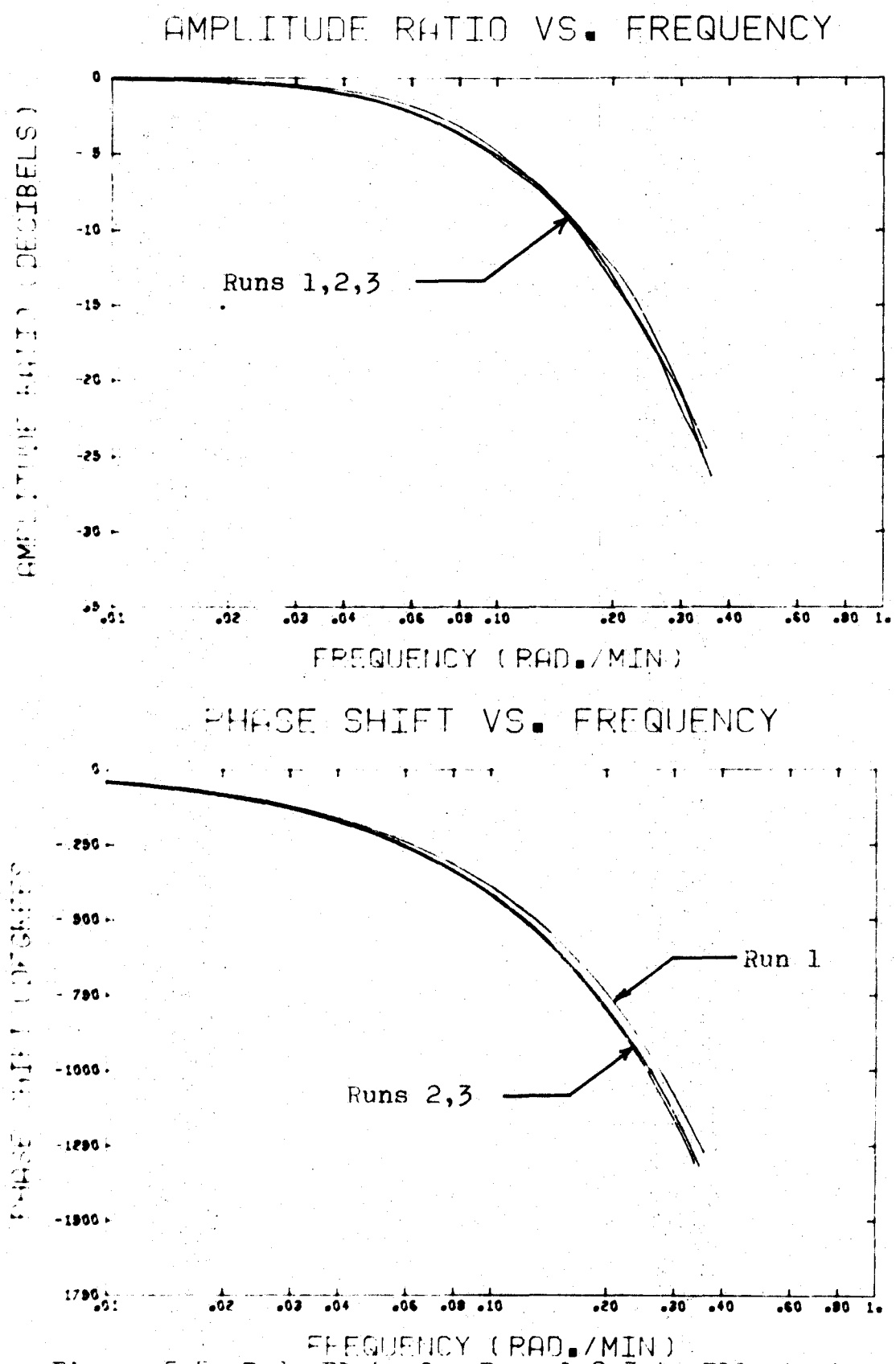

Figure 5-5 Bode Plots for Runs 1,2,3 to Illustrate the Effect of Different Types of Input

function. Even though all three runs were performed on the same day, the flume readings indicate that the flow for Run 1 is higher than that for Runs 2 and 3. This is evidenced in the output curves (Figure 5-4); the pulse for Run 1 arrived at the output site before the other two.

The corresponding Bode plots for these runs are shown in Figure 5-5. It can be seen that the amplitude ratio and phase shift curves are very close to each other. The difference or the variation between them is due to both experimental error and the fact that each run is at a slightly different flowrate. The fact that the flows for Runs 2 and 3 are relatively the same, yet less than that for Run 1, is clearly illustrated in the phase shift plot.

Even though all these inputs gave essentially the same result, it cannot be concluded that any input would do so. Other workers (31, 19, 55) have found that the results are unreliable for all frequencies greater than that frequency whose frequency content in the input pulse is less than .2 - .3. For all three of the inputs used, the input frequency content was never less than .84. It was, therefore, a matter of choosing from these the most convenient input pulse. The impulse was difficult to simulate and was rejected as a poor method. Also, use of the pumped input was not chosen because the resulting concentrations in the stream were too low to measure the tail of the output curve accurately. The 100 ml. 'shot' procedure turned out to be the best method. Not only

is there no extra injection apparatus required, but the method is easy to reproduce and a reasonable detection of the tail was possible.

5.7 Mathematical Modelling

5.7.1 Summary of Procedure

The procedure followed to mathematically fit a model to the experimental data has been discussed in detail in section 3.5 and is summarized here. First, the proposed model is formulated in terms of a transfer function in the Laplace domain. The frequency response is obtained by substitution of jw for s (this is done in the computer program used to do the fitting). A numerical search technique, patterned after the Rosenbroch Method (96), is used to minimize the function

$$\phi = \sum_{i=1}^{N}\left[(Re_{oi} - Re_{pi})^2 + (Im_{oi} - Im_{pi})^2\right] \qquad 5.7\text{-}1$$

where Re_{oi} and Im_{oi} are the real and imaginary parts of the observed complex number for the ith frequency and Re_{pi} and Im_{pi} are the real and imaginary parts of the predicted complex number for the ith frequency.

This function is similar to equation 3.5-7 except that the frequencies have been selected evenly spaced on the $\log_{10}w$ axis. This is equivalent to weighting the more accurate low frequency data. The computer program used, to carry out this search technique in evaluating the best parameter values of the

proposed model, is described in detail by Melnyk (75). Not only are the statistically best parameter values found, but the value of the function ϕ, the residual sum of squares (RSS), for these values is also evaluated. This RSS value can be used to compare different models for the same data.

5.7.2 Fitting Models to Run 1

The fitting of various models to Run 1 will be explained in detail to illustrate the procedure followed for an actual case. The input used for this run was an impulse and, as mentioned in the literature review, the response to such an input can be used to compare models in the time domain as well as the frequency domain. The various model parameters were evaluated using the frequency response data but the predicted models are plotted in the time domain for a graphical comparison with the time-concentration curve for Run 1. The graphical comparison in the frequency domain, using Bode plots, will be illustrated in section 5.7.3.

The dispersion model, since it has been applied to natural streams in the past, was attempted first. The transfer function for this model is given in Appendix C. The two parameters of the model are the average residence time and the Peclet number, Pe. The real and imaginary parts of the experimental response were calculated without the dead time removed. Both the average residence time, $\bar{t}$, and Pe were allowed to vary in the search routine. The best values

of these two parameters are shown, along with the RSS, in Table 5-4. The time domain solution (see Appendix C) was used to plot the predicted model for comparison with Run 1 (see Figure 5-6). It can be seen that the fit is very poor. The actual response rises more sharply and has a longer tail.

Then, a simple model consisting of N equal sized CSTR in series with one PFTR was fitted. Since the residence time of the PFTR component is simply the dead time, this factor was not included in the calculations of the real and imaginary parts of the experimental frequency response to be used to evaluate the parameters of the N CSTR part of the model. The parameters are the average residence time of one of the CSTRs and N, the number of CSTRs in series. An initial estimate of the residence times was obtained by calculating the time of the centroid of the response curve. Several values of N were tried and the best was chosen on the basis of the lowest RSS (see Table 5-4). The time solution of this model is well known (see Appendix C) and has been plotted in Figure 5-6 to compare with Run 1. Although the fit is better, as expected from the lower RSS, it still does not represent the peak or the tail portion well.

The long tail on the time-concentration curve indicates that stagnancy or the phenomenon of 'dead zones' may be significant. This was checked by evaluating the intensity function proposed by Noar and Shinnor (101).

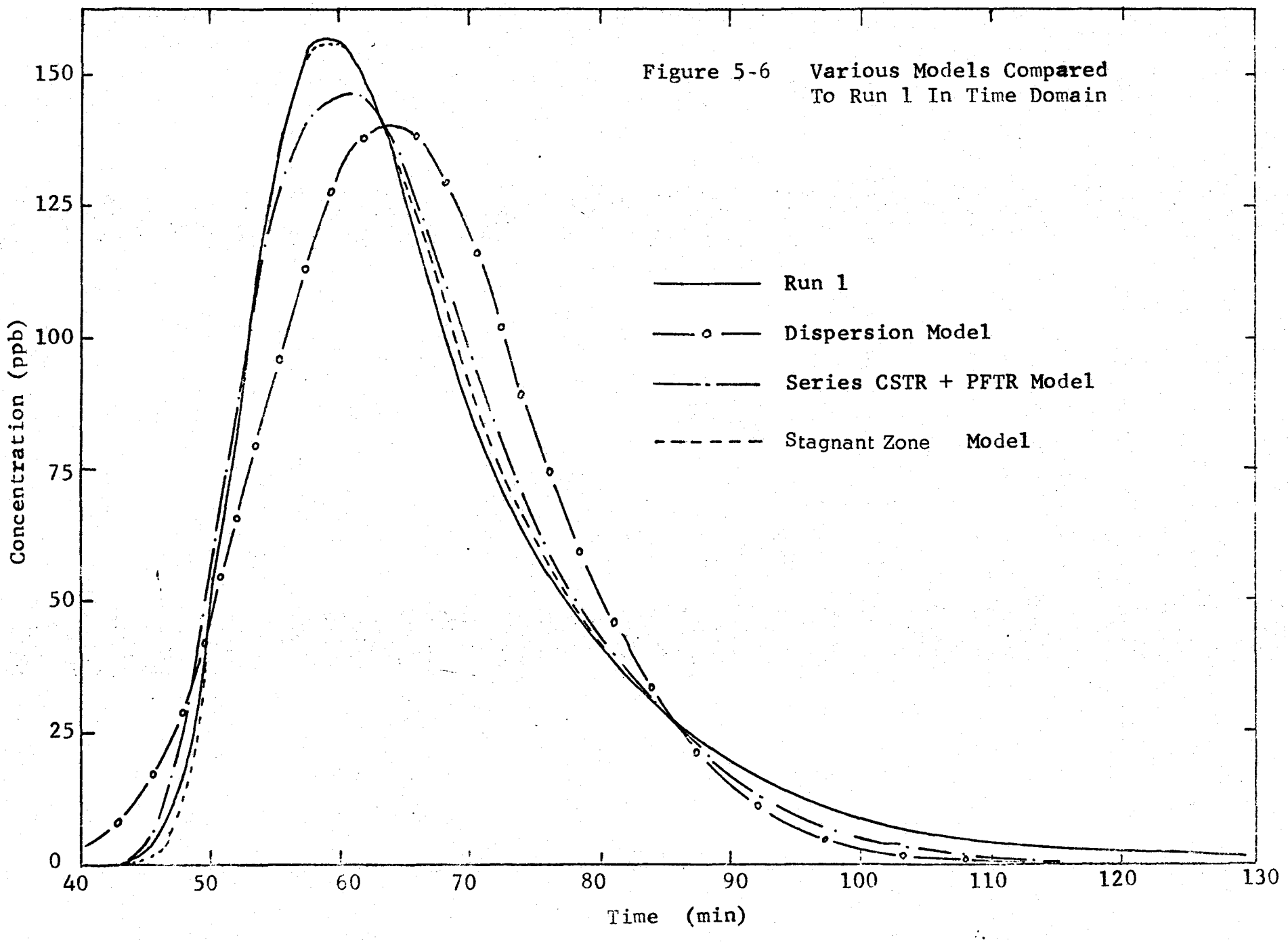

Figure 5-6 Various Models Compared To Run 1 In Time Domain

The function is defined as:

$$\lambda(t) = \frac{f(t)}{1 - F(t)} \qquad 5.7\text{-}2$$

where f(t) is the residence time distribution (i.e. the response to a unit impulse) and F(t) is the cumulative RTD. For this calculation it was assumed that ninety-nine percent of the dye was measured at the output. The calculated function is plotted in Figure 5-7. Stagnancy or parallel flow is indicated by the fact that the function decreases over some time interval. It was necessary, therefore, to propose a model that accounts for this factor.

The model proposed by Adler and Hovorka (1)(discussed in Appendix C) can be used to simulate mixing situations where regions of relatively long residence times are significant. As before, the total residence time of the PFTR components is equal to the dead time. The centroid was used as an initial estimate of the total average residence time of the CSTR portion of the model. In order to obtain an initial estimate of the other parameters, a grid search was performed. This involved the evaluation of the function ϕ for complete ranges of the three parameters N, k, F, and the initial estimate of $\bar{t}$. The three best sets of the parameters, where ϕ was a minimum, were used as starting values in the Rosenbrock program. For each of the three N's chosen, the best values of F, $\bar{t}$ and k were evaluated. From these sets of

Figure 5-7 Intensity Function for Run 1

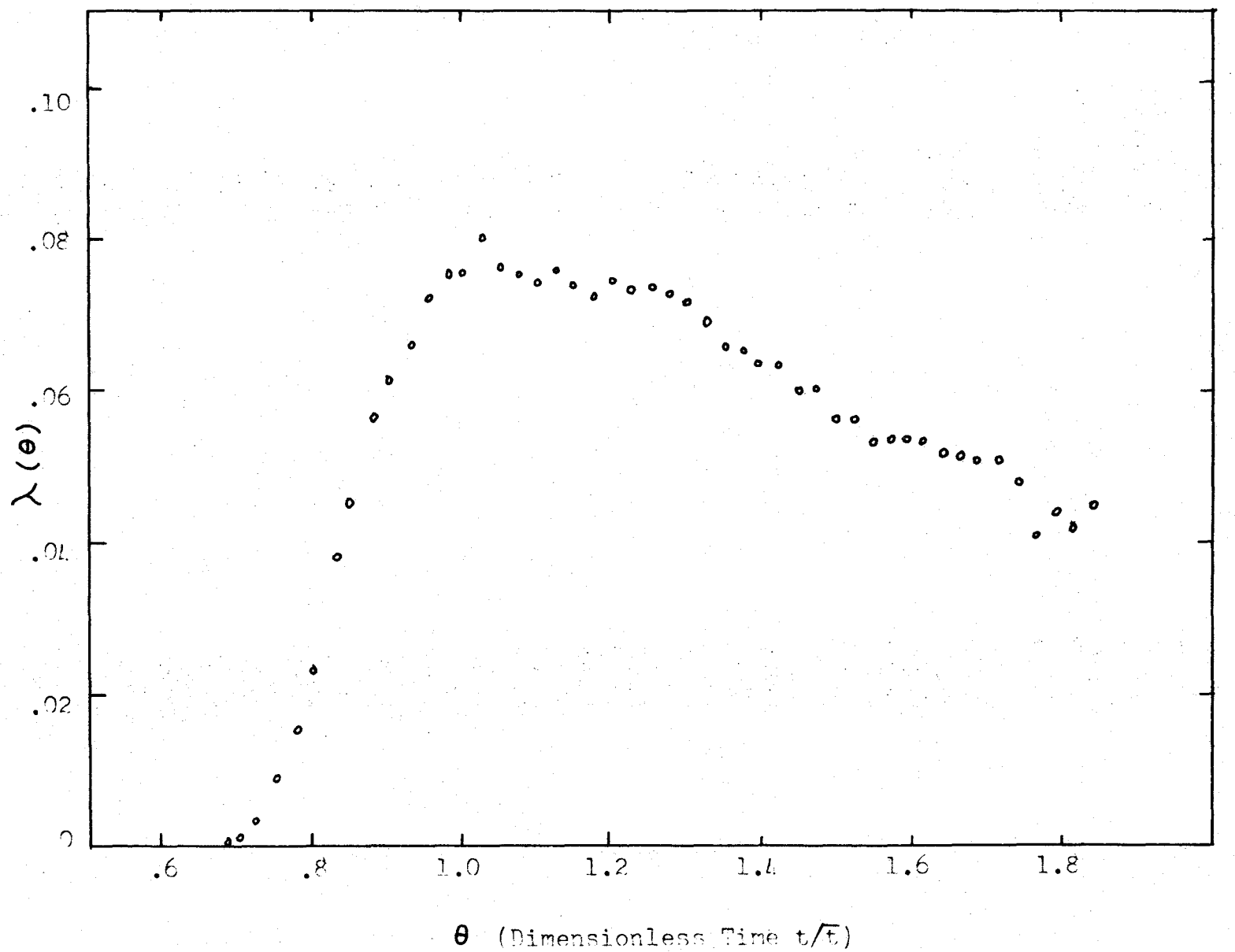

TABLE 5-4

MODELS FITTED TO RUN 1

Model	CSTRi	N_{CSTR}	PFTR	F	k	N_{AH}	$\bar{t}$	Pe	RSS x 10^{-2}
Dispersion							69.71	88.06	26.37
N CSTRs + 1 PFTR	5.657	4	48.0						6.18
Stagnant Zone (SZ)			48.0	.799	.0931	6	24.00		.229

values, the one with the lowest RSS was chosen (see Table 5-4). In comparing RSSs, their model gives a smaller value and therefore the fit should be better. The time domain solution given by Adler (1) was used to plot the predicted model in Figure 5-6. The fit of this model is excellent; the two curves are almost identical.

5.7.3 Model Parameters as a Function of Streamflow

Various models were fitted to six of the pulse runs. The flows for these runs cover the complete range of streamflow studied. Table 5-5 summarizes the parameter values and the RSS for each of the models fitted to the six runs.

In order to decide whether the addition of one or more parameters is justified (i.e. if the reduction in the RSS is significant) an F-test was used. Although this is not strictly true for this non-linear least squares analysis, it will serve as an indication of the statistically best model. The F statistic used here is defined as

$$F_{DF1,DF2} = \frac{RSS_x - RSS_y}{\frac{RSS_y}{N_{Data}-y}}$$

where DF1 = degrees of freedom of the numerator $= y-x$,

DF2 = degrees of freedom of the denominator

$= N_{Data} - y$,

RSS_x = residual sum of square for the x

TABLE 5-5

MODEL SUMMARY

Run	Model	τ_1 or τ_i (min)	τ_2 (min)	τ_3 (min)	τ_4 (min)	τ_{PFTR} (min)	N_{CSTR} or N_{AH}	F	k	$\bar{t}$ (min)	RSS x10^{-2}
3	UEC	2.2136	8.622	2.19	8.51	55.36					.721
	UEC	7.111	7.09	6.99		55.36					2.06
	EC	7.065				55.36	3				2.06
	SZ*					55.36	4	.843	.116	21.84	.480
6	SZ					36.23	4	.718	.517	13.08	.913
	EC	4.350				36.23	3				.719
	UEC	4.42	4.31	4.33		36.23					.719
	UEC*	5.64	3.85	3.46	.203	36.23					.578
8	SZ*					59.98	4	.835	.094	29.95	.333
	EC	9.49				59.98	3				2.69
	UEC	8.125	12.58	8.01		59.98					2.49
	UEC	16.60	4.31	4.37	4.35	59.98					.449
12	SZ*					47.76	5	.829	.112	21.27	.246
	SZ					47.76	4	.944	.031	20.86	1.64
	UEC	7.00	6.97	6.97		47.76					14.7
	UEC	9.01	3.95	3.96	3.96	47.76					1.8
	EC	5.10				47.76	4				4.65

TABLE 5-5 (Cont.)

MODEL SUMMARY

Run	Model	τ_1 or τ_i (min)	τ_2 (min)	τ_3 (min)	τ_4 (min)	τ_{PFTR} (min)	N_{CSTR} or N_{AH}	F	k	$\bar{t}$ (min)	RSS x10^{-2}
14	UEC	4.45	4.44	4.44		40.19					1.73
	UEC*	5.74	2.79	.634	4.29	40.19					.497
	SZ					40.19	4	.814	.238	13.45	.571
	EC	4.44				40.19	3				1.73
17	SZ					42.60	5	.774	.266	16.74	.608
	SZ*					42.60	4	.911	.060	16.75	.401
	EC	4.04				42.60	4				6.40
	UEC	5.53	5.52	5.53		42.60					.858
	UEC	7.68	2.61	2.89	3.52	42.60					.464

UEC = unequal CSTRs + PFTR model

EC = equal CSTRs + PFTR model

SZ = Stagnant Zone model

* models chosen

parameter model,

RSS_y = residual sum of square for the y parameter model,

and N_{Data} = number of points at which model is compared to the data.

This value was compared to the tabulated F at the ninety-five percent confidence level. The best models are indicated in Table 5-5 by an asterisk.

For the runs at the four lowest flows the A-H model is best, but at the higher flows, a model consisting of four unequal CSTRs in series with a PFTR is better. This probably indicates that the stagnant zones are not significant at these high flowrates. It would be more convenient, although not necessary, to use the three equal CSTRs in series with the PFTR since this three parameter model is a sub case of the Stagnant Zone model with F = 1.0. The predicted frequency response of these two models was plotted up and compared with the observed response for Runs 14 and 6. Since they did not differ greatly, the three parameter model was chosen for the sake of model consistency.

The Bode plots of the six runs with their corresponding models are shown in Figures 5-8 and 5-9. It can be seen that, on the whole, the agreement is very good. The greatest deviation is at the high frequencies. This was to be expected since the low frequencies were weighted in the fitting procedure.

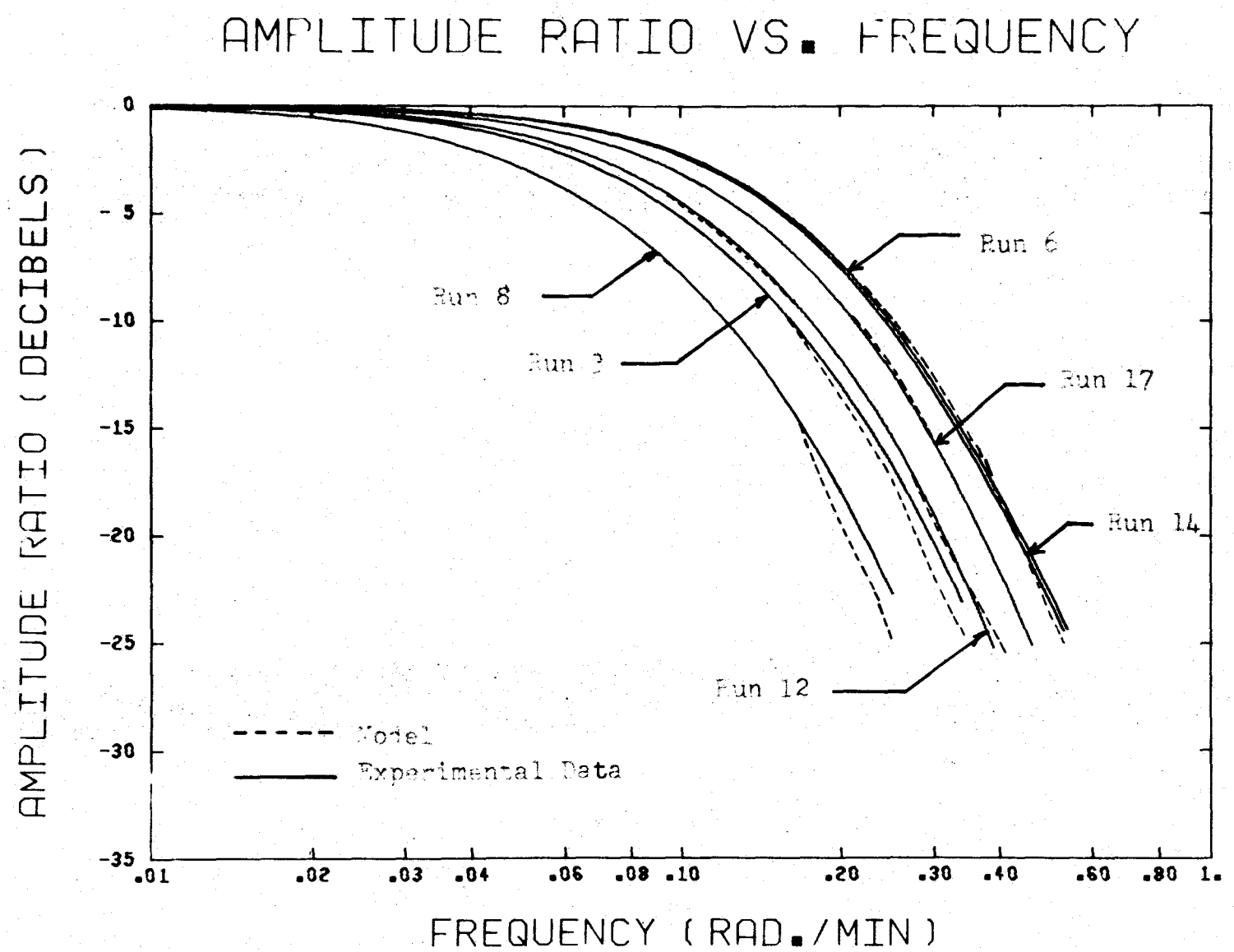

Figure 5-2 [illegible] (Amplitude Ratio Vs. Frequency) to Illustrate [illegible] Model and Experimental Data at Various [illegible]

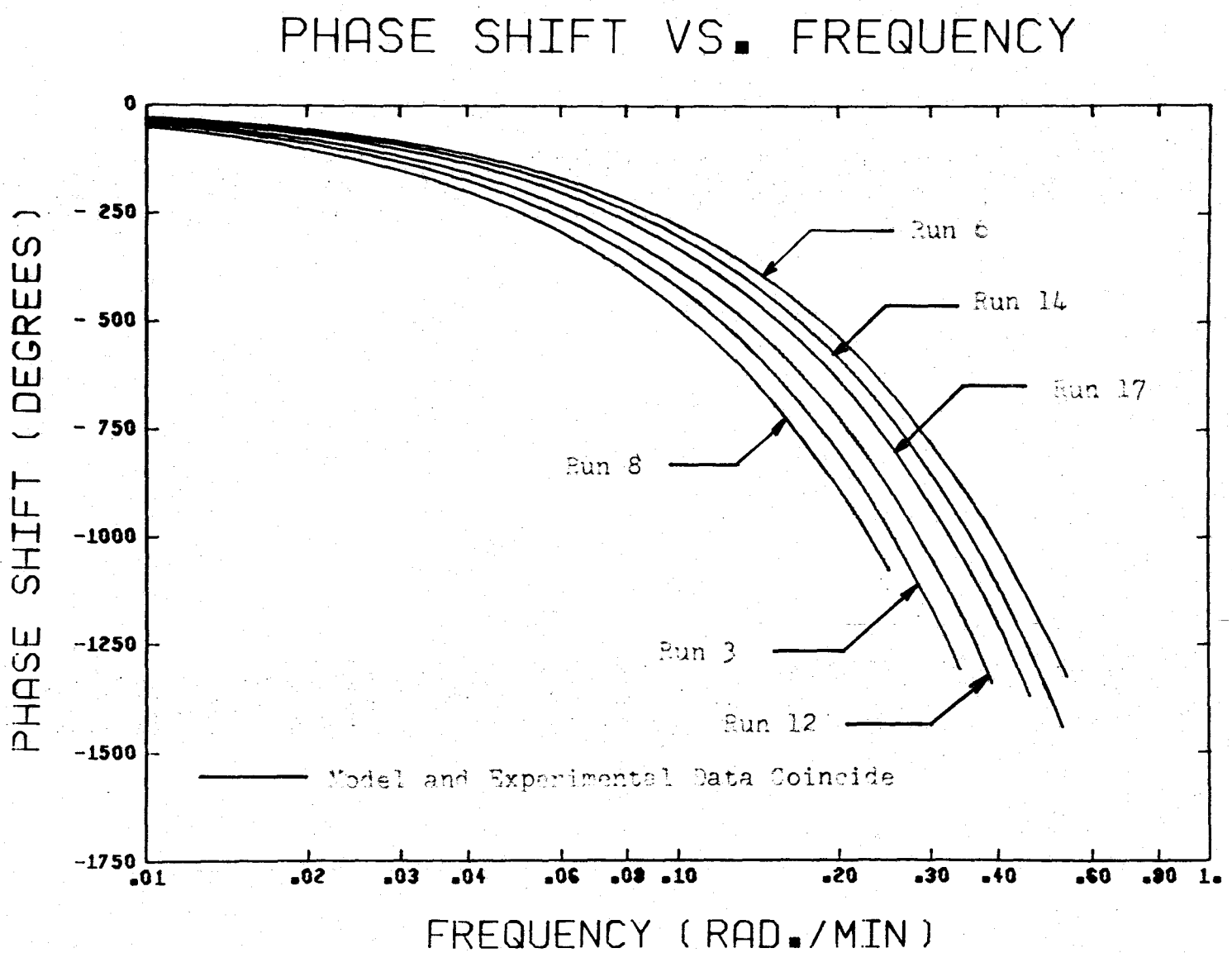

Figure 5-2 Bode Plot (Phase Shift Vs. Frequency) to Illustrate Model and Experimental Data at Various Flows

The parameters of the chosen models are plotted as a function of streamflow in Figure 5-10. The curves drawn through the points were only done by eye to show trends. If it is desired, for computational purposes, to describe the relationships between the parameters and flowrate mathematically, curves could be easily fitted to these points using some numerical linear regression technique. It appears that two sets of relationships would be needed for three of the parameters (F, k, N), one set for flows less than 6.3 cfs and the other for flows greater than this flow.

The best model for Run 12 at 4.3 cfs is inconsistent (N = 5 instead of N = 4) with the other models. A closer examination of the data for this run revealed that the problem discussed in section 5.1, in connection with Run 15, is also significant here. This makes the calculated frequency response unreliable. Therefore, this model could be ignored in the development of parameter flowrate relationships.

Some general statements can be made concerning the effect of flowrate on model parameters. For flows less than 6.3 cfs the F appears to be fairly constant. The active volume accounts for between .8 and .9 of the total volume of the creek for these flows. For flows greater than 6.3 cfs the total volume can be considered essentially active with F = 1.0. Similarly the exchange rate is about .1 of the flow-through rate for the whole range of lower flows. When F = 1.0, the parameter k is meaningless. The residence times of both

McMASTER UNIVERSITY LIBRARY

Figure 5-10 Model Parameters as a Function of Flow

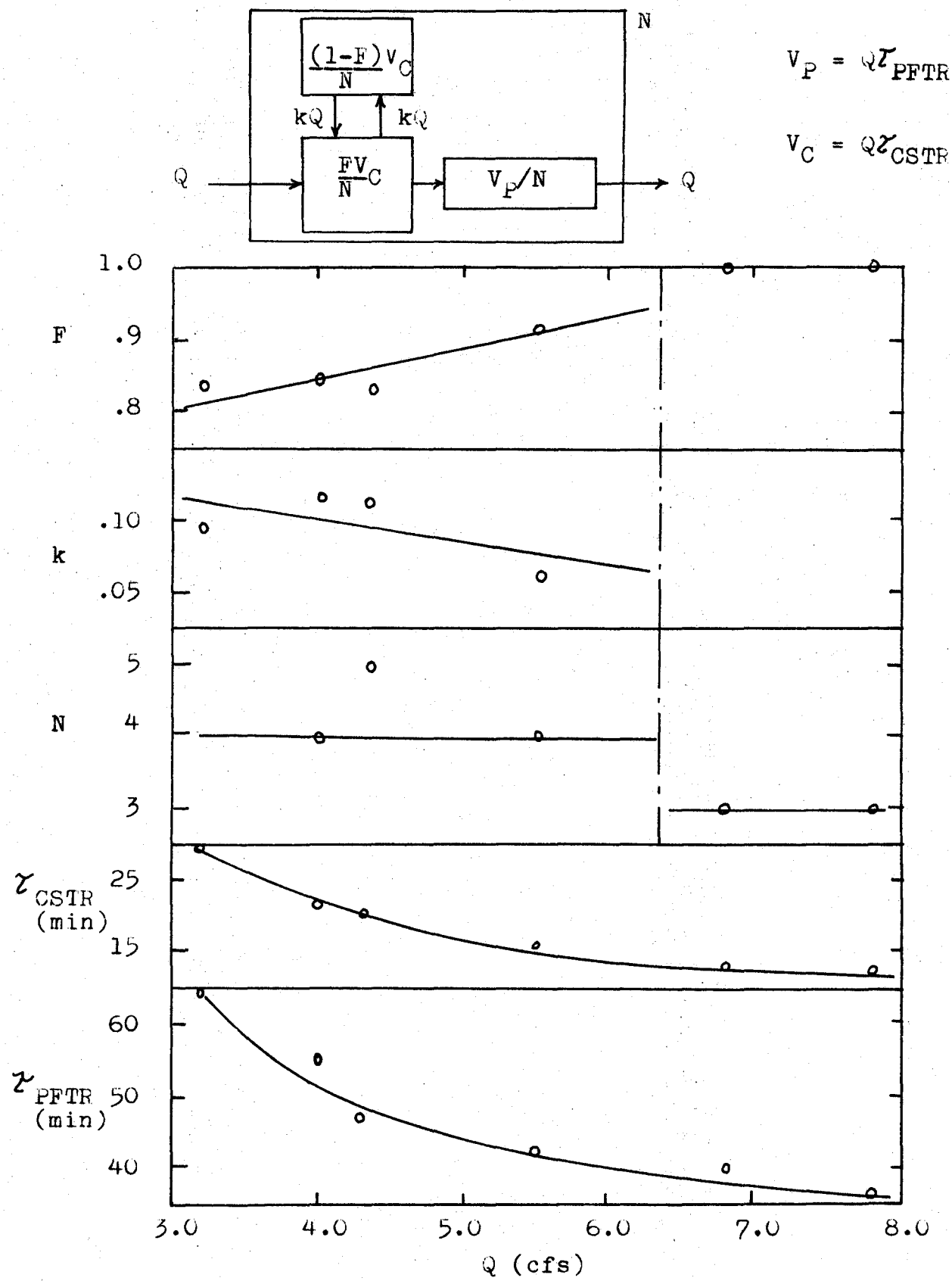

the CSTRs and PFTRs increase with decreasing flowrate as expected. Since the residence time is defined as V/Q this observation implies that the volume of the creek increases more slowly than the flowrate, a property common to most natural streams.

5.8 Recommendations for Future Work

The methods described in this study could be applied to a wide range of rivers and streams. Estuaries, however, require special consideration because of tidal action and their two dimensional or even three dimensional nature. It would be both useful and interesting to extend the modular approach to this type of mixing situation.

For large rivers and estuaries, radioactive tracer techniques offer more advantages than the fluorometric procedures used on the small creek in this work. Although the initial cost of the equipment would be high, data collection would be considerably easier for these systems.

CHAPTER 6

6. SUMMARY AND CONCLUSIONS

Several criteria, necessary to adequately characterize the mixing phenomena, were listed in the introduction (Chapter 1). All of these criteria have been satisfied by the modelling approach and techniques described in this paper.

The modular approach is extremely flexible and can be used to directly simulate the dominant mechanisms causing the mixing. The literature review amply illustrated how various networks of the ideal elements of a CSTR and a PFTR can be used to model a wide variety of mixing situations. The procedure outlined is not restricted to any one model such as the Stagnant Zone model. The manner in which stagnant zones were handled in this study (i.e. with the use of a parallel CSTR) illustrates how the physical situation can be directly simulated.

The use of frequency response techniques and a non-linear least squares analysis to evaluate model parameters is particularly useful. Models consisting of CSTRs and PFTRs are simple algebraic equations in the frequency domain as opposed to complex differential equations in the time domain. As discussed before, the advantage in using a least squares analysis is that both the statistically best values of the parameters and an estimate of model fit, are obtained.

A further advantage of the modular approach is that reaction kinetic information can be applied directly to predict conversions. In terms of systems and subsystems discussed in the statement of the problem, the mixing subsystem can be easily coupled to reaction kinetics subsystems using well established relations.

The field data required to evaluate these models is easily obtainable. Pulse techniques using fluorescent dyes, are extensively used for time-of-travel studies in natural streams. By employing the fluorometric procedures discussed in earlier chapters, these same tests could be used to supply all the data necessary to model the mixing. Not only pulses, but almost any input and the corresponding output can be used.

It has also been shown that the effect of streamflow can be included in the models. This would be especially useful in water quality studies where prediction of conditions at various flows is required.

REFERENCES

(1) Adler, R. J., "Finite Stage Modelling", Proceedings of the Fourth National Instrument Society of America Chemical and Instrumentation Symposium, 18A, 1962.

(2) Adler, R. J., W. M. Long, J. Rooze and H. Weinstein, "Use of Finite Stage Models For Analysis and Design of Continuous Chemical Reactors", World Petroleum Congress, Section VII, Paper 19, 1963, 103-120.

(3) Ambrose, E. R. Baumann and E. B. Fowler, "Three Tracer Methods for Determining Detention Times in Primary Clarifiers", Sewage and Industrial Wastes, Vol. 29, Jan., 1957, 24-33.

(4) Angus, R. M. and L. Lapidus, "Noise Characterization of Multiple Variable Linear System from Random Inputs", American Institute of Chemical Engineers Journal, Vol. 9, No. 6, Nov., 1963, 810-826.

(5) Archibald, R. S., "Radioactive Tracers in Flow Tests", Boston Society of Civil Engineers, 1949.

(6) Aris, R., "On the Dispersion of a Solute in a Fluid Flowing Through a Tube", Proceedings of the Royal Society of London, Vol. 235A, 1956, 67-77.

(7) Aris, R. and N. R. Amundson, "Some Remarks on Longitudinal Mixing or Diffusion in Fixed Beds", American Institute of Chemical Engineers Journal, Vol. 3, No. 2, June, 1957, 280-282.

(8) Aris, R. and N. R. Amundson, "Statistical Analysis of a Reactor", Chemical Engineering Science, Vol. 9, 1958, 250-262.

(9) Bailey, T. E., C. A. McCullough and C. G. Gunnerson, "Mixing and Dispersion Studies in San Francisco Bay", Journal of the Sanitary Engineering Division, ASCE, Vol. 92, No. SA5, 1966, p. 23.

(10) Barbagelata, A., "Chemical-Electric Measurement of Water", American Society of Civil Engineers, Papers, 1927-28, 789-802.

(11) Bischoff, K. B. and O. Levenspeil, "Fluid Dispersion-Generalization and Comparison of Mathematical Models", Chemical Engineering Science, Vol. 17, 1962, 245-264.

(12) Brown, M. C., T. Z. Wigley and D. C. Ford, "Water Budget Studies in Karst Aquifiers", Journal of Hydrology, Vol. 9, No. 1, 1969, 113-116.

(13) Buchanan, T. J., "Time of Travel of Soluble Contaminants in Streams", Journal of the Sanitary Engineering Division, ASCE, Vol. 90, No. SA3, June, 1964, 1-12.

(14) Buffham, B. A. and Gibilaro, "A Unified Time Delay Model for Dispersion in Flowing Media", Chemical Engineering Journal, Vol. 1, No. 1, 1970, p. 31.

(15) Butts, T. A., "Fluorometer Calibration Curves and Nomographs", Journal of the Sanitary Engineering Division, ASCE, Vol. 95, No. SA4, Aug., 1969, 705-714.

(16) Cederwall, K. and J. Hansen, "Tracer Studies on Dilution and Residence Time Distribution in Receiving Waters", Water Research, Vol. 2, 1968, 297-310.

(17) Chollette, A. and L. Cloutier, "Mixing Efficiency Determinations for Continuous Flow Systems", Canadian Journal of Chemical Engineering, Vol. 37, 1959, p. 105.

(18) Chollette, A., L. Cloutier and Blanchetet, "Performance of Flow Reactors at Various Levels of Mixing", Canadian Journal of Chemical Engineering, Vol. 38, 1960, p. 1.

(19) Clements, W. C. Jr., Pulse Testing for Dynamic Analysis, Ph.D. Thesis, Vanderbilt University, Nashville, Tenn., 1963.

(20) Clements, W. C. Jr., "A note on Determination of the Parameter of the Longitudinal Dispersion Model from Experimental Data ", Chemical Engineering Science, Vol. 24, 1969, p. 957.

(21) Clements, W. C. Jr. and K. B. Schnell Jr., "Pulse Testing for Dynamic Analysis", Industrial and Engineering Chemistry, Process Design and Development, Vol. 2, No. 2, 1963, p. 94.

(22) Corrigan, T. E. and W. O. Beavers, "Dead Space Interaction in Continuous Stirred Tank Reactor", Chemical Engineering Science, Vol. 23, 1968, 1003-1006.

(23) Dankwerts, R. N., "Continuous Flow Systems", Chemical Engineering Science, Vol. 2, No. 1, Feb., 1953, 1-13.

(24) Deans, H. A. and L. Lapidus, "A Computational Model for Predicting and Correlating the Behavior of Fixed-Bed Reactors", American Institute of Chemical Engineers Journal, Vol. 6, 1960, 656-668.

(25) Diachishin, A. N., "Dye Dispersion Studies", Journal of the Sanitary Engineering Division, ASCE, Vol. 89, No. SA1, 1963, p. 29.

(26) Dobbins, W. E., "BOD and Oxygen Relationships in Streams", Journal of the Sanitary Engineering Division, ASCE, Vol. 90, No. SA3, 53-78.

(27) Donaldson, Donald, "A Review of Tracer Material", Research Resources Progress, R. S. Kerr Water Research Centre.

(28) Dorf, R. C., Modern Control System, Addison-Wesley, Reading, Mass., 1969.

(29) Draper, C. S., N. McKay and S. Lees, Chapter 25, Instrument Engineering, Vol. II, McGraw Hill Book Co. Inc., New York, 1953, 651-705.

(30) Dreifke, G. E., Effects of Input Pulse Shape and Width on Accuracy of Dynamic Systems, Ph.D. Thesis, Washington University, 1961.

(31) Dreifke, G. E. and J. O. Hougen, "Experimental Determination of System Dynamics by Pulse Methods", Fourth Joint Automatic Control Conference, University of Minnesota, June, 1963, 608-633.

(32) Dreifke, G. E. and J. O. Hougen, "Process Diagnosis and Model Formulation by Pulse Methods", Paper presented at the Instrument Society of America, AID/CHEMPID Symposium, Montreal, May, 1965.

(33) Dreifke, G. E., J. O. Hougen and G. Mesmer, "Effects of Truncation on Time to Frequency Response Domain Conversions", Instrument Society of America, Transactions, Vol. 1, No. 4, 1962, 353-368.

(34) Dysinger, G. C., D. E. Griffin and W. S. Stewart, "Dynamics of Partially Mixed Stirred Tank Reactors", Joint Automatic Control Conference, 7th, Seattle, Washington, Aug. 17-19, 1966, 312-320.

(35) Elder, J. S., "The Dispersion of Marked Fluid in Turbulent Shear Flow", Journal of Fluid Mechanics, Vol. 5, 1959, 544-560.

(36) Esterson, G. L. and R. E. Hamilton, "Dynamic Response of Continuous Stirred Tank", Joint Automatic Control Conference, June 24-26, 1964, 155-161.

(37) Feuerstein, D. L. and R. E. Sellach, "Fluorescent Tracers for Dispersion Measurements", Journal of the Sanitary Engineering Division, ASCE, Vol. 89, No. SA4, Aug., 1963, 121-135.

(38) Filon, L. N. G., "On a Quadrature Formula for Trigonometric Integrals", Proceedings of the Royal Society of Edinburgh, Vol. 49, No. 38, 1928.

(39) Fisher, H. B., "Methods for Predicting Dispersion Coefficients In Natural streams With Applications to Lower Reaches of the Green and Duwamish Rivers, Washington", Geological Survey Professional Paper 582-A, United States Government Printing Office, Washington, 1968.

(40) Fisher, H. B., "Dispersion Predictions in Natural Streams", Journal of the Sanitary Engineering Division, ASCE, Vol. 94, No. SA5, Oct., 1968, 927-943.

(41) Fisher, H. B., "The Effect of Bends on Dispersion in Streams", Water Resources Research, Vol. 5, No. 2, April, 1969, p. 496.

(42) Fluorometry Reviews, "Fluorometry in Studies of Pollution and Movement of Fluids", G. K. Turner Assoc., No. 9941, 1968.

(43) Frederick, B. J. and R. G. Godfrey, "The Effect of Finite Boundaries on Measurement of Gold-198 with a Scintillation Detector", Geological Survey Professional Paper 424-D, United States Government Office, Washington, 1961.

(44) Gibilaro, L. C., H. W. Krophaller and D. J. Spihins, "Solution of Mixing Model due to Van de Vusse by Simple Probability Method", Chemical Engineering Science, Vol. 22, No. 4, April, 1967, 517-523.

(45) Glenne, B. and R. E. Sellach, "Longitudinal Estuarine Diffusion in San Francisco Bay, California", Water Research, Vol. 3, No. 1, 1969, 1-20.

(46) Godfrey, R. G. and B. J. Frederick, "Dispersion in Natural Streams", Open File Report, Geological Survey, U.S. Dept. of the Interior, Washington D.C., 1963.

(47) Harleman, D. R., "The Significance of Longitudinal Dispersion in the Analysis of Pollution in Estuaries", Advances in Water Pollution Research, Tokyo, Vol. 1, 1964, p. 279.

(48) Harleman, D. R. F., Chook-Heng Lee and L. C. Hall, "Numerical Studies of Unsteady Dispersion in Estuaries", Journal of the Sanitary Engineering Division, ASCE, Vol. 94, No. SA5, Oct., 1968, p. 897.

(49) Harris, E. K., "A New Statistical Approach to the One-Dimensional Diffusion Model", International Journal of Air and Water Pollution, Vol. 7, 1963, p. 799.

(50) Hays, J. R., Mathematical Modelling of the Turbulent Diffusion Phenomena, M.Sc. Thesis, Vanderbilt University, Nashville, Tenn., 1964.

(51) Hays, J. R., W. C. Clements and T. R. Harris, "Modelling Techniques in the Frequency Domain", American Institute of Chemical Engineers Journal, March, 1967, p. 374.

(52) Hays, J. R. and P. A. Krenkel, "Mathematical Modelling of Mixing Phenomena in Rivers", Advances in Water Quality Improvement, University of Texas Press, 1968, p. 111.

(53) Hays, J. R., K. B. Schnelle and P. A. Krenkel, "Application of Frequency-Response Techniques to Analysis of Turbulent Diffusion Phenomena", Nineteenth Industrial Waste Conference, Purdue, 1964, 777-795.

(54) Hoover, T. E. and R. A. Arnoldi, "Computer Model of Pollution of the Connecticut River", Journal of the Water Pollution Control Federation, 42, R67, 1970.

(55) Hougen, J. O. and Walsh, "Pulse Testing Method", Chemical Engineering Progress, Vol. 57, No. 3, March, 1961, 69-79.

(56) Hull, D. E. and J. W. Kent, "Radioactive Tracers to Mark Interfacer and Measure Intermixing in Pipelines", Industrial Engineering Chemistry, Vol. 44, Part 2, No. 11, 2745-2750.

(57) Hull, D. E. and M. Macomber, "Flow Measurements By The Total Count Method", Proceedings of the Second United Nations International Conference in the Peaceful Use of Atomic Energy, 19, 1958, 324-332.

(58) Hutton, S. P. and E. A. Spencer, "Gauging Water Flow by Salt Dilution Method", Institute of Civil Engineers, Proceedings, Vol. 16, 1960, 395-418.

(59) Kent, R., "Diffusion in a Sectionally Homogenous Estuary", Journal of the Sanitary Engineering Division, ASCE, Vol. 86, No. SA2, 1960, p. 15.

(60) Kilpatrick, F. A., "Flow Calibration by Dye-Dilution Measurement", Civil Engineering, ASCE, Feb., 1968, 74-76.

(61) Klinkenberg, A., "Distribution of Residence Times in a Cascade of Mixed Vessels with Backmixing", Industrial and Engineering Chemistry, Fundamentals, Vol. 5, No. 2, May, 1966, 283-285.

(62) Krambeck, F. J., R. Shinnar and Katz, "Stochastic Mixing Models for Chemical Reactors ", Industrial and Engineering Chemistry, Fundamentals, Vol. 6, 1967, p. 276.

(63) Kramers, H. and G. Alberda, "Frequency Response Analysis of Continuous Flow Systems", Chemical Engineering Science, Vol. 2, 1953, 173-181.

(64) Krenkel, P. A., "Waste Dispersion Characteristics of Streams Using Turbulent Diffusion Phenomena", Journal of the Water Pollution Control Federation, Vol. 34, No. 12, Dec., 1962, 1204-1212.

(65) Krenkel, P. A., Discussion of "The Significance of Longitudinal Dispersion in the Analysis of Estuaries", Advances in Water Pollution Research, Vol. 1, 1965.

(66) Lager, J. and G. Tchobanoglous, "Effluent Disposal in South San Francisco Bay", Journal of the Sanitary Engineering, Division, ASCE, Vol. 94, No. SA2, April, 1968, p. 213.

(67) Lecli, U., "Prediction of RTD from Unsteady Behavior of Chemical Reacting Systems", Industrial and Engineering Chemistry, Fundamentals, Vol. 4, No. 3, Aug., 1965, 360-361.

(68) Leeds, J. V. and H. H. Bybee, "Solution of Estuary Problems and Networks", Journal of the Sanitary Engineering Division, ASCE, Vol. 93, No. SA3, June, 1967, 29-36.

(69) Lees, S., "Interpreting Dynamic Measurements of Physical Systems", Transactions, American Society of Mechanical Engineers, Vol. 80, 1958, 857-883.

(70) Lees, S. and R. C. Dougherty, "Refinement of the Pulse Testing Procedure-Computer Simulation", David Taylor Model Basin, Dept. Navy, #NONR 3897(03), Oct., 1964, Thayer School of Engineering.

(71) Levenspiel, O., "Mixed Models to Represent Flow of Fluids through Vessels", Canadian Journal of Chemical Engineering, Vol. 40, Aug., 1962, 135-138, and Vol. 41, 1963, p. 132.

(72) Levenspiel, O. and W. K. Smith, "Notes on the Diffusion-type Model for the Longitudinal Mixing of Fluids in Flow", Chemical Engineering Science, Vol. 6, 1957, p. 227.

(73) Levich, V. G., V. S. Markin and Yu. A. Chismadzhev, "On Hydrodynamic Mixing in a Model of a Porous Medium with Stagnant Zones", Chemical Engineering Science, Vol. 22, 1967, 1357-1367.

(74) Matthews, T., "Simulating Dynamics of Reactor Systems", Chemical Engineering, Vol. 71, No. 18, Aug. 31, 1964, 77-79.

(75) Melnyk, P. B., The Representation of the Non-ideal Mixing in a Flow Reactor by a Network of Idealized Components, M.Eng. Thesis, McMaster, 1970.

(76) Murphy, K. L. and B. Boyko, "Longitudinal Mixing in Spiral Flow Aeration Tanks", Journal of the Sanitary Engineering Division, ASCE, Vol. 96, No. SA2, April, 1970, 211-220.

(77) Murphy, K. L. and P. Timpany, "Design and Analysis of Mixing for an Aeration Tank", Journal of the Sanitary Engineering Division, ASCE, Vol. 93, No. SA5, Oct., 1967, 1-15.

(78) Murrill, P. N., R. W. Pike and C. L. Smith, "Dynamic Mathematical Models, Parts I-XII", Chemical Engineering, CE. Refresher Series, Sept. 1968 - Aug. 1969.

(79) Muszkalay, L. and I. Va'ga's, "Modification of the Tracer Measuring Method in Settling Basins", Sewage and Industrial Wastes, Vol. 30, No. 9, Sept., 1958, 1101-1107.

(80) Nyquist, J. K., R. M. Schendler and R. E. Gilbert, "Determination of Frequency Response from Step Response", Process Systems Engineering, Chemical Engineering Process Symposium Series, Vol. 59, No. 46, p. 98.

(81) O'Connell, R. L. and C. M. Walter, "Hydraulic Model Tests of Estuarial Waste Dispersion", Journal of the Sanitary Engineering Division, ASCE, Vol. 89, No. SA1, 1953, p. 51.

(82) O'Connor, D. J., "Oxygen Balance of an Estuary", Journal of the Sanitary Engineering Division, ASCE, Vol. 86, No. SA3, 1960, p. 35.

(83) O'Connor, D. J., "Estuarine Distribution of Non-Conservative Substances", Journal of the Sanitary Engineering Division, ASCE, Vol. 91, No. SA1, 1965, P. 23.

(84) Orlob, G. T., A. R. Shubinski and K. D. Feigner, "Mathematical Modelling of Water Quality in Estuarial Systems", ASCE National Symposium on Estuary Pollution, Stanfield University, California, Aug., 1967.

(85) Otto, R. E. and L. E. Stout, "The Moments Method of Analysis and Its Application to Mixing Dynamics", Chemical Engineering Progress Symposium, Series 57, No. 36, 1961, p. 69.

(86) Patterson, C. C., A Discussion of "Mathematical Modelling of Mixing Phenomena in Rivers", Advances in Water Quality Improvement, University of Texas Press, 1968, p. 124.

(87) Patterson, C. C. and E. F. Gloyna, "Dispersion Measurement in Open Channels", Journal of the Sanitary Engineering Division, ASCE, Vol. 91, No. SA3, 1965, p. 17.

(88) Paulson, R. W., "The Longitudinal Diffusion Coefficient in the Delaware River Estuary as Determined from a Steady-State Model", Water Resources Research, Vol. 5, No. 1, Feb., 1969.

(89) Quirk, T. P. and L. J. Eder, "Evaluation of Alternative Solutions for Achievement of River Standards", Journal of the Water Pollution Control Federation, Vol. 42, 1970, p. 272.

(90) Rebhun, M. and Y. Argaman, "Evaluation of Hydraulic Efficiency of Sedimentary Basins", Journal of the Sanitary Engineering Division, ASCE, Vol. 91, No. SA5, Oct., 1965, 37-45.

(91) Resnick, W. and D. Wolf, "RTD in Real Systems", Industrial and Engineering Chemistry, Fundamentals, Vol. 2, No. 4, Nov., 1963, 287-293.

(92) Retallick, W. B., "Distribution of Residence Times in a Cascade of Mixing Vessels with Backmixing", Industrial and Engineering Chemistry, Fundamentals, Vol. 4, No. 4, Feb., 1965, 88-90.

(93) Rippin, D. W. T., "Recycle Reactor as Model of Incomplete Mixing", Industrial and Engineering Chemistry, Fundamentals, Vol. 6, No. 4, Nov., 1967, 488-492.

(94) Roemer, M. H. and L. D. Darbin, "Transient Response and Moments Analysis of Backflow Cell Model for Flow Systems with Longitudinal Mixing", Industrial and Engineering Chemistry, Fundamentals, Vol. 6, No. 1, Feb., 1967, 120-129.

(95) Rooze, J. W., Determination of RTD using Deterministic and Random Signals, MSc. Thesis, Case Institute of Technology, 1963.

(96) Rosenbrock, H. H., "An Automatic Method for Finding the Greatest or Least Value of a Function", Computer Journal, Vol. 3, No. 3, 1960, p. 175.

(97) Sawyer, C. M., Tracer Studies on a Model Chlorine Contact Tank, M.Sc. Thesis, Virginia Polytechnical Institute.

(98) Sawyer, C. M. and P. H. King, "The Hydraulic Performance of a Chlorine Contact Tank", Purdue Industrial Wastes Conference, May, 1969, p. 20.

(99) Scalf, M. R. and B. L. DePrater, "Dye Tracer Method for Sewage Treatment Basins", Research Resources Progress, R. S. Kerr Water Research Centre, 1967.

(100) Schechter, R. S. and E. H. Wissler, "Frequency Response from Step Input Response", Industrial and Engineering Chemistry, Vol. 51, No. 8, Aug., 1959, 945-948.

(101) Shinnar, R. and P. Naor, "Representation and Evaluation of Residence Time Distribution", Industrial and Engineering Chemistry, Fundamentals, Vol. 2, No. 4, Nov., 1963, 278-286.

(102) Shinnar, R. and P. Naor, "Residence Time Distributions in Systems with Internal Reflux", Chemical Engineering Science, Vol. 22, No. 10, Oct., 1967, 1369-1381

(103) Shubinski, R. P., J. C. McCarty and M. R. Lindorf, "Computer Simulation of Estuarial Networks", Journal of the Hydraulics Division, ASCE, Vol. 91, No. HY5, Sept., 1965, p. 33.

(104) Simmon, H. B., "Application and Limitation of Estuary Models in Pollution Analyses", Waste Disposal in the Marine Environment, E. A. Pearson, Ed., Pergamon Press Inc., New York, N. Y., 1960, 540-546.

(105) Streeter, H. W. and Phelps, E. B., "A Study on the Pollution and Natural Purification of the Ohio River, III", Public Health Bulletin, No. 146, Washington, 1925.

(106) Taylor, G. I., "Dispersion of a Soluble Material in a Solvent Flowing Slowly Through a Tube", Proceedings of the Royal Society of London, Vol. 219A, 1953, p. 186.

(107) Taylor, G. I., "The Dispersion of Matter in Turbulent Flow Through a Pipe", Proceedings of the Royal Society of London, Vol. 223A, 446-468.

(108) Taylor, G. I., "Conditions under which Dispersion of a Solute in a Stream of Solvent can be used to Measure Molecular Diffusion", Proceedings of the Royal Society of London, Vol. 225A, 1954a, p. 473.

(109) Teasdale, A. R. and J. B. Reynolds, "Two Ways to Get Frequency Response from Transient Data", Control Engineering, Oct., 1955, 55-63.

(110) Thackston, E. L, J. R. Hays and P. A. Krenkel, "Least Squares Estimation of Mixing Coefficients", Journal of Sanitary Engineering Division, ASCE, Vol. 93, No. SA3, June, 1967, 47-58.

(111) Thackston, E. L. and P. A. Krenkel, "Longitudinal Mixing in Natural Streams", Journal of the Sanitary Engineering Division, ASCE, Vol. 93, No. SA5, Oct., 1967, 67-90.

(112) Thackston, E. L. and K. B. Schnelle, "Predicting Effects of Dead Zones on Stream Mixing", Journal of the Sanitary Engineering Division, ASCE, Vol. 96, No. SA2, April, 1970, p. 319.

(113) Thayer, R. P. and R. G. Krutchkoff, "Stochastic Model for BOD and DO in Streams", Journal of the Sanitary Engineering Division, ASCE, Vol. 93, No. SA3, June, 1967, 59-72.

(114) Thomann, R. V., "Mathematical Model for Dissolved Oxygen", Journal of the Sanitary Engineering Division, ASCE, Vol. 89, No. SA5, Oct., 1963.

(115) Thomas, H. A. Jr. and J. M. Archibald, "Longitudinal Mixing Measured by Radioactive Tracers", American Society of Civil Engineers, Transactions, Paper #2518, 1951.

(116) Van De Vusse, J. C., "A New Method for Stirred Tank Reactor", Chemical Engineering Science, Vol. 17, 1962, 507-521.

(117) Wen, C. Y. and S. F. Chang, "Dynamic Response Equations for Various Reactor Models", Canadian Journal of Chemical Engineering, Vol. 43, No. 3, June, 1965, 101-109.

(118) White, E. T., "On Deadwater Regions and Stagnant Zones in Mixing", Canadian Journal of Chemical Engineering, June, 1963, p. 131.

(119) Williams, J. A., R. J. Adler and W. J. Zolner, "Parameter Estimation of Unsteady State Distributed Models in the Laplace Domain", Industrial and Engineering Chemistry, Fundamentals, Vol. 9, No. 2, 1970.

(120) Wilson, J. F. Jr., "Fluorometric Procedures for Dye Tracing", Techniques of Water-Resources Investigation of U. S. Geological Survey, Chapter A12.

(121) Wright, R. R. and M. R. Collings, "Application of Fluorescent Tracing Techniques to Hydrologic Studies", Journal of the American Water Works Association, June, 1964, 748-754.

APPENDIX A

A EXPERIMENTAL APPARATUS

A.1 Dye Injection Apparatus

1 Sigmamotor kinetic clamp pump, AL4E40

1 Mechanical low frequency sine generator (75)

1 Set of 100:1 gear reducers

1 1,500 watt portable gasoline generator

1 5 gallon polyethylene container

20 ft. of rubber tubing

A.2 Monitoring Apparatus

2 Turner 111 fluorometers

2 5 ml. flowthrough doors

2 Primary filters, narrow pass, color spec. #546

2 Secondary filters, narrow pass, color spec. #590

2 Far UV lamps

1 10" Honeywell Electronik 194 single pen recorder, multi-span, 11-position zero

1 10" Honeywell Electronik 194 single pen recorder, multi-span 2-position zero

2 3,000 watt portable gasoline generators

2 Constant voltage transformers, 120VA*, SOLA23-22-112

2 Selfix -6213 voltmeters

2 Self-priming pumps, JABSCO -B3M6

1 YSI-TELE-Thermometer

10 B-4J NUPRO valves

50 ft. of polyethylene tubing, .25" I.D.

1 Stop clock

2 litres of Rhodamine WT, 20% sol.

1 pair of hip waders

Assorted lengths of 1/2" diam. aluminum rods, with clamps and connectors (sampling frame)

* Constant voltage transformer was too small. At least 240 VA would be preferable.

A.3 Extra Calibration Equipment

4 1,000 ml. volumetric flasks

2 Powerstat variable transformers

5 Pipettes, 5 ml., 10 ml., 20 ml., 50 ml., and 100 ml.

A.4 Miscellaneous

1 1.5' throat Parshall flume, constructed from 3/4" plywood and 2" x 2" cedar

200 Sand bags

3 Platforms for injection and monitoring apparatus, made from 3/4" plywood and 2" x 2" cedar

3 Black polyethylene tarps to cover platforms

APPENDIX B

B.1 FLUOROMETER CALIBRATIONS

B.1.1 Procedure

Since all three scales of light intensity were used, a wide range of dye concentrations were necessary to give an adequate calibration of fluorometer reading vs. concentration. Standard solutions of 2.4 ppb to 800 ppb were made up from a twenty percent concentrated dye solution and distilled water. Various pipettes and 1,000 ml. volumetric flasks were used to carry out the series of dilutions necessary to make up these solutions. Table B-1 illustrates how this was done.

TABLE B-1

Dilute x ml. of y solution to z ml.				
Solution	x	y	z	Final concentration
A*				2.38×10^8 ppb
B**	10	A	595	4.0×10^6 ppb
C	10	B	1,000	4.0×10^4 ppb
D	20	C	1,000	800 ppb
E	15	C	1,000	600 ppb
F	10	C	1,000	400 ppb
G	500	F	1,000	200 ppb
H	250	F	1,000	100 ppb
I	150	F	1,000	60 ppb
J	100	F	1,000	40 ppb
K	75	F	1,000	30 ppb

TABLE B-1 (Continued)

Solution	x	y	z	Final concentration
L	50	F	1,000	20 ppb
M	150	I	1,000	9 ppb
N	100	I	1,000	6 ppb
O	40	I	1,000	2.4 ppb

*A Initial solution 20% Rhodamine WT, S.G. 1.19

Initial conc. = $1.19 \times .2 = 2.38 \times 10^8$ ppb.

**B First dilution

$$(V_a + V_i)\, C_f = C_i V_i$$

where C_i = initial concentration

V_i = initial volume

C_f = desired final concentration

V_a = volume of dilutent

Using V_i = 10 ml., $C_f = 4.00 \times 10^6$ ppb

$$V_a = \frac{2.38 \times 10^8 \times 10}{4.0 \times 10^6} - 10 = 585 \text{ ml.}$$

Both fluorometer and recorder were allowed to warm up for two hours in the laboratory. Veriacs were used to set the line voltage to the output voltage of the generators in the field. The standard solutions were pumped through the fluorometer using the same pump and tubing as in the field. At least 1,000 ml. of each standard solution was required for each fluorometer. Background readings were taken using distilled water. For each solution, readings were taken on

all possible scales. The temperature of the sample after it has passed through the fluorometer was continuously monitored.

B. 1.2 Results

Since three different calibrations were undertaken, the amount of data collected is excessive. Only an example set of results is shown here. Table B-2 gives the results for the 30x scale of the input fluorometer. It may appear, from looking at the numbers in this table, that the results from the various calibrations would probably agree within experimental error. However, when these results were plotted, each set was consistently different from the others. On this basis, it was concluded that the calibration had changed slightly over the period of testing and that it would be necessary to use different calibration curves for different runs.

The fluorometers are designed so that the relationship between fluorometer reading and concentration is linear. However, for the older of the two fluorometers, the relationship was found to be non-linear at very low concentrations. A standard computer subroutine was used to regress these calibration curves. A summary of the coefficients of the regression equations is listed in Table B-3.

TABLE B-2

Calibration Results for Input Fluorometer, 30x Scale

Calibration #1

Concentration of Stand. Sol.	Reading	Reading-Background	Temp. (°C)*	$Reading_{25}$
Background	.2			
2.4	2.8	2.6	29.5	3.00
6.0	9.0	8.8	29.0	10.00
9.0	13.3	13.1	29.0	14.89
12.0	19.0	18.8	29.0	21.38
20.0	31.5	31.3	29.0	35.59
30.0	49.5	49.3	29.0	56.05
40.0	63.0	62.8	29.5	72.53
50.0	79.0	78.8	29.5	91.01
60.0	91.0	90.8	29.0	103.24

TABLE B-2 (Continued)

Calibration Results for Input Fluorometer, 30x Scale

Calibration #2

Concentration of Stand. Sol.	Reading	Reading-Background	Temp. (°C)*	Reading 25
Background	.2			
2.4	2.8	2.6	29.5	2.91
6.0	8.2	8.0	30.0	9.39
9.0	13.4	13.2	30.0	15.5
20.0	30.0	29.8	31.0	34.88
30.0	46.2	46.0	30.5	54.83
40.0	60.2	60.0	30.0	70.44
60.0	87.2	87.0	30.0	102.14

TABLE B-2 (Continued)

Calibration Results for Input Fluorometer, 30x Scale

Calibration #3

Concentration of Stand Sol.	Reading	Reading-Background	Temp. (°C)*	Reading 25
Background	.8			
2.4	3.0	2.2	26.7	2.32
6.0	8.2	7.4	26.9	7.87
9.0	13.0	12.2	27.1	13.05
20.0	31.2	29.4	27.1	32.53
30.0	43.8	43.0	25.9	44.25
40.0	63.0	62.2	27.9	68.23
60.0	90.0	89.2	28.5	99.81

*Temperature correction factor discussed in section B.2.

TABLE B-3

Calibration Coefficients

Code: A - 30x scale, 0 - intercept, 1 - non-linear portion

B - 10x scale, 1 - first order term, 2 - linear portion

C - 3x scale, 2 - second order term

D - 1x scale

BRx - Reading on the x scale above which the relationship is linear

Calibration	Scale	A-30x Input	A-30x Output	B-10x Input	B-10x Output	Remark
#3	01		.173		1.01	Input and Output to Runs 14,15, 16,17
	11		.645		1.70	
	21		-1.02E-02		-2.40E-02	
	BR		11.28		5.54	
	02	1.11	2.30	-.984	4.70	
	12	5.91E-01	.336	7.10	.866	
#2	01		.611		.685	Input and Output to Runs 8,11,12
	11		.895		7.30	
	21		-2.32E-02		-1.95	
	31				.143	
	BR		15.9		9.91	
	02	.0903	3.55	4.19	11.08	
	12	.575	.350	6.50	.801	
#1	01		.879		1.18	Input and Output to Run 6 Input = Output to Runs 1-4
	11		.429		1.21	
	21					
	BR		12.5		15.6	
	02	.185	1.23	4.08	7.87	
	12	.559	.360	6.70	.809	

TABLE B-3 (Continued)

Calibration Coefficients

Calibration	Scale	C-3x Input	C-3x Output	D-1x Input	D-1x Output	Remark
#3	01					Input and Output to Runs 14,15, 16,17
	11					
	21					
	BR					
	02	13.4				
	12	22.47				
#2	01					Input and Output to Runs 8,11,12
	11					
	21					
	31					
	BR					
	02	-11.55				
	12	19.18				
#1	01					Input and Output to Run 6 Input = Output to Runs 1-4
	11					
	21					
	BR					
	02	-3.58			20.43	
	12	19.53			8.85	

B.2 TEMPERATURE EFFECT

B.2.1 Procedure

The fluorometer reading is dependent on the temperature as well as the concentration of the sample. This effect was measured over a range of 10°C - 35°C. To do this, five standard solutions were prepared as in section B.1. The concentrations were selected so that the effect could be measured on all the scales used on both fluorometers.

The dye solutions were first cooled to about 10°C using an ice bath. The solution was then recycled through the fluorometer using the pump as before. This continual pumping slowly heated the solution up. The temperature was continually monitored at the outlet of the fluorometer. Periodically, the fluorometer dial reading and the corresponding temperature were recorded.

B.2.2 Results

A complete list of the experimental results for these tests is given in Table B-4.

A base temperature of 25°C was chosen. If the relationship

$$\frac{F_t}{F_{25}} = e^{n(t-25)}$$

where F_t = fluorometer reading at t°C

F_{25} = fluorometer reading at 25°C

and n = constant to be evaluated,

TABLE B-4

TEMPERATURE VS. FLUOROMETER READING

(i) Input

Sample Conc.	Scale	Temp.	Read.	Read-Back	F/F_{25}
Background	30x	28.2	1.0		
	10x	27.9	.5		
	3x	27.7	.3		
30 ppb	30	14.3	61.0	60.0	1.36
		15.8	57.0	56.0	1.27
		17.2	55.0	54.0	1.225
		19.6	52.0	51.0	1.16
		21.0	50.0	49.0	1.11
		23.5	47.0	46.0	1.04
		25.9	44.0	43.0	.975
		27.5	42.0	41.0	.93
		29.3	40.0	39.0	.885
		30.9	38.0	37.0	.84
		32.0	36.0	35.0	.794
		34.1	32.0	31.0	.704
400 ppb	10x	15.2	90.0	89.5	1.388
		16.5	85.0	84.5	1.31
		18.4	81.0	80.5	1.25
		20.2	77.0	76.5	1.19

TABLE B-4 (Continued)

(i) Input (Continued)

Sample Conc.	Scale	Temp.	Read.	Read-Back	F/F_{25}
400 ppb	10x	21.3	74.0	73.5	1.14
		22.7	71.0	70.5	1.09
		24.3	67.0	66.5	1.03
		25.0	65.0	64.5	1.0
		26.8	62.0	61.5	.955
		28.0	60.0	59.5	.92
		29.3	58.0	57.5	.89
		30.2	56.0	55.5	.86
		32.9	52.0	51.5	.80
500 ppb	3x	11.5	51.0	50.7	1.51
		12.9	49.0	49.7	1.48
		15.2	45.0	44.7	1.34
		17.2	42.0	41.7	1.24
		19.5	40.0	39.7	1.18
800 ppb	3x	22.0	37.0	36.7	1.095
		23.9	35.0	34.7	1.035
		25.9	33.0	32.7	.975
		28.1	31.0	30.7	.916
		30.3	29.0	28.7	.857
		32.5	27.0	26.7	.797

TABLE B-4 (Continued)

(ii) Output

Sample Conc.	Scale	Temp.	Read.	Read-Back	F/F_{25}
Background	30x		.7		
	10x		.4		
20 ppb	30x	13.0	80.0	79.3	1.50
		14.5	76.0	75.3	1.43
		15.9	73.0	72.3	1.37
		17.7	69.0	68.3	1.30
		19.4	66.0	65.3	1.24
		20.9	63.0	62.3	1.18
		22.7	58.0	57.3	1.09
		25.3	53.0	52.3	.993
		26.7	50.0	49.3	.938
		27.9	48.0	47.3	.898
		30.7	43.0	42.3	.805
		32.2	41.0	40.3	.765
		33.6	39.0	38.3	.728

TABLE B-4 (Continued)

(ii) Output (Continued)

Sample Conc.	Scale	Temp.	Read.	Read-Back	F/F_{25}
60 ppb	10x	13.9	93	92.6	1.44
		15.0	90	89.6	1.395
		16.2	87	86.6	1.35
		17.2	84	83.6	1.30
		18.3	81	80.6	1.255
		19.3	78	77.6	1.21
		20.5	75	74.6	1.16
		21.7	72	71.6	1.12
		23.0	69	68.6	1.07
		24.2	66	65.6	1.02
		25.8	63	62.6	.975
		27.1	60	59.6	.93
		28.5	57	56.6	.883
		29.9	54	53.6	.835
		31.5	51	50.6	.788
		33.2	48	47.6	.74

is to hold, then a plot of F_t/F_{25} vs t on semi-log paper will be a straight line. The slope of this line would be equal to n. Figure B-1 shows such a plot. The cluster of data definitely indicates a straight line relationship. The line shown was fitted by eye and has a slope of $n = -.032$. This value was used to correct readings for temperature on all pulse and sine runs.

Figure B-1 Temperature Calibration

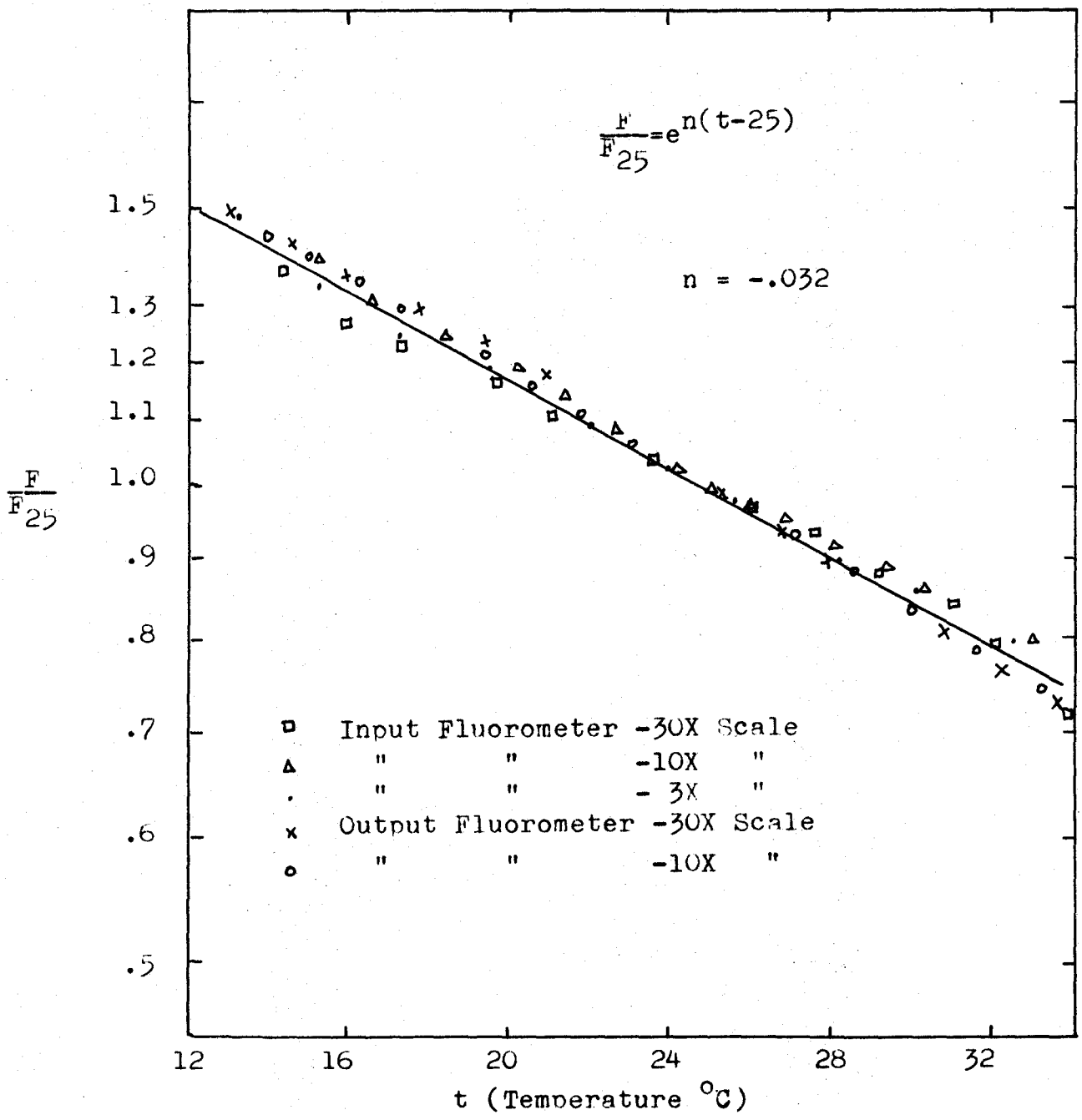

APPENDIX C

C MODEL TRANSFER FUNCTIONS AND TIME DOMAIN SOLUTIONS

C.1 CSTR

C.1.1 Derivation of the Transfer Function of a CSTR

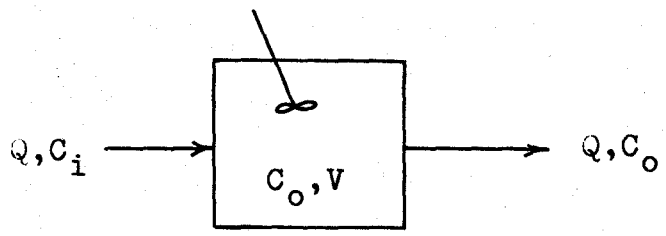

Doing a mass balance for a CSTR we obtain

$$V \frac{dC_o}{dt} = Q(C_i - C_o) \qquad \text{C.1-1}$$

where V = volume of the reactor,

Q = inlet feed rate,

t = time,

C_o = outlet concentration, and

C_i = inlet concentration.

Defining τ, the residence time, as

$$\tau = V / Q \qquad \text{C.1-2}$$

we can write C.1-1 as

$$\tau \frac{dC_o}{dt} = C_i - C_o \qquad \text{C.1-3}$$

Taking the Laplace transform of C.1-3 with initial conditions zero we obtain

$$\tau s\bar{C}_o = \bar{C}_i - \bar{C}_o$$

or with rearrangement

$$\frac{\bar{C}_o}{\bar{C}_i} = \frac{1}{\tau s + 1} \qquad \text{C.1-4}$$

where the bar denotes a transformed quantity. A transfer function is defined as the Laplace transform of the output over the Laplace transform of the input. Therefore, the transfer function of a CSTR, $G_{CSTR}(s)$, is

$$G_{CSTR}(s) = \frac{1}{\tau s + 1} \qquad \text{C.1-5}$$

C.1.2 Time Domain Solution of the CSTR

The time domain solution of the CSTR, for an impulse input, is

$$\frac{C_o}{C_i} = \frac{1}{\tau} e^{-t/\tau} \qquad \text{C.1-6}$$

This is the solution of the differential equation C.1-3. The transfer function could also have been derived by taking the Laplace transform of C.1-6.

C.2 PFTR

C.2.1 Time Domain Solution of the PFTR

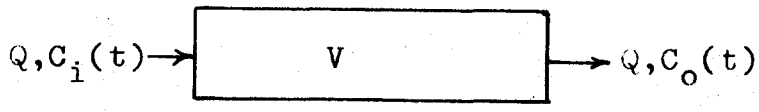

The general solution of a PFTR for any input is defined in the time domain as

$$C_o(t) = C_i(t-\tau) \qquad \text{C.2-1}$$

C.2.2 Derivation of the Transfer Function of a PFTR

The transfer function is derived by taking the Laplace transform of equation C.2-1. Employing the property of these transforms that $L[f(t-c)] = e^{-cs}F(s)$ we can write

$$\frac{\overline{C}_o(s)}{\overline{C}_i(s)} = e^{-\tau s} \qquad \text{C.2-2}$$

Therefore,

$$G_{PFTR}(s) = e^{-\tau s} \qquad \text{C.2-3}$$

C.3 Stagnant Zone Model

C.3.1 Derivation of the Transfer Function of the Stagnant Zone Model

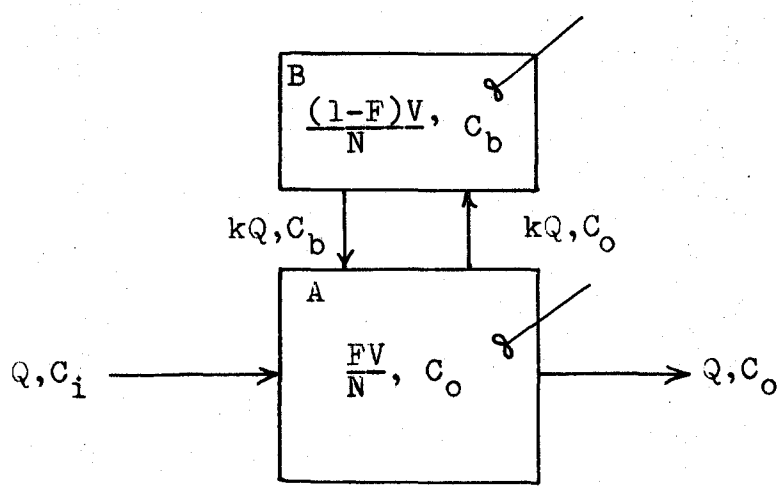

In the above figure, the new parameters are:

F = fraction of a single stage volume occupied by vessel A,

k = fraction of total flow Q which interchanges between vessel A and vessel B, and

N = number of units making up the entire system.

The volume of A vessel = FV/N and the volume of B vessel is (1-F)V/N. A material balance on A gives

$$\frac{FV}{N}\frac{dC_o}{dt} = Q(C_i - C_o) + kQ(C_b - C_o) \qquad \text{C.3-1}$$

A similar balance on B vessel gives

$$\frac{(1-F)V}{N}\frac{dC_b}{dt} = kQ(C_o - C_b) \qquad \text{C.3-2}$$

Introducing a dimensionless time

$$\theta = \tau t \qquad \text{C.3-3}$$

equation C.3-1 becomes

$$\frac{F}{N}\frac{dC_o}{d\theta} = C_i - C_o + k(C_b - C_o) \qquad \text{C.3-4}$$

and equation C.3-2 becomes

$$\frac{1-F}{N}\frac{dC_b}{d\theta} = k(C_o - C_b) \qquad \text{C.3-5}$$

Taking the Laplace transform of C.3-5 and C.3-4 with initial conditions zero we have

$$\frac{F}{N}s\bar{C}_o = \bar{C}_i - \bar{C}_o + k(\bar{C}_b - \bar{C}_o) \qquad \text{C.3-6}$$

and

$$\frac{1-F}{N}s\bar{C}_b = k(\bar{C}_o - \bar{C}_b) \qquad \text{C.3-7}$$

Solving equation C.3-6 and equation C.3-7 simultaneously

for $\bar{C}_o$ by eliminating $\bar{C}_b$ and simplfying we obtain

$$\bar{C}_o \left[\frac{F}{N} s + 1 + k - \frac{k^2}{\frac{1-F}{N}s + k} \right] = \bar{C}_i \qquad \text{C.3-8}$$

Therefore, the transfer function for a single stage is

$$\frac{\bar{C}_o}{\bar{C}_i} = \frac{\frac{1-F}{kN} s + 1}{\frac{F(1-F)}{kN^2} s^2 + \frac{k + 1-F}{kN} s + 1} \qquad \text{C.3-9}$$

and for N in series it is

$$G_{AH}(s) = \left[\frac{\frac{1-F}{kN} s + 1}{\frac{F(1-F)}{kN^2} s^2 + \frac{k+1-F}{kN} s + 1} \right]^N$$

The above derivation is from Clements (19).

C.3.2 Time Domain Solution of the Stagnant Zone Model

Those interested in the time domain solution for this model are referred to Adler et al (1, 2).

C.4 Dispersion Model

C.4.1 Transfer Function for the Dispersion Model

The function has been derived by Clements (19).

$$G_{DIS.}(s) = \exp \frac{Pe}{2} \left[1 - \sqrt{1 + 4s/Pe} \right] \qquad \text{C.4-1}$$

where Pe is the Peclet number.

C.4.2 Time Domain Solution of the Dispersion Model

This solution for an impulse input has been given by many (53, 110).

$$C_o(t) = \frac{M}{V} \sqrt{\frac{Pe}{4\ t/\tau}} \times \exp\left[- \frac{Pe(1-t/\tau)^2}{4t/\tau} \right] \qquad \text{C.4-2}$$

where M = mass of tracer used and the other parameters are as defined before.

C.5 Series CSTR + PFTR Model

C.5.1 Transfer Function of the Series CSTR + PFTR Model

The transfer function is a combination of the transfer function of sections C.1 and C.2.

$$G_{SCP}(s) = \left(\frac{1}{\tau_1 s + 1}\right)\left(\frac{1}{\tau_2 s + 1}\right) \cdots \left(\frac{1}{\tau_N s + 1}\right) e^{-\tau_{PFTR}\, s} \qquad \text{C.5-1}$$

where τ_1, τ_2 ... τ_N are the residence times of the first, second, and Nth CSTR in series, and τ_{PFTR} is the residence time of the PFTR in series.

C.5.2 Time Domain Solution of the Series CSTR + PFTR Model

The solution for an impulse input for equal sized CSTRs in series is

$$C_o(t) = \frac{M}{V} \frac{1}{\tau_N} \frac{N(t/\tau_N)^{N-1}}{(N-1)!} e^{-Nt/\tau_N + \tau} \qquad \text{C.5-2}$$

(parameters are all defined above)

APPENDIX D

D. COMPUTER PROGRAM FRRED

D.1 Description of Program

This program was used to do the bulk of the pulse data analysis. The general purpose is to calculate the experimental frequency response and transfer function from raw data. Any one of three types of inputs, an impulse, a pulse or step, could be used to collect the data. Points are taken directly from the graphs at two different time intervals. Smaller intervals can be used for quickly changing portions of the pulse and a large interval for slowly changing sections. The program converts the readings to temperature corrected dye concentration using read-in calibration coefficients. The required integrals can be evaluated using either the trapezoidal rule or Filon's quadrature. Included in the output are: the calculated frequency response (phase shift is calculated with and without the dead time), the frequency content of both the input and output pulses, the real and imaginary parts of the experimental transfer function, the areas under the pulses, the percent recovery, and the average residence time calculated from the first moments. Data can be punched for plotting or for curve fitting purposes. The program was used on a CDC 6400 machine.

D.2 Program Input

Each line is a different data card unless otherwise noted.

1. TITLE -Identification information - 80 spaces.
2. IN -Type of input, I1, IN=1 if step input used
   IN=2 if impulse input used
   IN=3 if pulse input used
3. JOB, M JOB = No. of sets of data being processed
   M = No. of frequencies at which output is required. I2, 8X, I3
4. NRS, NPD, NCFD If NRS = 1 -omit trapezoidal rule
   if NPD = 1 -plot data desired
   if NCFD = 1 -curve fit data desired.
   3I1
5. W(J), J=1, M -Frequencies at which output is required
   8F10.5
6. DTIME -Time before any output pulse is detected (consistent time units) F10.5
7. SUBINT -No. of subdivisions used for each time interval in trapezoidal method. F10.5
8. NX1, NX2, NY1, NY2 -No. of data points
   NX1, NY1 must be odd numbers
   NX2, NY2 must be even numbers
   I3, 7X, I3, 7X, I3, 7X, I3
   Only NY1, NY2 required if impulse data.

9. XINT1, XINT2, YINT1, YINT2 - time interval between data points

4F10.5

Only YINT1, YINT2 required if impulse data.

10. XBACK(I), I = 1, 4 -Background readings for scale I, input 1 - 30x, 2 - 10x, 3 - 3x, 4 - 1x

4F10.5, (Omit for impulse data)

11. YBACK(I), I= 1, 4 -As above for output

12. X(I), XNSC(I), XTEMP(I), I = 1, NX -input data

X(I) Read directly from recorder chart (span 0-100)

XNSC(I) -scale being used

XTEMP(I) -temperature in ^{o}C

NX = NX1 + NX2

F10.5, 10X, I1, 10X, F10.5

Omit for impulse data

13. Y(I), YNSC(I), YTEMP(I), I = 1, NY -output data as above

14. A01, A11, A21, A31 -calibrate constants for input

4(E15.8)

15. A02, A12 " " " "

16. B01, B11, B21, B31 " " " "

17. B02, B12 " " " "

18. C01, C11, C21, C31 " " " "

19. C02, C12 " " " "

20. D01, D11, D21, D31 " " " "

21. D02, D12 " " " "

22. BR30, BR10, BR3, BR1 as described in Appendix B -4F10.4

Repeat 14 - 22 for output

Only one set required for impulse input

I = Integer format, F = Floating point format,

E = Exponential format, X = Space

```
      PROGRAM FRFD(INPUT,OUTPUT,PUNCH,TAPE5=INPUT,TAPE6=OUTPUT,
     1   TAPE7=PUNCH)
C     FREQUENCY RESPONSE DATA IS OBTAINED FROM STEP DATA, IMPULSE, OR PULSE
C                                                                      DATA
      COMMON W(100),NR,SSIR,SSII,SSOR,SSOI
      COMMON AROUT,ARIN,PREC,SUBINT
      COMMON DTIME,TBAR
      DIMENSION  SI(100),SO(100),TREFR(100),
     1PHASE(1000),GAINM(100),GAIND(100),TREFI(100)
      DIMENSION TITLE(8),PHASP(100)
C     TITLE IS AN ALPHANUMERIC ARRAY WITH IDENTIFICATION INFORMATION
C     INTEGRALS ARE EVALUATED USING TRAPEZOIDAL RULE IF NR = 1
C     INTEGRALS ARE EVALUATED USING FILON QUADRATURE IF NR = 2
C     ONLY FILON QUADRATURE USED IF NRS=1
C     IF NPD=1 PLOTTING DATA WILL BE PUNCHED
C     IF NCFD=1 CURVE FITTING DATA WILL BE PUNCHED
C
C     COMMON INPUT DATA
C     TYPE OF INPUT, IN=1 FOR STEP INPUT, IN=2 FOR IMPULSE INPUT, AND IN=3
C     PULSE INPUT (I3)
C
C     NO OF SETS OF DATA, NO OF OMEGA VALUES, I2, 8X, I3
C     OMEGA VALUES, F10.5
C     DEAD TIME F10.5
C     DTIME IS THE TIME BEFORE ANY OUTPUT PULSE IS DETECTED-USE CONSISTENT
      READ(5,161) TITLE                                                UNITS
      WRITE(6,161) TITLE
      READ(5,119)  IN
      READ(5,100) JOB,M
      READ(5,119) NRS,NPD,NCFD
      READ(5,101) (W(J), J = 1,M)
      READ(5,101) DTIME
      DO 99 JN = 1,JOB
      NR=2
   30 CONTINUE
      DO 98 J= 1,M
      IF(IN-2) 200,201,202
  200 CALL FRESR(J)
      GO TO 203
  201 CALL FRFIR(J)
      GO TO 203
  202 CALL FRFPR(J)
  203 CONTINUE
C     CALCULATION OF TRANSFER FUNCTION FOR GIVEN OMEGA
C     TREFR IS TRANSFER FUNCTION REAL PART
C     TREFI IS TRANSFER FUNCTION IMAGINARY PART
C
      TREFR(J) = (SSOR * SSIR + SSOI * SSII) / (SSIR * SSIR + SSII *
     1SSII)
      TREFI(J) = (SSII * SSOR - SSOI * SSIR) / (SSIR * SSIR + SSII *
     1SSII)
C
C     CALCULATION OF MAGNITUDE RATIO
      GAINM(J) = SQRT(TREFR(J) * TREFR(J) + TREFI(J) * TREFI(J))
C
C     MAGNITUDE RATIO IN DECIBELS
      GAIND(J) = 20.0 * ALOG10(GAINM(J))
C
C     CALCULATION OF PHASE SHIFT
      PHASE(J)= 57.29578 * (ATAN(TREFI(J) / TREFR(J)))
      IF (TREFR(J))  11, 14,17
```

```
   11 IF (TRFFI(J)) 12, 13, 12
   12 TAN = PHASE(J) - 180.0
      GO TO 20
   13 TAN = -180.0
      GO TO 20
   14 IF (TRFFI(J)) 15, 21, 16
  15  TAN = -90.0
      GO TO 20
   16 TAN = -270.0
      GO TO 20
   17 IF (TRFFI(J)) 21, 21, 18
   18 TAN=PHASE(J) - 360.
   20 PHASE(J) = TAN
   21 PHASP(J)=PHASE(J)
C
C     THE EFFECT OF DEAD TIME ON PHASE ANGLE IS SUBTRACTED OUT
      PHASE(J)=PHASE(J)-DTIME*W(J)*57.29578
C
C     CALCULATION OF FREQUENCY CONTENT(SO(J)) OF OUTPUT PULSE
      IF(IN.EQ.1) GO TO 22
      SO(J)=SQRT(SSOR*SSOR+SSOI*SSOI)/ARIN
      IF(J.EQ.1)  SO(1) = 1.0
   22 IF(IN-2)  801,801,800
C     CALCULATION OF FREQUENCY CONTENT(SI(J)) OF INPUT PULSE
  800 SI(J)=SQRT(SSIR*SSIR+SSII*SSII)/ARIN
      IF(J.EQ.1)  SI(1) = 1.0
  801 CONTINUE
      IF(J.EQ.36) GO TO 24
      IF(J.EQ.76) GO TO 24
      IF(J.GT.1) GO TO 26
      IF(IN-2) 400,401,402
  400 WRITE(6,120)
      GO TO 403
  401 WRITE(6,121)
      GO TO 403
  402 WRITE(6,106)
  403 CONTINUE
      IF(NR.EQ.2) GO TO 25
   23 WRITE(6,107)
      GO TO 24
   25 WRITE(6,108)
   24 IF(IN-2) 241,242,240
  242 WRITE(6,134)
      GO TO 26
  240 WRITE(6,109)
      GO TO 26
  241 WRITE(6,129)
   26 B=J
      B1=B/5.0
      J1=J/5
      B2=J1
      IF(B1-B2) 27,28,27
   27 IF(IN-2) 272,270,271
  271 WRITE(6,110) GAINM(J),PHASE(J),PHASP(J),GAIND(J),W(J),SI(J),SO(J),
     1J
      GO TO 98
  272 WRITE(6,130) GAINM(J),PHASE(J),PHASP(J),GAIND(J),W(J),J
      GO TO 98
  270 WRITE(6,132) GAINM(J),PHASE(J),PHASP(J),GAIND(J),W(J),SO(J),J
      GO TO 98
```

```
 28 IF(IN-2) 282,280,281
282 WRITE(6,131) GAINM(J),PHASE(J),PHASP(J),GAIND(J),W(J),J
    GO TO 98
281 WRITE(6,111) GAINM(J),PHASE(J),PHASP(J),GAIND(J),W(J),SI(J),SO(J),
   1 J
    GO TO 98
280 WRITE(6,133) GAINM(J),PHASE(J),PHASP(J),GAIND(J),W(J),SO(J),J
 98 CONTINUE
    WRITE(6,117)
    WRITE(6,113) (TRFFR(J),TRFFI(J),W(J),J,J=1,M)
    WRITE(6,162) DTIME,TBAR
    IF(IN-2) 50,51,52
 51 WRITE(6,125) AROUT
    GO TO 50
 52 WRITE(6,116) ARIN,AROUT,PREC
 50 CONTINUE
    IF(NR.EQ.1) GO TO 99
    IF(NCFD.NE.1) GO TO 93
    DO 90 I=2,M
 90 WRITE(7,160) W(I),TRFFR(I),TRFFI(I)
 93 IF(NPD.NE.1) GO TO 91
    DO 92 I=1,M
 92 WRITE(7,163) W(I),GAIND(I),PHASE(I),PHASP(I)
 91 CONTINUE
    IF(NRS.EQ.1) GO TO 99
    NR=1
    GO TO 30
 99 CONTINUE
100 FORMAT(I2,8X,I3)
101  FORMAT(8F10.5)
102 FORMAT(4(I3,7X))
104 FORMAT(8F10.4)
106 FORMAT(1H1,15X,27HFREQUENCY RESPONSE RESULTS ,14HFOR PULSE TEST)
107 FORMAT(16X,23HUSING TRAPEZOIDAL RULE //)
108 FORMAT(16X,23HUSING FILON QUADRATURE //)
109 FORMAT(//9X,9HMAGNITUDE,5X,11HPHASE ANGLE,5X,11HPHASE ANGLE,7X,
   14HGAIN,9X,
   2 9HFREQUENCY,6X,17HINPUT FREQ. CONT.,6X,18HOUTPUT FREQ. CONT.,/
   311X,5HRATIO,8X,10HWITH DTIME,4X,13HWITHOUT DTIME,
   4 4X,8HDECIBELS,6X,11HRADIANS/MIN, 7X,13HDIMENSIONLESS,10X,
   513HDIMENSIONLESS/)
110 FORMAT(7X,F9.4,F16.2,F16.2,F14.4,F15.4,9X,F11.4,12X,F11.4,12X,I3)
111 FORMAT(7X,F9.4,2F16.2,F14.4,F15.4,9X,F11.4,12X,F11.4,12X,I3//)
113 FORMAT(3F15.5,40X,I3)
114 FORMAT(1H1,(4(F10.5,10X,I3))
115 FORMAT(10X,I3,2F15.6)
116 FORMAT(///,10X,5HARIN=,E12.4,10X,6HAROUT=,E12.4,10X,
   1 17HPERCENT RECOVERY=,F8.1)
117 FORMAT(1H1)
119 FORMAT(3I1)
120 FORMAT(1H1,15X,27HFREQUENCY RESPONSE RESULTS ,13HFOR STEP TEST//)
121 FORMAT(1H1,15X,27HFREQUENCY RESPONSE RESULTS ,16HFOR IMPULSE TEST/
   1/)
125 FORMAT(///,13X,6HAROUT=,E12.4)
129 FORMAT(//9X,9HMAGNITUDE,5X,11HPHASE ANGLE,5X,11HPHASE ANGLE,7X,
   1 4HGAIN,9X,
   2 9HFREQUENCY,9X,/11X,5HRATIO,8X,10HWITH DTIME,4X,13HWITHOUT DTIME,
   3 4X,8HDECIBELS,6X,11HRADIANS/MIN/)
130 FORMAT(7X,F9.4,2F16.2,F14.4,F15.4,12X,I3)
131 FORMAT(7X,F9.4,2F16.2,F14.4,F15.4,12X,I3//)
132 FORMAT(7X,F9.4,2F16.2,F14.4,F15.4,9X,F11.4,12X,I3)
```

```
  133 FORMAT(7X,F9.4,2F16.2,F14.4,F15.4,9X,F11.4,12X,I3//)
  134 FORMAT(//9X,9HMAGNITUDE,5X,11HPHASE ANGLE,5X,11HPHASE ANGLE,7X,
     1 4HGAIN,9X,
     2 9HFREQUENCY,6X,17HOUTPUT FREQ. CONT,/11X,5HRATIO,8X,10HWITH DTIME
     3,4X,13HWITHOUT DTIME,
     5 4X,8HDECIBELS,6X,11HRADIANS/MIN, 7X,13HDIMENSIONLESS/)
  160 FORMAT(3E15.8)
  161 FORMAT(8A10)
  162 FORMAT(//,10X,6HDTIME=,F10.6,20X,5HTBAR=,F10.6)
  163 FORMAT(4E15.8)
      STOP
      END
      SUBROUTINE FREPR(J)
C     SUBROUTINE CALCULATES NECESSARY INTEGRALS FOR PULSE INPUTS AND
C     CORRESPONDING OUTPUTS.
      COMMON W(100),NR,SSIR,SSII,SSOR,SSOI
      COMMON AROUT,ARIN,PREC,SUBINT
      COMMON DTIME,TBAR
      DIMENSION X(600),Y(600),PIN(600),POUT(600)
      DIMENSION NSCX(600),NSCY(600),XTEMP(600),YTEMP(600)
      DIMENSION YBACK(4),XBACK(4)
      IF(J.GT.1)  GO TO 6
      IF(NR.EQ.1) GO TO 6
C     NUMBER OF SUBDIVISIONS PER TIME INTERVAL F10.5
C     NUMBER OF DATA POINTS, NX1, NX2, NY1, NY2, (I3,7X,I3,7X,I3,7X,I3)
C     TIME INTERVAL BETWEEN DATA POINTS, XINT1, XINT2, YINT1, YINT2, 4F10.5
C
C     XINT1 IS THE TIME INTERVAL FOR NX1 POINTS
C     XINT2 IS THE TIME INTERVAL FOR NX2 POINTS
C     YINT1 IS THE TIME INTERVAL FOR NY1 POINTS
C     YINT2 IS THE TIME INTERVAL FOR NY2 POINTS
C     NX2, NY2 MUST BE EVEN NUMBERS
C     NX1, NY1 MUST BE ODD NUMBERS                                      PTS)
C     TOTAL NUMBER OF INPUT  DATA POINTS IS NX=NX1+NX2 ( INCLUDING ZERO END
C     TOTAL NUMBER OF OUTPUT DATA POINTS IS NY=NY1+NY2 ( INCLUDING ZERO END
C     SUBINT IS THE NUMBER OF SUBDIVISIONS PER TIME INTERVAL            PTS)
C     XBACK(I), YBACK(I) ARE THE BACKGROUND CHART READINGS FOR SCALE(I) OF
C     INPUT AND OUTPUT RESP. (4F10.5)
C     NSC(I) SIGNIFIES ON WHICH SCALE THE READING WAS TAKEN (I1)
C        1 - 30X SCALE
C        2 - 10X SCALE
C        3 -  3X SCALE
C        4 -  1X SCALE
C     TEMP(I) IS THE TEMPERATURE IN DEG. C AT WHICH THE READING WAS TAKEN
C     FORMAT FOR DATA, NSC, TEMP IS F10.5,I1,10X,F10.5                  F10.5
C
      READ(5,101) SUBINT
      READ(5,102) NX1,NX2,NY1,NY2
      READ(5,101) XINT1,XINT2,YINT1,YINT2
      NX= NX1 + NX2
      NY= NY1 + NY2
      READ(5,137) (XBACK(I),I=1,4)
      READ(5,137) (YBACK(I),I=1,4)
      READ(5,140) (X(I),NSCX(I),XTEMP(I),I=1,NX)
      READ(5,140)(Y(I),NSCY(I),YTEMP(I),I=1,NY)
C
C     DATA IS CONVERTED TO CONC. AFTER TEMP. ADJUSTMENT IN SUBR. CALIB.
      CALL CALIB(X,NSCX,XTEMP,XBACK,NX)
      CALL CALIB(Y,NSCY,YTEMP,YBACK,NY)
      DO 3 I=1,NY
      PIN(I)=X(I)
```

```
    3 POUT(I) = Y(I)
C
C     FINAL DATA TO BE ANALYSED IS PRINTED OUT
      WRITE(6,114) XINT1,NX1,XINT2,NX2,YINT1,NY1,YINT2,NY2
      WRITE(6,141) (XBACK(I),I=1,4)
      WRITE(6,141) (YBACK(I),I=1,4)
      WRITE(6,142) (X(I),NSCX(I),XTEMP(I),I=1,NX)
      WRITE(6,142) (Y(I),NSCY(I),YTEMP(I),I=1,NY)
C
C     SERIES SUMMATION
C
C     INDEX J CHANGES OMEGA
C
C     INDEX I CONTROLS THE DATA POINT LOCATION
C
    6 OMEGA = W(J)
C     EVALUATION OF INPUT INTEGRALS
C
C     INTEGRATION UP TO NX1
      TIST = 0.0
      IF(NR.EQ.2) GO TO 500
      CALL  TRAP(J,1,NX1,XINT1,OMEGA,PIN,TIST,SSIR1,SSII1)
      GO TO 501
  500 CALL FILON(J,1,NX1,XINT1,OMEGA,PIN,TIST,SSIR1,SSII1)
C     INTEGRATION UP TO NX FROM NX1
  501 RNX1=FLOAT(NX1)
      TIST = (RNX1-1.)*XINT1
      IF(NR.EQ.2) GO TO 502
      CALL  TRAP(J,NX1,NX,XINT2,OMEGA,PIN,TIST,SSIR2,SSII2)
      GO TO 503
  502 CALL FILON(J,NX1,NX,XINT2,OMEGA,PIN,TIST,SSIR2,SSII2)
C     INTEGRALS FOR TWO DIFFERENT REGIONS ARE SUMMED
  503 SSIR = SSIR1 + SSIR2
      SSII = SSII1 + SSII2
C
C     EVALUATION OF OUTPUT PRODUCT INTEGRAL
C
C     INTEGRATION UP TO NY1
      TIST = 0.0
      IF(NR.EQ.2) GO TO 504
      CALL TRAP (J,1,NY1,YINT1,OMEGA,POUT,TIST,SSOR1,SSOI1)
      GO TO 505
  504 CALL FILON (J,1,NY1,YINT1,OMEGA,POUT,TIST,SSOR1,SSOI1)
C     INTEGRATION UP TO NY FORM NY1
  505 RNY1 = FLOAT(NY1)
      TIST = (RNY1-1.)*YINT1
      IF(NR.EQ.2) GO TO 506
      CALL  TRAP(J,NY1,NY,YINT2,OMEGA,POUT,TIST,SSOR2,SSOI2)
      GO TO 507
  506 CALL FILON(J,NY1,NY,YINT2,OMEGA,POUT,TIST,SSOR2,SSOI2)
C     INTEGRALS FOR TWO DIFFERENT REGIONS ARE SUMMED
  507 SSOR = SSOR1 + SSOR2
      SSOI = SSOI1 + SSOI2
      IF(J.GT.1)  GO TO 450
C     AREA UNDER INPUT AND OUTPUT PULSES ARE CALCULATED FOR FREQUENCY CONTENT
C     CALCULATION AND FOR TRACER RECOVERY CHECK
      ARIN = SSIR
      AROUT = SSOR
      PREC = (AROUT/ARIN)*100.0
C     CALCULATION OF THE MEAN AVERAGE RESIDENCE TIME FOR THE CSTR COMPONENTS
C     FIRST THE MEAN AVG. RES. TIME FOR INPUT PULSE IS CALC AND THEN FOR THE
                                                                      OUTPUT
```

```
C     FOR EACH PULSE THERE ARE RESIDENCE TIMES FOR EACH TIME INTERVAL
      N1=NX1-1
      TXNUM1=0.0
      DO 200 N=1,N1
      RN=N
  200 TXNUM1=TXNUM1+(RN*XINT1-XINT1/2.)*(PIN(N)+PIN(N+1))/2.
      SFX1=0.0
      DO 201 N=1,NX1
  201 SFX1=SFX1+PIN(N)
      TX1=TXNUM1/SFX1
      TXNUM2=0.0
      DO 202 N=1,NX2
      RN=N
  202 TXNUM2=TXNUM2+(RN*XINT2-XINT2/2.)*(PIN(NX1+N-1)+PIN(NX1+N))/2.
      SFX2=0.0
      DO 203 N=NX1,NX
  203 SFX2=SFX2+PIN(N)
      TX2=TXNUM2/SFX2
      TX=((TX1*SSIR1)+((NX1-1)*XINT1+TX2)*SSIR2)/SSIR
      N1=NY1-1
      TYNUM1=0.0
      DO 300 N=1,N1
      RN=N
  300 TYNUM1=TYNUM1+(RN*YINT1-YINT1/2.)*(POUT(N)+POUT(N+1))/2.
      SFY1=0.0
      DO 301 N=1,NY1
  301 SFY1=SFY1+POUT(N)
      TY1=TYNUM1/SFY1
      TYNUM2=0.0
      DO 302 N=1,NY2
      RN=N
  302 TYNUM2=TYNUM2+(RN*YINT2-YINT2/2.)*(POUT(NY1+N-1)+POUT(NY1+N))/2.
      SFY2=0.0
      DO 303 N=NY1,NY
  303 SFY2=SFY2+POUT(N)
      TY2=TYNUM2/SFY2
      TY=((TY1*SSOR1)+((NY1-1)*YINT1+TY2)*SSOR2)/SSOR
      TBAR=TY-TX
C
      WRITE(6,103)  TXNUM1,TXNUM2,TX
      WRITE(6,103)  TYNUM1,TYNUM2,TY
      WRITE(6,103)  SSIR1,SSIR2,SSIR
      WRITE(6,103)  SSOR1,SSOR2,SSOR
C
C     OUTPUT DATA IS ALTERED SO THAT PERCENT RECOVERY = 100
      DO 10 I=1,NY
   10 POUT(I) = POUT(I)*ARIN/AROUT
      SSOR=1.
      SSIR=1.
  450 CONTINUE
 101  FORMAT(8F10.5)
  102 FORMAT(4(I3,7X))
  103 FORMAT(3(E15.8,10X))
  114 FORMAT(1H0,(4(F10.5,10X,I3))
  137 FORMAT(4F10.5)
  140 FORMAT(F10.5,10X,I1,10X,F10.5)
  141 FORMAT(1H-,8(5X,F10.5)//)
  142 FORMAT(1H ,F10.5,20X,I1,20X,F10.5)
      RETURN
      END
      SUBROUTINE FRFIR(J)
```

```
C     SUBROUTINE CALCULATES NECESSARY INTEGRALS FOR IMPULSE INPUTS AND
C     CORRESPONDING OUTPUTS
      COMMON W(100),NR,SSIR,SSII,SSOR,SSOI
      COMMON AROUT,ARIN,PREC,SUBINT
      DIMENSION Y(600),POUT(600)
      DIMENSION NSCY(600),YTEMP(600),YBACK(4)
      IF(J.GT.1)  GO TO 6
      IF(NR.EQ.1) GO TO 6
C
C     NUMBER OF SUBDIVISIONS PER TIME INTERVAL F10.5
C     NUMBER OF DATA POINTS, NY1, NY2, (I3,7X,I3)
C     TIME INTERVAL BETWEEN DATA POINTS, YINT1,YINT2,2F10.5
C
C     YINT1 IS THE TIME INTERVAL FOR NY1 POINTS
C     YINT2 IS THE TIME INTERVAL FOR NY2 POINTS
C     NX2, NY2 MUST BE EVEN NUMBERS
C     NX1, NY1 MUST BE ODD NUMBERS
C     TOTAL NUMBER OF OUTPUT DATA POINTS IS NY=NY1+NY2 ( INCLUDING ZERO END
C     SUBINT IS THE NUMBER OF SUBDIVISIONS PER TIME INTERVAL              PTS)
C     YBACK(I) IS THE BACKGROUND CHART READING FOR SCALE I OF OUTPUT 4F10.5
C     NSC(I) SIGNIFIES ON WHICH SCALE THE READING WAS TAKEN (I1)
C        1 - 30X SCALE
C        2 - 10X SCALE
C        3 -  3X SCALE
C        4 -  1X SCALE
C     TEMP(I) IS THE TEMPERATURE IN DEG. C AT WHICH THE READING WAS TAKEN
C     FORMAT FOR DATA, NSC, TEMP IS F10.5,I1,10X,F10.5                F10.5
C
      READ(5,101) SUBINT
      READ (5,102) NY1,NY2
      READ(5,101) YINT1,YINT2
      NY= NY1 + NY2
      READ(5,143) (YBACK(I),I=1,4)
      READ(5,140)(Y(I),NSCY(I),YTEMP(I),I=1,NY)
C
C     DATA IS CONVERTED TO CONC. AFTER TEMP. ADJUSTMENT IN SUBR. CALIB.
      CALL CALIB(Y,NSCY,YTEMP,YBACK,NY)
C
C     FINAL DATA TO BE ANALYSED IS PRINTED OUT
      WRITE(6,114) YINT1,NY1,YINT2,NY2
      WRITE(6,144) (YBACK(I),I=1,4)
      WRITE(6,142) (Y(I),NSCY(I),YTEMP(I),I=1,NY)
C     FREQUENCY CONTENT OF IMPULSE = 1.0 FOR ALL FREQUENCYS
      NYD=110
      DO 1 I=1,NYD
    1 POUT(I)=0.0
      DO 3 I=1,NY
    3 POUT(I+110)=Y(I)
      NY1=NY1+NYD
      NY=NY1+NY2
C
C     INPUT INTEGRALS ARE DEFINED AS FOLLOWS
      SSIR=1.0
      SSII=0.0
      ARIN = 1.0
C
C     INDEX J CHANGES OMEGA
C
C     INDEX I CONTROLS THE DATA POINT LOCATION
C
C
```

```
C     EVALUATION OF OUTPUT PRODUCT INTEGRAL
C
C     INTEGRATION UP TO NY1
    6 OMEGA = W(J)
      TIST = 0.0
      IF(NR.EQ.2) GO TO 504
      CALL TRAP (J,1,NY1,YINT1,OMEGA,POUT,TIST,SSOR1,SSOI1)
      GO TO 505
  504 CALL FILON (J,1,NY1,YINT1,OMEGA,POUT,TIST,SSOR1,SSOI1)
C     INTEGRATION UP TO NY FORM NY1
  505 RNY1 = FLOAT(NY1)
      TIST = (RNY1-1.)*YINT1
      IF(NR.EQ.2) GO TO 506
      CALL  TRAP(J,NY1,NY,YINT2,OMEGA,POUT,TIST,SSOR2,SSOI2)
      GO TO 507
  506 CALL FILON(J,NY1,NY,YINT2,OMEGA,POUT,TIST,SSOR2,SSOI2)
C     INTEGRALS FOR TWO DIFFERENT REGIONS ARE SUMMED
  507 SSOR = SSOR1 + SSOR2
      SSOI = SSOI1 + SSOI2
      IF(J.GT.1) GO TO 460
      TX=0.0
      N1=NY1-1
      TYNUM1=0.0
      DO 300 N=1,N1
      RN=N
  300 TYNUM1=TYNUM1+(RN*YINT1-YINT1/2.)*(POUT(N)+POUT(N+1))/2.
      SFY1=0.0
      DO 301 N=1,NY1
  301 SFY1=SFY1+POUT(N)
      TY1=TYNUM1/SFY1
      TYNUM2=0.0
      DO 302 N=1,NY2
      RN=N
  302 TYNUM2=TYNUM2+(RN*YINT2-YINT2/2.)*(POUT(NY1+N-1)+POUT(NY1+N))/2.
      SFY2=0.0
      DO 303 N=NY1,NY
  303 SFY2=SFY2+POUT(N)
      TY2=TYNUM2/SFY2
      TY=((TY1*SSOR1)+((NY1-1)*YINT1+TY2)*SSOR2)/SSOR
      TBAR=TY-TX
      WRITE(6,103) TYNUM1,TYNUM2,TY
      WRITE(6,103) SSOR1,SSOR2,SSOR
C     THE OUTPUT DATA IS NORMALIZED SO THAT AREA UNDER OUTPUT PULSE=1.0
      AROUT=SSOR
      SSOR=1.0
      DO 450 I=1,NY
  450 POUT(I) = POUT(I)/AROUT
 460  CONTINUE
 101  FORMAT(8F10.5)
  102 FORMAT(2(I3,7X))
  103 FORMAT(3(E15.8,10X))
  114 FORMAT(1H1,(2(F10.5,10X,I3))
  140 FORMAT(F10.5,10X,I1,10X,F10.5)
  142 FORMAT(1H ,F10.5,20X,I1,20X,F10.5)
  143 FORMAT(4F10.5)
  144 FORMAT(1H-,4(F10.5,10X)//)
      RETURN
      END
      SUBROUTINE FRFSR(J)
C     SUBROUTINE CALCULATES NECESSARY INTEGRALS FOR STEP INPUT AND CORRES -
C     OUTPUT.                                                          PONDING
```

```
      COMMON W(100),NR,SSIR,SSII,SSOR,SSOI
      COMMON AROUT,ARIN,PREC,SUBINT
      DIMENSION X(600),Y(600),PIN(600),POUT(600)
      IF(J.GT.1)  GO TO 6
      IF(NR.EQ.1) GO TO 6
C     NUMBER OF SUBDIVISIONS PER TIME INTERVAL F10.5
C     NUMBER OF DATA POINTS, NX1, NX2, NY1, NY2, (I3,7X,I3,7X,I3,7X,I3)
C     TIME INTERVAL BETWEEN DATA POINTS, XINT1, XINT2, YINT1, YINT2, 4F10.5
C
C     XINT1 IS THE TIME INTERVAL FOR NX1 POINTS
C     XINT2 IS THE TIME INTERVAL FOR NX2 POINTS
C     YINT1 IS THE TIME INTERVAL FOR NY1 POINTS
C     YINT2 IS THE TIME INTERVAL FOR NY2 POINTS
C     NX2, NY2 MUST BE EVEN NUMBERS
C     NX1, NY1 MUST BE ODD NUMBERS
C     TOTAL NUMBER OF INPUT  DATA POINTS IS NX=NX1+NX2 ( INCLUDING ZERO END PT)
C     TOTAL NUMBER OF OUTPUT DATA POINTS IS NY=NY1+NY2 ( INCLUDING ZERO END PT)
C     SUBINT IS THE NUMBER OF SUBDIVISIONS PER TIME INTERVAL
C     XBACK(I), YBACK(I) ARE THE BACKGROUND CHART READINGS FOR SCALE(I) OF
C     INPUT AND OUTPUT RESP. (4F10.5)
C     NSC(I) SIGNIFIES ON WHICH SCALE THE READING WAS TAKEN (I1)
C        1 - 30X SCALE
C        2 - 10X SCALE
C        3 -  3X SCALE
C        4 -  1X SCALE
C     TEMP(I) IS THE TEMPERATURE IN DEG. C AT WHICH THE READING WAS TAKEN
C     FORMAT FOR DATA, NSC, TEMP IS F10.5,I1,10X,F10.5
C
      READ(5,101) SUBINT
      READ(5,102) NX1,NX2,NY1,NY2
      READ(5,101) XINT1,XINT2,YINT1,YINT2
      NX= NX1 + NX2
      NY= NY1 + NY2
      READ(5,137) (XBACK(I),I=1,4)
      READ(5,137) (YBACK(I),I=1,4)
      READ(5,140) (X(I),NSCX(I),XTEMP(I),I=1,NX)
      READ(5,140)(Y(I),NSCY(I),YTEMP(I),I=1,NY)
C
C     DATA IS CONVERTED TO CONC. AFTER TEMP. ADJUSTMENT IN SUBR. CALIB.
      CALL CALIB(X,NSCX,XTEMP,XBACK,NX)
      CALL CALIB(Y,NSCY,YTEMP,YBACK,NY)
      DO 3 I=1,NY
      PIN(I)=X(I)
    3 POUT(I) = Y(I)
C
C     FINAL DATA TO BE ANALYSED IS PRINTED OUT
      WRITE(6,114) XINT1,NX1,XINT2,NX2,YINT1,NY1,YINT2,NY2
      WRITE(6,141) (XBACK(I),I=1,4)
      WRITE(6,141) (YBACK(I),I=1,4)
      WRITE(6,142) (X(I),NSCX(I),XTEMP(I),I=1,NX)
      WRITE(6,142) (Y(I),NSCY(I),YTEMP(I),I=1,NY)
C
C     STEP INPUT AND OUTPUT MODIFIED TO USE REGULAR PRODUCT INTEGRALS
C     AMM, AKK ARE THE STEP HEIGHTS OF INPUT AND OUTPUT RESPECTIVELY
C
      AMM=PIN(NX)
      AKK=POUT(NY)
      DO 5 I=1,NY
      PIN(I) = AMM-PIN(I)
    5 POUT(I)=AKK-POUT(I)
```

```
C     FINAL DATA TO BE ANALYSED IS PRINTED OUT TO BE CHECKED
C
      WRITE(6,114) XINT1,NX1,XINT2,NX2,YINT1,NY1,YINT2,NY2
      WRITE(6,115) (J, PIN(J),POUT(J),J=1,NY)
C
C     SERIES SUMMATION
C
C     INDEX J CHANGES OMEGA
C
C     INDEX I CONTROLS THE DATA POINT LOCATION
C
    6 OMEGA = W(J)
C     EVALUATION OF INPUT INTEGRALS
C
C     INTEGRATION UP TO NX1
      TIST = 0.0
      IF(NR.EQ.2) GO TO 500
      CALL  TRAP(J,1,NX1,XINT1,OMEGA,PIN,TIST,SSIR1,SSII1)
      GO TO 501
  500 CALL FILON(J,1,NX1,XINT1,OMEGA,PIN,TIST,SSIR1,SSII1)
C     INTEGRATION UP TO NX FROM NX1
  501 RNX1=FLOAT(NX1)
      TIST = (RNX1-1.)*XINT1
      IF(NR.EQ.2) GO TO 502
      CALL  TRAP(J,NX1,NX,XINT2,OMEGA,PIN,TIST,SSIR2,SSII2)
      GO TO 503
  502 CALL FILON(J,NX1,NX,XINT2,OMEGA,PIN,TIST,SSIR2,SSII2)
C     INTEGRALS FOR TWO DIFFERENT REGIONS ARE SUMMED
  503 SSIR = SSIR1 + SSIR2
      SSII = SSII1 + SSII2
C
C     EVALUATION OF OUTPUT PRODUCT INTEGRAL
C
C     INTEGRATION UP TO NY1
      TIST = 0.0
      IF(NR.EQ.2) GO TO 504
      CALL TRAP (J,1,NY1,YINT1,OMEGA,POUT,TIST,SSOR1,SSOI1)
      GO TO 505
  504 CALL FILON (J,1,NY1,YINT1,OMEGA,POUT,TIST,SSOR1,SSOI1)
C     INTEGRATION UP TO NY FORM NY1
  505 RNY1 = FLOAT(NY1)
      TIST = (RNY1-1.)*YINT1
      IF(NR.EQ.2) GO TO 506
      CALL  TRAP(J,NY1,NY,YINT2,OMEGA,POUT,TIST,SSOR2,SSOI2)
      GO TO 507
  506 CALL FILON(J,NY1,NY,YINT2,OMEGA,POUT,TIST,SSOR2,SSOI2)
C     INTEGRALS FOR TWO DIFFERENT REGIONS ARE SUMMED
  507 SSOR = SSOR1 + SSOR2
      SSOI = SSOI1 + SSOI2
C
C     USUAL PRODUCT INTEGRALS MODIFIED FOR STEP FUNCTIONS
C
      SSOI=AKK-W(J)*SSOI
      SSOR=-W(J)*SSOR
      SSII=AMM-W(J)*SSII
      SSIR=-W(J)*SSIR
  101 FORMAT(8F10.5)
  102 FORMAT(4(I3,7X))
  114 FORMAT(1H1,(4(F10.5,10X,I3))
  137 FORMAT(4F10.5)
```

```
  140 FORMAT(F10.5,10X,I1,10X,F10.5)
  141 FORMAT(1H-,8(5X,F10.5)//)
  142 FORMAT(1H ,F10.5,20X,I1,20X,F10.5)
      RETURN
      END
      SUBROUTINE  TRAP(J,NST,NFIN,TINT,OMEGA,FUN,TIST,PICOS,PISIN)
C      SUBROUTINE CALCULATES TRIGNOMETRIC INTEGRALS USING TRAPEZOIDAL RULE
      DIMENSION FUN(600)
      COMMON W(100),NR,SSIR,SSII,SSOR,SSOI
      COMMON AROUT,ARIN,PREC,SUBINT
      SSR =0.0
      SSI =0.0
      A=0.0
      NEND=NFIN-1
      TINC=TINT/SUBINT
      DO 10 I=NST,NEND
      DELI=(FUN(I+1)-FUN(I))/SUBINT
      DELI1 = FUN(I)
      IT=SUBINT
      DO 9 K=1,IT
      DELI2 = DELI1 + DELI
      FUNTI = (DELI1 + DELI2)/2.
      A = A+1.
      T=(TIST+(2.*A-1.)/2.*TINC)*OMEGA
      SSR = SSR + FUNTI*COS(T)
      SSI = SSI + FUNTI*SIN(T)
    9 DELI1=DELI2
   10 CONTINUE
      PICOS = TINC*SSR
      PISIN = TINC*SSI
      RETURN
      END
      SUBROUTINE FILON(J,NST,NFIN,TINT,OMEGA,FUN,TIST,PICOS,PISIN)
C     SUBROUTINE CALCULATES TRIGNOMETRIC INTEGRALS USING FILONS QUADRATURE
      DIMENSION FUN(600)
      NN=(NFIN-1)/2+1
      NO=NN-1
      TSEV = 0.0
      TSODD= 0.0
      TCEV = 0.0
      TCODD= 0.0
      NFS=(NST+1)/2
      R=TINT*OMEGA
      DO 420 I=NFS,NN
      K=2*I-1
      II=(I+1-NFS)
      XI=FLOAT(II)
      TEV =(TIST+2.*(XI-1.)*TINT)*OMEGA
      SEV =FUN(K) * SIN(TEV)
      TSEV=TSEV+SEV
      CEV = FUN(K) * COS(TEV)
      TCEV = TCEV + CEV
  420 CONTINUE
      DO 440 I=NFS,NO
      L=2*I
      III=2*(I+1-NFS)
      XL=FLOAT(III)
      TODD=(TIST+(XL-1.)*TINT)*OMEGA
      SODD = FUN(L) * SIN(TODD)
      TSODD = TSODD + SODD
```

```
      CODD = FUN(L) * COS(TODD)
      TCODD= TCODD + CODD
  440 CONTINUE
      TSEV=TSEV-.5*(FUN(NST)*SIN(OMEGA*TIST) + FUN(NFIN)*SIN(TEV))
      TCEV=TCEV-.5*(FUN(NST)*COS(OMEGA*TIST) + FUN(NFIN)*COS(TEV))
C     CONSTANTS ARE EVALUATED IN SUBROUTINE CONST
      CALL CONST(R,ALPHA,BETA,GAMMA)
      PISIN=TINT*(ALPHA*(FUN(NST)*COS(OMEGA*TIST) -FUN(NFIN)*COS(TEV ))
     1+BETA*TSEV + GAMMA*TSODD)
      PICOS= TINT*(ALPHA*(FUN(NFIN)*SIN(TEV)-FUN(NST)*SIN(OMEGA*TIST))
     1+BETA*TCEV + GAMMA*TCODD)
      RETURN
      END
      SUBROUTINE CONST(R,ALPHA,BETA,GAMMA)
C     SUBROUTINE EVALUATED CONSTANTS USED IN THE INTEGRATION
      IF(R.LT.0.35) GO TO 405
      R2=R+R
      RR=R*R
      RRR=R*R*R
      SR=SIN(R)
      CR=COS(R)
      SR2=SIN(R2)
      ALPHA=1./R + SR2/(RR+RR) - 2.*SR*SR/RRR
      BETA=2.*((1.+CR*CR)/RR-SR2/RRR)
      GAMMA = 4.*(SR/RRR-CR/RR)
      RETURN
  405 CONTINUE
C     EVALUATION OF CONSTANTS IF R IS SMALL
      ALPHA = 2.*R**3/45. - 2.*R**5/315. + 2.*R**7/4725.
      BETA = 2./3. + 2.*R*R/15.- 4.*R**4/105. + 2.*R**6/567.-
     1 4.*R**8/22275.
      GAMMA = 4./3. - 2.*R*R/15. + R**4/210. - R**6/11340.+R**8/997920.
      RETURN
      END
      SUBROUTINE CALIB(PT,NSC,TEMP,BACKG,N)
C     SUBROUTINE PERFORMS THE FOLLOWING FUNCTIONS
C        1. READS IN THE NECESSARY CALIBRATION COEFFICIENTS FOR EACH SCALE
C           AND FOR EACH PORTION OF THE CALIBRATION CURVE- LINEAR AND NON-
C        2. BACKGROUND IS SUBTRACTED FROM DATA                          LINEAR
C        3. TEMPERATURE CORRECTION TO 25 C IS MADE
C        4. CORRECTED SCALE READING IS CONVERTED TO CONC. IN PPB
      DIMENSION PT(600),NSC(600), TEMP(600),BACKG(4)
C
C     THE FOLLOWING CODE IS USED FOR CALI RATION COEFFS.
C        A - 30X              0 - INTERCEPT            1 - NON LINEAR PORTION
C        B - 10X              1 - LINEAR TERM          2 - LINEAR PORTION
C        C -  3X              2 - QUADRATIC TERM
C        D -  1X              3 - CUBIC TERM
C
      READ(5,136) A01,A11,A21,A31
      READ(5,136) A02,A12
      READ(5,136) B01,B11,B21,B31
      READ(5,136) B02,B12
      READ(5,136) C01,C11,C21,C31
      READ(5,136) C02,C12
      READ(5,136) D01,D11,D21,D31
      READ(5,136) D02,D12
C     BR30,BR10, ETC. ARE THE READINGS AT WHICH THE CALIBRATION CURVE CHANGES
C
      READ(5,137) BR30,BR10,BR3,BR1
```

```
      DO 2 I=1,N
      NNN=NSC(I)
      GO TO (3,4,5,6) NNN
    3 PT(I) = (PT(I)-BACKG(1))*EXP(+.032*(TEMP(I)-25.))
      IF(PT(I).GT.BR30) GO TO 7
      PT(I) = A01 + A11*PT(I) + A21*PT(I)**2 + A31*PT(I)**3
      GO TO 2
    7 PT(I) = A02 + A12*PT(I)
      GO TO 2
    4 PT(I) = (PT(I)-BACKG(2))*EXP(+.032*(TEMP(I)-25.))
      IF(PT(I).GT.BR10) GO TO 8
      PT(I) = B01 + B11*PT(I) + B21*PT(I)**2 + B31*PT(I)**3
      GO TO 2
    8 PT(I) = B02 + B12*PT(I)
      GO TO 2
    5 PT(I) = (PT(I)-BACKG(3))*EXP(+.032*(TEMP(I)-25.))
      IF(PT(I).GT.BR3) GO TO 9
      PT(I) = C01 + C11*PT(I) + C21*PT(I)**2 + C31*PT(I)**3
      GO TO 2
    9 PT(I) = C02 + C12*PT(I)
      GO TO 2
    6 PT(I) = (PT(I)-BACKG(4))*EXP(+.032*(TEMP(I)-25.))
      IF(PT(I).GT.BR1)  GO TO 10
      PT(I) = D01 + D11*PT(I) + D21*PT(I)**2 + D31*PT(I)**3
      GO TO 2
   10 PT(I) = D02 + D12*PT(I)
    2 CONTINUE
  136 FORMAT(5E15.8)
  137 FORMAT(4F10.5)
      RETURN
      END
         6400 END OF RECORD
```

CD TOT 0759

RUN 8

XINT1	NX1	XINT2	NX2	YINT1	NY1	YINT2	NY2
.18000	57	.45000	14	.50500	43	2.02000	44

XBACK			
-0.00000	-0.00000	-0.00000	-0.00000

YBACK			
.60000	.50000	-0.00000	-0.00000

0.00000	3	26.00000
51.81823	3	26.00000
255.78300	3	26.00000
473.60945	3	26.00000
592.42388	3	26.00000
594.40412	3	26.00000
507.61021	2	26.00000
477.40520	2	26.00000
430.41962	2	26.00000
403.57072	2	26.00000
383.43405	2	26.00000
356.58515	2	26.00000
326.38014	2	26.00000
306.24346	2	26.00000
284.76434	2	26.00000
265.13376	2	25.90000
241.71603	2	25.90000
226.32724	2	25.90000
211.60752	2	25.90000
194.88057	2	25.90000
179.49177	2	25.90000
161.42667	2	25.90000
148.71418	2	25.90000
143.36156	2	25.90000
127.97277	2	25.90000
117.93660	2	25.90000
105.89319	2	25.90000
103.21688	2	25.90000
97.86425	2	25.90000
92.51163	2	25.90000
86.89394	2	25.80000
78.89066	2	25.80000
76.22289	2	25.80000
67.55267	2	25.80000
62.88409	2	25.80000
57.54856	2	25.80000
52.21304	2	25.80000
47.54446	2	25.80000
44.20975	2	25.80000
34.57435	1	25.80000
31.92173	1	25.80000
29.26911	1	25.80000
27.20596	1	25.80000
24.55334	1	25.80000
22.71242	1	25.70000
20.65587	1	25.70000
18.89310	1	25.70000
16.54275	1	25.70000
14.77999	1	25.70000
13.01723	1	25.70000
11.84205	1	25.70000

Input
Data after calibration
and temperature correction
has been applied

McMASTER UNIVERSITY

10.96067	1	25.70000
10.37308	1	25.70000
9.49170	1	25.70000
8.61032	1	25.70000
8.02273	1	25.70000
7.61142	1	25.70000
6.08369	1	25.70000
4.89313	1	25.60000
4.19027	1	25.60000
3.83885	1	25.60000
2.55028	1	25.60000
2.37457	1	25.60000
1.72505	1	25.50000
1.25798	1	25.50000
1.25798	1	25.50000
1.14121	1	25.50000
.96606	1	25.50000
.84929	1	25.50000
.73252	1	25.50000
.55737	1	25.50000
.61066	1	27.50000
.70730	1	27.50000
.70730	1	27.50000
.80339	1	27.50000
.89894	1	27.50000
1.08839	1	27.50000
1.08839	1	27.50000
2.52551	1	27.50000
2.77942	1	27.50000
3.19171	1	27.50000
4.98087	1	27.50000
6.28868	1	27.50000
7.57464	1	27.50000
8.24893	1	27.50000
9.30735	1	27.50000
10.89774	1	27.50000
11.84441	1	27.50000
13.92707	1	27.50000
15.28990	1	27.60000
17.18930	1	27.60000
19.46857	1	27.60000
21.48193	1	27.60000
23.15340	1	27.60000
25.35670	1	27.60000
27.63598	1	27.60000
28.85159	1	27.60000
30.82696	1	27.60000
33.12475	1	27.70000
34.76346	1	27.70000
36.47840	1	27.70000
38.38388	1	27.70000
39.90827	1	27.70000
40.17275	2	27.70000
40.87173	2	27.70000
42.01905	2	27.80000
42.63262	2	27.80000
42.89558	2	27.80000
44.47333	2	27.80000
44.12272	2	27.80000
44.82394	2	27.80000

Output Data
after calibration and
temperature correction
has been applied

McMASTER UNIVERSITY

44.99925	2	27.80000
44.91160	2	27.80000
45.17455	2	27.80000
44.93210	2	27.90000
42.99756	2	27.90000
40.53542	2	27.90000
40.83614	1	28.00000
36.60363	1	28.00000
33.33306	1	28.00000
30.06249	1	28.00000
26.48410	1	28.00000
23.63678	1	28.00000
20.86642	1	28.00000
18.13453	1	28.00000
16.21066	1	28.00000
14.28680	1	28.00000
12.86314	1	28.00000
11.59339	1	28.00000
10.59298	1	28.00000
9.43866	1	28.00000
8.49190	1	28.00000
7.80640	1	28.00000
7.09581	1	28.00000
6.46826	1	28.00000
5.63364	1	28.00000
4.54462	1	28.00000
4.17474	1	28.00000
3.63325	1	28.00000
3.47347	1	28.00000
2.98062	1	28.00000
2.81183	1	28.00000
2.64079	1	28.00000
1.93410	1	28.00000
1.47411	1	28.00000
1.47411	1	28.00000
1.38042	1	28.00000
1.28617	1	28.00000
1.28617	1	28.00000
1.28617	1	28.00000
1.28617	1	28.00000
1.09599	1	28.00000
1.00005	1	28.00000
1.00005	1	28.00000
1.00005	1	28.00000
1.00005	1	28.00000
.80648	1	28.00000
.70885	1	28.00000
2.22506685E+04	6.82533517E+01	2.63381333E+00
1.40943647E+04	9.84731997E+03	3.15405842E+01
1.57689045E+03	1.60353413E+01	1.59292579E+03
4.71794979E+02	1.07591416E+03	1.54770914E+03

Intermediate Residence Time Calculations

Experimental Transfer Function

Real	Imaginary	Freq.	
1.00000	0.00000	0.00000	1
.94184	-.28514	.01000	2
.91723	-.33699	.01200	3
.88890	-.38617	.01400	4
.84017	-.45424	.01700	5
.78512	-.51470	.02000	6
.72514	-.56694	.02300	7
.66166	-.61065	.02600	8
.59606	-.64577	.02900	9
.52968	-.67250	.03200	10
.46371	-.69125	.03500	11
.35740	-.70645	.04000	12
.29707	-.70717	.04300	13
.22178	-.70002	.04700	14
.16956	-.68965	.05000	15
.09092	-.66510	.05500	16
.02247	-.63407	.06000	17
-.03666	-.59882	.06500	18
-.08753	-.56088	.07000	19
-.13109	-.52113	.07500	20
-.16801	-.48008	.08000	21
-.19863	-.43815	.08500	22
-.22312	-.39583	.09000	23
-.24156	-.35377	.09500	24
-.25420	-.31282	.10000	25
-.26430	-.23761	.11000	26
-.26026	-.17495	.12000	27
-.24991	-.12450	.13000	28
-.23749	-.08181	.14000	29
-.22211	-.04296	.15000	30
-.20087	-.00827	.16000	31
-.17352	.01840	.17000	32
-.14419	.03395	.18000	33
-.11865	.03952	.19000	34
-.09995	.04005	.20000	35
-.08666	.04041	.21000	36
-.07507	.04197	.22000	37
-.06304	.04275	.23000	38
-.05173	.04058	.24000	39
-.04385	.03596	.25000	40

DTIME= 59.980000 (Dead Time) TBAR= 28.906771 (Average residence time without Dead Time)

ARIN= 1.5929E+03 AROUT= 1.5477E+03 PERCENT RECOVERY= 97.2

ARIN = area under input pulse

AROUT = area under output pulse

FREQUENCY RESPONSE RESULTS FOR PULSE TEST
USING FILON QUADRATURE

MAGNITUDE RATIO	PHASE ANGLE WITH DTIME	PHASE ANGLE WITHOUT DTIME	GAIN DECIBELS	FREQUENCY RADIANS/MIN
1.0000	0.00	0.00	0.0000	0.0000
.9841	-51.21	-16.84	-.1396	.0100
.9772	-61.41	-20.17	-.2005	.0120
.9692	-71.59	-23.48	-.2721	.0140
.9551	-86.82	-28.40	-.3990	.0170
.9388	-101.98	-33.25	-.5486	.0200
.9205	-117.06	-38.02	-.7199	.0230
.9004	-132.06	-42.70	-.9115	.0260
.8788	-146.95	-47.29	-1.1221	.0290
.8560	-161.75	-51.77	-1.3500	.0320
.8324	-176.43	-56.15	-1.5936	.0350
.7917	-200.63	-63.16	-2.0286	.0400
.7670	-214.99	-67.21	-2.3037	.0430
.7343	-233.94	-72.42	-2.6824	.0470
.7102	-248.02	-76.19	-2.9725	.0500
.6713	-271.23	-82.22	-3.4618	.0550
.6345	-294.17	-87.97	-3.9519	.0600
.5999	-316.88	-93.50	-4.4378	.0650
.5677	-339.43	-98.87	-4.9181	.0700
.5374	-361.87	-104.12	-5.3947	.0750
.5086	-384.22	-109.29	-5.8720	.0800
.4811	-406.50	-114.39	-6.3558	.0850
.4544	-428.70	-119.41	-6.8517	.0900
.4284	-450.80	-124.33	-7.3635	.0950
.4031	-472.76	-129.10	-7.8921	.1000
.3554	-516.07	-138.04	-8.9855	.1100
.3136	-558.48	-146.09	-10.0726	.1200
.2792	-600.28	-153.52	-11.0816	.1300
.2512	-642.12	-160.99	-12.0002	.1400
.2262	-684.54	-169.05	-12.9092	.1500
.2010	-727.50	-177.64	-13.9344	.1600
.1745	-770.28	-186.05	-15.1643	.1700
.1481	-811.84	-193.25	-16.5868	.1800
.1251	-851.38	-198.42	-18.0579	.1900
.1077	-889.16	-201.84	-19.3577	.2000

MCMASTER UNIVERSITY
DATA PROCESSING AND COMPUTER CENTRE

MAGNITUDE RATIO	PHASE ANGLE WITH DTIME	PHASE ANGLE WITHOUT DTIME	GAIN DECIBELS	FREQUENCY RADIANS/MIN
.0956	-926.68	-205.00	-20.3892	.2100
.0860	-965.26	-209.21	-21.3099	.2200
.0762	-1004.56	-214.14	-22.3650	.2300
.0658	-1042.90	-218.11	-23.6419	.2400
.0567	-1078.51	-219.36	-24.9270	.2500

FREQUENCY RADIANS/MIN	INPUT FREQ. CONT. DIMENSIONLESS	OUTPUT FREQ. CONT. DIMENSIONLESS	
0.0000	[illegible]	[illegible]6	1
.0100	.9998	.9838	2
.0120	.9997	.9769	3
.0140	.9996	.9687	4
.0170	.9994	.9545	5
.0200	.9991	.9379	6
.0230	.9988	.9194	7
.0260	.9985	.8990	8
.0290	.9981	.8772	9
.0320	.9977	.8541	10
.0350	.9973	.8301	11
.0400	.9964	.7889	12
.0430	.9959	.7639	13
.0470	.9951	.7307	14
.0500	.9944	.7062	15
.0550	.9933	.6668	16
.0600	.9920	.6294	17
.0650	.9906	.5943	18
.0700	.9891	.5615	19
.0750	.9875	.5307	20
.0800	.9858	.5014	21
.0850	.9841	.4734	22
.0900	.9822	.4463	23
.0950	.9802	.4199	24
.1000	.9781	.3943	25
.1100	.9736	.3460	26
.1200	.9688	.3038	27
.1300	.9636	.2690	28
.1400	.9581	.2407	29
.1500	.9523	.2154	30
.1600	.9461	.1902	31
.1700	.9397	.1640	32
.1800	.9330	.1382	33
.1900	.9260	.1158	34
.2000	.9188	.0989	35

FREQUENCY RADIANS/MIN	INPUT FREQ. CONT. DIMENSIONLESS	OUTPUT FREQ. CONT. DIMENSIONLESS	
.2100	.9114	.0871	36
.2200	.9038	.0777	37
.2300	.8960	.0682	38
.2400	.8880	.0584	39
.2500	.8799	.0499	40

APPENDIX E

E. SAMPLE CALCULATION OF FREQUENCY RESPONSE FROM SINE RUN DATA

E.1 Amplitude Ratio Calculation

Input	Maximum Reading	85.0	
	Background	.5	
	Temperature	26.8°C	
	Corrected Reading -25°C	89.49	Concentration = 51.42 ± 1.03 ppb
	Minimum Reading	52.5	
	Background	.5	
	Temperature	26.7°C	
	Corrected Reading	7.92	Concentration = 5.83 ± .1
		Amplitude	45.59 ± 1.13
			= 45.59 ± 2.5%
Output	Maximum Reading	79.5	
	Background	.5	
	Temperature	28.0°C	
	Corrected Reading -25°C	86.9	Concentration = 33.92 ± .68
	Minimum Reading	52.5	
	Background	.5	
	Temperature	28.0°C	
	Corrected Reading	57.2	Concentration = 23.54 ± .47
		Amplitude	10.38 ±1.15
			= 10.38 ± 11%

$$\text{Amplitude Ratio} = \frac{10.38}{45.59} = .228 \pm 13.5\%$$

$$= -12.85 \begin{smallmatrix} + 1.12 \\ - 1.26 \end{smallmatrix} \text{ decibels}$$

E.2 Frequency and Period

Frequency of sine input = .174 rad/min.

Period = 36.2 min.

E.3 Phase Shift

Input minimum at 98.9 ± 1.0 min.

Corresponding Output

minimum at 172.5 ± 1.5 min.

Difference = 73.6 ± 2.5 min.

$$\text{Phase Shift} = \frac{73.6}{36.2} \times 360 = 732 \pm 25 \text{ degrees}$$